Modelling Microbial Populations

in Variable Environments.

The research presented is this thesis was carried out at the Department of Theoretical Biology, Vrije Universiteit Amsterdam, The Netherlands and at the Laboratory of Microbiology Geochemistry and Marin Ecology, University of Aix-Marseille II, Marseille France.

VRIJE UNIVERSITEIT

MODELLING MICROBIAL POPULATIONS IN VARIABLE ENVIRONMENTS

ACADEMISCH PROEFSCHRIFT

ter verkrijging van de graad van doctor aan
de Vrije Universiteit Amsterdam,
op gezag van de rector magnificus
prof.dr. T. Sminia,
in het openbaar te verdedigen
ten overstaan van de promotiecommissie
van de faculteit der Aard- en Levenswetenschappen
op donderdag jour mois 2006 om 15.45 uur
in de aula van de universiteit,
De Boelelaan 1105

door

Caroline Tolla

geboren te Marseille (France)

Double Doctorate Degree:	Netherland/ France
promotoren:	prof.dr. S.AL.M. Kooijman prof.dr. J.C. Poggiale
Dutch Reading Committee:	prof.dr. P. Auger dr.ir. P.M. van Bodegom prof.dr. U. Dieckmann prof.dr. R. Hengeveld dr.ir. B.W. Kooi dr. J. van der Meer
French Reading Committee:	prof.dr. P. Auger prof.dr. J.C. Bertrand dr. P. Bonin dr. S. Pouvreau dr. C. Rabouille

To my mother

The important thing is not to stop questioning. Curiosity has its own reason for existing.

Einstein, Albert

Thesis 2006 of the Institute of Molecular and Cellular Biology, Vrije Universiteit, Amsterdam, the Netherlands.

Contents

Preface

Modelling finds all of its importance in its reasoning. Indeed, the model formulation for a phenomenon implies having identified the problem previously and putting forward knowledge-based assumptions about the environment in which this phenomenon takes place. Indeed, apart from assumptions about biota, knowledge of the environment is necessary to model e.g. population dynamics. Modelling allows to: (*i*) put in evidence, quantify and simplify the process descriptions in the considered environment; (*ii*) determine not-measured parameters and understand non expected experimental results; (*iii*) structure next experiments, if the formulated model describes the studied phenomenon correctly. Finally, modelling may lead to a prediction step.

The spatial and temporal scale that is chosen for the formulation is crucial as each process and interaction has its own scale at which it is important. The models which were proposed to study the bacterial population dynamics are mostly empirical: they don't describe the processes at the individual level but they aim to represent the results at the population level. Moreover, they are mostly formulated on the basis of experiments done in equilibrium situations, making them inappropriate in changing environmental conditions.

This thesis finds its basis in such problems. It improves mathematical formulations for the study of variable environments through the development of a mechanistic approach for the model construction. More precisely, we focused here on bacterial communities dynamics and the corresponding biogeochemical processes. Several steps were achieved: (*i*) the treatment of bacterial dynamics by classical models analysing the organic matter degradation, (*ii*) the comparison of classical models analysing the bacterial dynamics (the models by Monod and Droop) and a mechanistic one based on the Dynamics Energy Budget theory (DEB), (*iii*) the improvement of the description of bacterial communities dynamics and the biogeochemical processes. Firstly, as the variable environments imply starvation conditions, we described one of the possible adaptation strategies: the shrinking process of the cell in unfavourable conditions. Then, we developed a complete mechanistic model describing the biogeochemical processes of the nitrogen cycle and we study the impact of benthic population on the expression of bacterial metabolism.

1

General introduction

Microbial activities play an important role in ecosystems and are used in different fields: health sciences (pathogen capacity, epidemiology, vaccination); agronomy and food research (optimization of plant and animal productions); environmental protection (mineral and organic cleanup, degradation of xenobiotics, and sprouts dissemination control). Among others, microbial activities are responsible for biogeochemical processes at the root of organic matter degradation. This degradation process releases minerals that serve as source for the first level of the trophic chain in the ecosystems.

Modelling finds all of its importance in its reasoning. Indeed, formulating some model for biological processes and thus expressing the relations between variables implies having identified the problem previously and putting forward knowledge-based assumptions about the environment in which they occur. Indeed, modelling and experimentation should be done in parallel. The experimental results allow model formulations that lead to a better understanding of the system and to a structuring of other experiments, as a cycle. First, modelling permits to understand and quantify the role of each process in the environment under consideration. Then, it allows to underline and simplify the description of the predominant processes, testing some assumptions. Moreover, it can be a useful step in data verification, if the formulated model describes the phenomenon correctly. But modelling can also help to structure the experiments by a preliminary analysis. Furthermore, this approach can determine not-measured parameters and enable to understand interactions between processes and in particular when some experimental results are unexpected. Finally, modelling may achieve the prediction step.

The degradation of organic matter has been modelled in different ways. Some biogeochemical models describe the interaction between organic matter and bacteria in the water column, but also include other processes such as carbon production, the transfer of matter to higher trophic levels and the different carbon pools (Anderson and Williams, 1998; Anderson and Williams, 1999; Anderson and Ducklow, 2001; Baretta-Bekker *et al.*, 1995; Blackburn *et al.*, 1996; Dearman *et al.*, 2003; Lancelot *et al.*, 2002; Spitz *et al.*, 2001). For the benthic system, the early diagenesis models (Berner, 1980; Boudreau, 1996; Boudreau, 1997; Soetaert *et al.*, 1996) are actually the most employed models. They use either Partial Differential Equations (PDE's) (Berner, 1980; Crank, 1976; Guinasso and Schink, 1975; Matisoff, 1982), or Ordinary Differential Equations (ODE's) (François-Carcaillet, 1999), and allow the analysis and the quantification of the mixing activity at the macroscopic scale (François-Carcaillet, 1999; Lawton, 1994; Wardle *et al.*, 1997). The considered biological processes are: (*i*) the non-local mixing processes of particles and interstitial water linked to macro-meiobenthic organisms (compound distributions as a function of depth); (*ii*) the degradation processes linked to the bacterial compartment. The various physical characteristics of the sediment, such as the sedimentation rate or the sediment porosity, can also intervene.

However, their assumptions remain simplistic leading to some intrinsic problems to their formulation. Firstly, they are essentially based on empirical mathematical formulations. By definition, empirism (emperia in Greek means experiments) is based on experiments (in the broad sense) as the unique source of knowledge [(1)]. Then, these empirical models are obtained from experimentations realised in equilibrium situations. But, natural environments are rarely at equilibrium. Finally, only few benthic models describe the microbial communities which are supposed to be in stationary state and large environmental perturbations will inevitably affect these communities. These perturbations can be natural such as the temperature, nutrient or salinity variations or can be anthropic such as the deposit of a hydrocarbon layer on the sediment that can quickly create an anoxic environment. Thus, their response to these perturbations must be described precisely in order to better represent the ecosystem response to environmental perturbations.

(1) "Empirism" is a late school in Greek medicine in which practice was based on the observation of symptoms keeping off any speculation on invisible causes that were only accessible by reasoning. At that time, people believed that the earth was a disc and the sun turned around it, deducing that the earth was the centre of the universe and humans were superior. Galilee put the solar system in evidence by a scientific approach.

1.1 Variable environments

We take an interest in variable environments because environments vary in reality. Indeed, even in "*in vitro*" experiments, the environment is not really constant depending on the considered scale. Different factors can have an impact on the considered ecosystem. The nature of the interactions is not always clearly determined and it can be difficult to judge the real effects. Since environments are complex, with lots of interactions between many variables, it cannot be always clearly decided when an environment is homogeneous and constant.

The fate of the organic matter is conditioned by: physical (particles, size distribution, erosion, and porosity), biological (sedimentary mixing by benthic organisms), biochemical (metabolism by microbial communities) and chemical processes in the environment, which all interact.

We will focus on the sedimentary column system. Among the biological processes, the mixing activity of macrobenthic organisms, known as the bioturbation process, is one of the major processes in the aquatic ecosystem functioning. The consumption, digging and movement activities of the macrobenthic fauna lead to significant sediment reworking and alter physical and chemical properties of lakes, rivers and oceans. Indeed, the bioturbation activity in the sedimentary column leads to different particles and solute fluxes.

Moreover, this macrobenthic fauna has a direct impact on the bacterial biomass distribution (Fig. 1.1, case of an upward - conveyor belt). It ensures (*i*) a « passive » vertical fall in the burrow of sediment and adsorbed bacteria; (*ii*) an « active » transport of sediment and adsorbed bacteria through the digestive tract; (*iii*) a transport of bacteria attached on the organism; (*iv*) the development of some bacterial populations on excretion products; (*v*) macrobenthic organisms produce nutrients that support and feed on some bacterial populations (the « gardening » effect).

Finally, the bioturbation activity leads to the formation of anaerobic micro niches in the aerobic sediment and the other way around (Fig. 1.2, the intake of reduced matter from the surface and of oxidised matter from the depth); these oxygenation modifications (spatial and temporal) affect bacterial metabolism and bring bacterial communities to a recomposition and a restructuration, modifying the organic matter degradation rates.

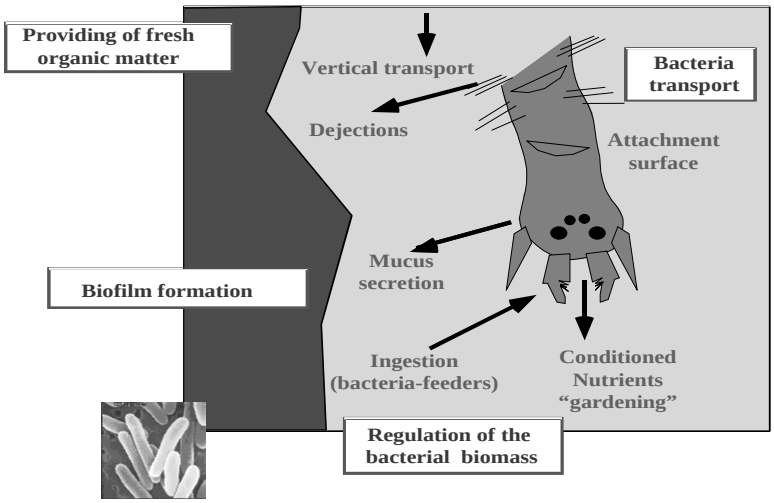

Fig. 1.1. The effect of bioturbation activity on bacterial biomass distribution.

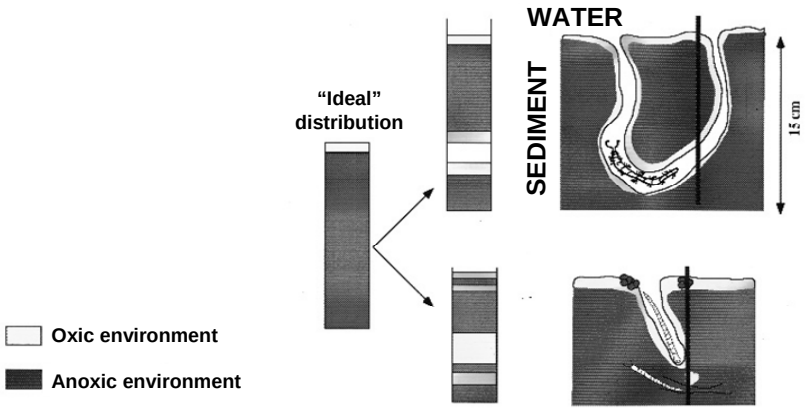

Fig. 1.2. In the sediment, the distribution of dissolved dioxygen is linked to the mixing activity of macrobenthic organisms.

Thus, macro fauna has a significant impact on bacterial communities: a direct effect on bacterial transport and an indirect effect on the formation of micro niches. Due to this complexity and to understand the environment changes, it is crucial to model the microbial communities dynamics that is responsible for biogeochemical processes.

1.2 Modelling bacterial dynamics

The individual is usually not the main study subject in population dynamic models; the different species are grouped in functional units. The choice of the temporal and spatial scale for the formulation is important. Each process and interaction has its own characteristic domain in the time-space scale. By changing the scale, some processes become more important while others negligible (Fig. 1.3).

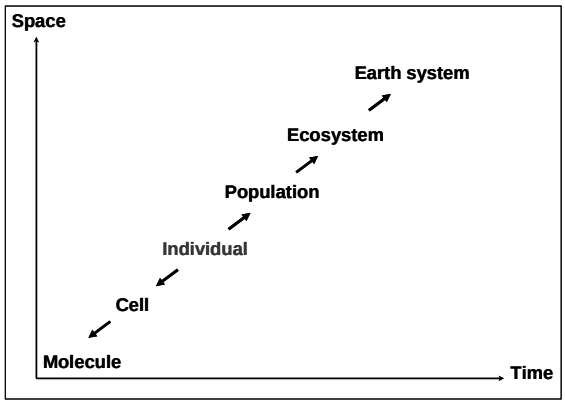

Fig. 1.3. The scales in space and time at which the different levels can successfully be modelled are interlinked. Dynamics Energy Budget theory starts at the individual, because mass and energy balances are most clear at this level, and evolution affects this level as primary target.

1.2.1 Classical models

At the moment, some classical models, formulated at the individual scale (as Monod, Marr-Pirt and Droop), enable to analyse and quantify the dynamics of bacterial communities. All of them assume first an absorption process of the substrate from the environment, which is described by a hyperbolic function, and then the use of this substrate for growth. They differ in the way the substrate is used. We can distinguish:

(*i*) The Monod model (Monod, 1942) considers a growth rate proportional to the absorption rate.

(*ii*) The Marr-Pirt model (Marr and Ingraham, 1962; Marr *et al.*, 1963; Pirt, 1965) introduces the maintenance notion, that is the continuous use of matter in order to satisfy the needs of the individual.

(*iii*) The Droop model (Droop, 1968) introduces the quota or reserve notion, stored matter which fuels growth. Thus there are two steps: assimilation then growth.

All of these model formulations are extensively presented in Chapter 3. However, since their formulation is simple, their assumptions are strong and differences in properties cannot always be translated in differences in population dynamics because of this simplicity. Indeed, they all assume a constant and homogeneous environment and they describe a system with only one limiting substrate by the use of the empirical hyperbolic function. Consequently, they offer a non-appropriate description of bacterial dynamics in case of perturbations in environmental conditions, such as those generated by macrobenthic organisms, or in case of multiple substrates.

1.2.2 The Dynamical Energy Budget (DEB) theory

The Dynamic Energy Budget theory (DEB, Kooijman, 1993) is formulated for individuals and quantifies the input and output fluxes of matter precisely, respecting the mass conservation law. In a general theoretic framework, it proposes a growth model for an individual based on mechanistic assumptions for the acquisition and the use of energy. Indeed, the DEB theory describes (Fig. 1.4) the way the individual assimilates substrates (S: food, light, nutrients) in the reserve compartment (E) and uses this stored energy, firstly for the maintenance and then for the growth process leading to the increase of structural biomass (V).

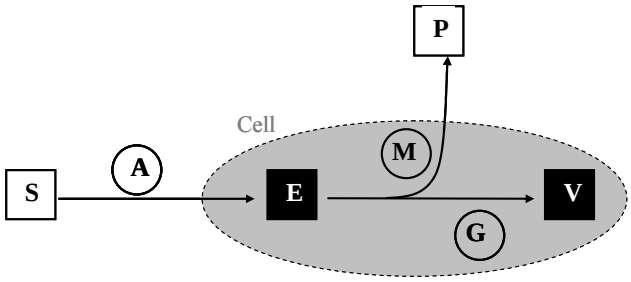

Fig. 1.4. Representative scheme of the key processes of the Dynamic Energy Budget theory applied to a bacterial cell - A: assimilation, G: growth, M: maintenance. S represents the substrate, V the structural mass, E the reserve and P the maintenance product. The total biomass is: $B = V + \varepsilon E$ where ε is the conversion coefficient of energy into mass. These processes are linked to respiration processes.

The uptake of substrates is based on fluxes of arriving substrates, not on substrate concentrations. The interest to work with fluxes is evident; it can capture photons and nutrients in one formulation and allows spatially heterogeneous environments. This theory was successfully applied to different organisms (microorganisms, Brandt, 2002; Evers, 1991b; insects, Péry *et al.*, 2002; flat fishes, van der Veer *et al.*, 2001; molluscs, van Haren and Kooijman, 1993). I took here a particular interest in the modelling of microorganisms.

Absorption/consumption

The organism extracts energy, electrons and building blocks (carbon, nitrogen, vitamins, etc.) from substrates by the absorption process. For unicellulars, substrates can be chemically simple (glucose) or complex (heptadecane), according to the species. For example, the chemio-organotrophic bacteria obtain their energy through oxydo-reduction reactions and their carbon from the organic compounds.

Assimilation

The intracellular storage of matter is realised through the assimilation process. Energy and building blocks are fixed in reserves (E: carbohydrates, triglycerides and lipids, RNA, proteins); if mobilised, it becomes available for metabolic use. During assimilation, a part of the absorbed matter is rejected in the environment as faeces and other products. The amount of stored matter depends on the nutritional conditions. Indeed, the assimilation rate is proportional to the absorption rate with a constant conversion coefficient defined as the assimilation yield. But, the use of reserve does not depend on substrate availability. The reserve notion allows growth to depend on the internal state of the cell and not directly on the external nutrient density. Furthermore, we define a reserve density ($e = E/V$, reserve per unit of structure) in order to deal with its dynamics. Indeed, reserves cannot be considered as concentrations as their dispersion is not homogeneous in the individual.

Maintenance

The cell needs to maintain itself to conserve its integrity and the gradients in concentrations of metabolites across the cellular membrane; this is well accepted in microbiology. Maintenance does not depend on the available material but is a necessity, depending on the amount of structural mass. This is predominant whatever the environmental conditions are. It is a collection of processes: biomass turnover, transport, movement and defence. But it excludes the net production (growth and the reproduction) as they have their own cost and dynamics. There is no maintenance for the reserves

therefore we talk about somatic maintenance. Garby and Larsen (1995) have shown that the efforts linked to the mechanical work can be neglected.

Growth

Once maintenance is realised, the growth of structural biomass (proteins, carbohydrates, lipids, DNA) can occur from the remaining mobilised reserves. It depends on the reserve density and on structural mass. The differentiation in mobile (reserve) and non-mobile (structural biomass) matter allows a changing composition of the whole individual, depending on the environmental state. Indeed, structural biomass and reserve don't change in their composition, but their relative amounts can change.

Other processes: maturation and reproduction

Maturation and reproduction (spore formation in some bacteria) are realised from reserves. Events in the cell cycle, such as the initiation of DNA duplication, are linked to the state of maturity. Then DNA duplication itself takes a fixed amount of time, followed by cell division. A cell divides itself by binary fission which can be considered to be fast. Furthermore, if the maturity and somatic maintenance costs relate to each other in a special way, the division takes place at a fixed structural mass. In the case of V1-morphs, which change in shape during growth such that their surface area is proportional to their volume, the individual and population levels coincide; it makes no difference if the population consists of many small or a few large individuals. The difference between these two levels is small for all organisms that divide into two for reasons given in Kooijman (2000, p118).

Respiration

The processes previously described, assimilation, maintenance and growth, all contribute to the respiration process, i.e. heat production or dioxygen consumption, or carbon dioxide production. For aerobic micro-organisms, dioxygen consumption is linked to a substantial decrease of reserves. The respiration rate increases with the reserve density and decreases during starvation. We will study the nitrogen cycle and all the biogeochemical processes that are involved.

The reserve dynamics and the specific growth rate for a microbial population (V1-morph model) are described in Appendix 1.A.

1.3 Enzymatic kinetics

We take an interest in the substrate interactions, which involves enzyme kinetics, in order to study the uptake of multiple substrates. The classical models described previously mostly use products of hyperbolic functions for the absorption, which is based on Michaelis-Menten kinetics (Eq. 1.1). Indeed, Leonor Michaelis and Maud Menten defined an expression corresponding to Fig. 1.5, which is at the root of absorption models, for the determination of the enzymatic reaction rate j_X of a limiting substrate X.

$$j_X = j_{Xm} \frac{X}{X + K_X} \tag{1.1}$$

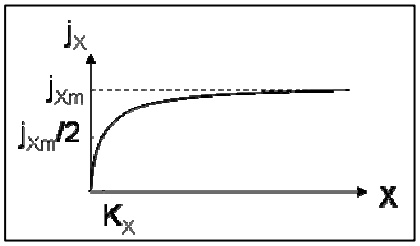

Fig.1.5. Michaelis-Menten kinetics - X is the substrate, j_X the enzymatic reaction rate, j_{Xm} the maximal reaction rate, K_X the half saturation constant.

All the variables and parameters are described in Appendix A, at the end of the manuscript.

1.3.1 Synthesizing Units (SU)

Compounds used by organisms for metabolism require enzymes for their chemical transformation. The synthesizing units (SUs) can be considered as a simple generalisation of the classical concept of enzyme (Kooijman, 1998). More specifically, SUs are generalised enzymes or complexes of enzymes which bind substrate molecules to synthesize molecules of product or a set of products. Compared to the classical kinetics of enzyme-mediated binding and dissociation, there is one simplification and one generalisation. The generalisation is that product fluxes are linked to arriving substrate fluxes, not to substrate concentrations. In spatially homogeneous environments the arriving flux can be taken proportionally to the concentration using a diffusion/advection argument; however more complex relationships are also possible. The simplification is that the back dissociation rate (the enzyme reversibility in their reaction), without any transformation, is supposed to occur at a negligible rate.

To simplify the dynamics, DEB theory uses time scale separation for the processes at molecular and individual scale. To this end, it considers changes in fractions of SUs that are in the various binding states, and expresses processes at the individual level as function of these fractions at steady state. Considering fractions instead of numbers is a good simplification. Firstly, as a substrate molecule will be used by only one enzyme molecule, the number of enzyme molecules doesn't necessarily increase the velocity of the reaction. Enzyme molecules can compete for substrate in an arriving flux of substrate molecules; spatial organization matters here. Secondly, if we take the number of enzyme molecules into account, we must describe precisely the formation and disappearance processes of enzymes in order to respect the mass conservation law but also the interaction processes (as the competition for substrate). This can complicate the model formulation.

The fraction of SUs in the different binding states is indicated by θ_{**} for binding state **, so that:

$$\sum \theta_{**} = 1$$

In a supply system (i.e. a system that depends on the availability of material), the change in the fractions of bound SUs can be written as linear ordinary differential equations as: $d\theta / dt = A\theta$ where θ is the vector of the fractions in the different binding states of the SU and A the matrix of kinetic velocities. In this case, the kinetic velocities fulfil the following constraints whatever the environmental conditions are:

$$a_{ii} = -\sum_{j \neq i} a_{ij} \text{ and } 1^T A = 0^T$$

where 1^T is the transposed vector filled with the value one.

We will see later than in the other case, in demand systems (i.e. systems that are controlled by production), contrary to supply systems, the change in fractions is no longer linear, and the constraints no longer apply.

The concept of SUs can further be generalised and represent states of an entity, several compartments, and not necessarily a generalised enzyme in a biogeochemical process. The link between the different states, mostly represented by arrows in this manuscript, corresponds to the transformation conditions, from one state to another one, defining the interactions within any system.

1.3.2 Substrate interactions

Brandt (2002) depicted the way substrates are subjected to transformation (Fig. 1.6). We can define 4 modes of transformation of two substrates *S* and *X* into product *C* according to the relative role of substrates in product formation and to their interaction during processing.

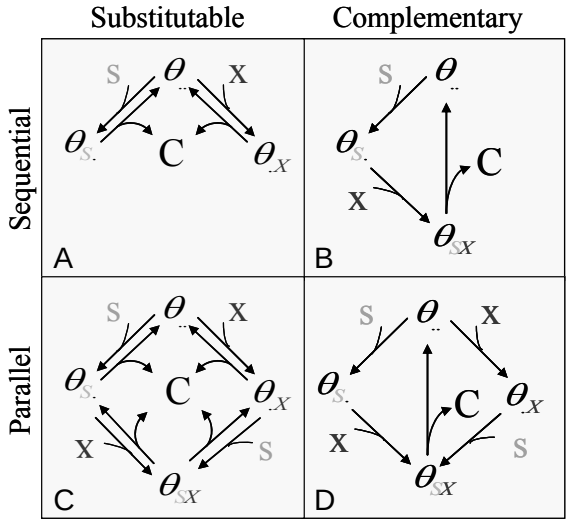

Fig. 1.6. Transformation modes of two substrates *S* and *X* into products *C* (Brandt, 2002). θ_{**} is the fraction of Synthesizing Units in a particular binding state. Substrates can be either substitutable or complementary. Bindings can be either sequential or parallel.

Substrates can be:

(*i*) either substitutable, meaning that substrates can independently be transformed in *C* products. For two substrates *A* and *B*, we have:

$$y_{AC}\ A \rightarrow C \quad \text{and} \quad y_{BC}\ B \rightarrow C$$

(*ii*) or complementary, meaning that the process requires several substrates simultaneously, in fixed relative amounts to synthesize the final product. The lack of one substrate prevents the consumption of the other. For two substrates *A* and *B*, we have:

$$y_{AC}\ A + y_{BC}\ B \rightarrow C$$

Moreover, the binding process can be either: (*i*) parallel meaning that the substrates do not interfere with each other in the binding process; or (*ii*)

sequential meaning that the different substrates interfere in the binding process. Indeed, they can be in competition or in inhibition. The Fig. 1.6 represents the competition interaction.

The inhibition process can control the transformation at three levels: (*i*) the accessibility of initial substrate – to achieve an enzymatic reaction, the substrate has to be accessible for the enzyme and thus to penetrate in the cellular compartment where the reaction occurs; (*ii*) the enzyme activity (the retroactive inhibition) – when the product of the transformation is accumulated. This can inhibit the enzyme which controls the first reaction, changing its form, and thus blocks the transformation; (*iii*) the synthesis of enzymes that catalyse the transformation.

1.3.3 Particular case: the organic matter degradation in the nitrogen cycle

In this manuscript, we will study only bacterial chemo-organo-heterotrophs: organisms that obtain their energy from oxidation of organic compounds. Many organic molecules are potential substrates for the microbial growth and the number of reactions is huge. Nitrogen is the most important element of living organisms after oxygen, hydrogen and carbon and it mostly limits the primary productivity rate in most ecosystems. Thus, we will focus on the main processes taking place in the nitrogen cycle in the marine sediments: mineralization of organic matter (OM) (Eq. 1.2 for oxic and Eq. 1.3 for anoxic), nitrification (Eq. 1.4) and denitrification (Eq. 1.5).

$$OM + O_2 \xrightarrow{k_{MinOx}} P_{MinOx} + NH_3 + CO_2 + H_2O \tag{1.2}$$

$$OM + \text{An Oxidant} \xrightarrow{k_{MinAnox}} P_{MinAnox} + NH_3 + CO_2 + H_2O \tag{1.3}$$

$$NH_3 + 2O_2 \xrightarrow{k_{Nit}} HNO_3 + H_2O \tag{1.4}$$

$$OM + HNO_3 \xrightarrow{k_{Denit}} P_{Denit} + NH_3 + CO_2 + N_2 + H_2O \tag{1.5}$$

where $P_{Process}$ is the product of the considered biogeochemical process and an oxidant can be methane, sulphate, etc.

Bacteria can use the different electron acceptors of the nitrogen cycle for the functioning of its respiratory chain. I will consider the competition between the different electron acceptors. For the OM degradation, the most energetically favourable is the oxic mineralization (O_2), then the denitrification (NO_3) and finally the anoxic mineralization (an oxidant). But,

all these respiration processes have also regulation rules, depending on the environmental conditions.

The oxic mineralization (Eq. 1.2) reduces the organic matter (OM) to ammonium using dioxygen. The nitrification (Eq. 1.4) is principally an aerobic microbial process where reduced nitrogen compounds (ammonia) are oxidized to nitrate with a consumption of dioxygen. The denitrification (Eq. 1.5, Gayon and Dupetit, 1882) is an important step in the nitrogen cycle. This anaerobic respiration process is generally defined as the dissimilative reduction of nitrate to the dinitrogen (N_2). It is realised by a whole range of enzymes. Dioxygen inhibits these enzymes with different sensitivity. Thus, depending on the dioxygen concentration, we will obtain a different final product of the denitrification. The anoxic mineralization (Eq. 1.3) is an anaerobic process (inhibited by dioxygen) which allows the transformation of OM in ammonium through an oxidant. It is inhibited by dioxygen and nitrate at the enzyme activity level.

1.4 Thesis outline

This work aims to improve present models analysing the bacterial dynamics by considering a mechanistic approach in order to study variable environments. This approach consists of describing the bacterial compartment at the enzymatic level, the interactions between different substrates and the relation between substrates and the considered community. Among others, the mechanistic approach allows a reuse of the parameter values. For example, if the composition of one species is known and the studied species has similar properties from a biological point of view, we could assume that its composition is identical to the first one. This will lead:

(*i*) for degradation aspects, to the study of interactions between processes playing a preponderant role in the nitrogen cycle; for example, to determine the use of nitrate as function of the oxygenation conditions or to assess the role of the oxygenation oscillations on some biogeochemical processes. This model will help to quantify the velocity of organic matter degradation in variable conditions.

(*ii*) for bacterial aspects, to determine the physiological state of bacteria in the different environmental conditions.

For this, we have (*i*) to put assumptions on the role of each process and their interactions, (*ii*) to quantify them, (*iii*) to determine non measurable parameters, (*iv*) to interpret experimental results and (*v*) to verify the original assumptions.

This thesis improves the models analysing the organic matter degradation in the sedimentary column (based on the early diagenesis equation of Berner (1980)) by taking the bacterial dynamics into account. Chapter 2 shows the importance of bacterial dynamics using simulations. This work refers to a paper published in *Acta Biotheoretica* (Talin *et al.*, 2003) as described in Appendix B at the end of the manuscript.

Then, it compares and improves the present models for bacterial dynamics by accounting for their functionality. For this, we have constructed a mechanistic model for the dynamics of bacterial communities in sediments, developed from the DEB theory (Kooijman, 2000). This new formulation is tested against experimental data. Chapter 3 makes a comparative analysis of classical microbial populations models, with an application to a set of data (Bonin *et al.*, 1992).

Chapter 4 presents an improvement of the DEB theory (see Appendix 1.A for the problems of the DEB theory) by giving a new description of adaptation in case of nutrients limitation: the shrinking process (Appendix 1.B). Structure will be used only when reserve is not enough. This leads to an inhibition formulation for maintenance which is controlled by product formation (demand system). This work is submitted to *Journal of Theoretical Biology* (Tolla *et al.*, Submitted) as presented in Appendix C at the end of the manuscript. We compare the new formulation with existing ones (Unilateral Binding Inhibition = UBI; Brandt, 2002; Kuijper, 2004, p35) and some simplified forms (Appendix 4.D).

Finally, Chapter 5 analyses the effect of bioturbation on the nitrogen cycle. In this case, we assume that the principal effect of macrobenthic activities on microbial communities is changing the environmental oxygenation (RedOx oscillations). We applied here the new inhibition formulation developed in Chapter 4 on a supply system corresponding to biogeochemical processes: inhibition of a biogeochemical process of the nitrogen cycle by the presence of an inhibitory compound (as dioxygen for anaerobic processes).

Work that has not been included in this thesis and has been submitted to *Canadian Journal of Fisheries Aquatic Sciences* (Appendix D at the end of the manuscript) simulates the influence of tubificids (*Tubifex* and *Limnodrilus*) on O_2 concentrations in hyporheic sediments. The model took the hydrodynamic properties into account, the microbial respiration, and the paper stimulated effects of tubificids on microbial activity in the system. This study leads to a lot of problems, however, because of its assumptions. First, the bacterial composition is fixed and the populations are supposed to grow exponentially, thus it doesn't vary with the presence of tubificids. Then, the

dioxygen concentration depends significantly on the interaction between tubificids and bacterial communities, and the tubificids distribution has an important impact on the biogeochemical functioning of the sediment. However, the interaction between *Tubifex* and bacteria is not well described. Indeed, the model is empirical and takes the different interactions into account in a comprehensive way. Thus in case of environmental perturbations, the model will not explain the change in the ecosystem correctly. These observations allow to identify the next steps in sediment research.

Appendix 1.A. The reserve dynamics – construction of the specific growth rate in the DEB model.

We treat bacterial cells as V1-morphs, i.e. individuals that change in shape during growth such that their surface area is proportional to their volume. This has as consequence that the dynamics of a population, i.e. a set of individuals, has a very simple relationship with changes of individuals. The change in the total amounts of structure and reserve is the sum of the change of the individual amounts. We have the following balance equation for reserve dynamics:

$$\frac{d}{dt}E = J_E^A - J_E^C \text{ with } J_E^C = J_E^G + J_E^M \qquad (1.A.1)$$

where
- J_E^A : the absolute reserve flux allocated to assimilation
- J_E^C : the absolute catabolic flux of reserve i.e. the reserve turnover
- J_E^G : the absolute reserve flux allocated to growth
- J_E^M : the absolute reserve flux allocated to maintenance

Appendix A at the end of the manuscript gives more variables and parameters description.

Assumption 1: strong homeostasis

The DEB theory assumes a constant composition for the reserve (E) and the structure (V) but a variable ratio between both generalised compounds, thus biomass composition can vary; biomass is a weighted sum of structure and reserve ($B = V + \varepsilon E$ with ε a constant)

With the reserve density $e = E/V$ and from Eq. 1.A.1, we obtain the following equality:

$$\frac{d}{dt}E = \frac{d}{dt}(eV) = V\frac{de}{dt} + e\frac{dV}{dt} \quad \Leftrightarrow \quad \frac{de}{dt} = \frac{1}{V}\frac{d}{dt}E - \frac{e}{V}\frac{dV}{dt} \tag{1.A.2}$$

Only the growth process has an impact on the amount of the structure of the individual:

$$\frac{dV}{dt} = rV \Rightarrow \frac{dV}{dt}\Big/V = r \tag{1.A.3}$$

where r is the specific growth rate.

The absolute flux J_*^{Π} of the substrate * allocated to the process Π is linked to the specific flux (by unit of structure) by $J_*^{\Pi} = j_*^{\Pi}V$. By replacing Eqs. 1.A.1 and 1.A.3 in Eq. 1.A.2, we obtain:

$$\frac{de}{dt} = j_E^A - j_E^C - re \text{ with } j_E^C = j_E^G + j_E^M \tag{1.A.4}$$

The specific catabolic flux (Eq. 1.A.4) is determined by some restrictions on the reserve density dynamics.

Assumption 2: weak homeostasis

If substrate density in the environment is constant, the reserve density becomes constant, even if the total biomass is changing: a small and a big population will have the same reserve density.

Thus, the Eq. 1.A.4 becomes:

$$\frac{d}{dt}e = j_E^A - f(?)$$

where *f(?)* is the unknown function of the reserve density, independent on the structural volume. Moreover, *f(?)* does not depend directly on the absorption/ assimilation process as the reserve use only depends on the individual states, given by the reserve and the structure.

Assumption 3: reserve partitionability

The DEB theory assumes that any particular compound in a single reserve system follows the same dynamics (Fig. 1.A.1). The catabolic flux, i.e. the flux that is mobilised from the reserve, depends on the amounts of reserve and structure. Multiplying this flux by an arbitrary factor has the same effect as multiplying the reserve with that factor. This condition is required to reduce the number of reserves smoothly, as has occurred in evolution (Kooijman *et al.*, 2003).

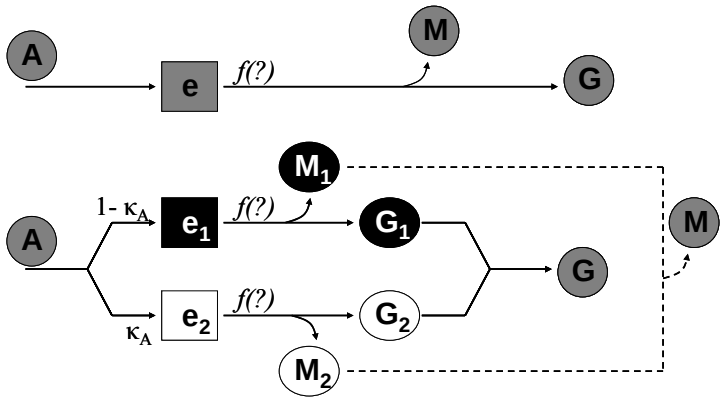

Fig. 1.A.1. The reserve partitionability assumption in the DEB theory where maintenance is realised only from reserve. A: assimilation, M: maintenance, G: growth and e: reserve density. κ_A is an arbitrary fraction of assimilation. *f(?)* is the unknown function of the reserve density dynamics.

So f must be homogeneous in the first degree in e such as $\alpha f(e|\theta) = f(\alpha e|\theta)$ with θ a set of parameters. Furthermore, from the weak homeostasis assumption, at substrate steady state, the reserve density is constant.

$$\frac{d}{dt}e = 0 \quad \Rightarrow \quad j_E^A - \theta e = 0 \quad \Rightarrow \quad \theta = j_E^A / e$$

The assimilation flux is maximal (j_{AEm}), if the substrate density is high. Reserve density is maximal (e_m) if assimilation flux is maximal.

$$\theta = j_{AEm} / e_m$$

θ corresponds to the reserve turnover rate h_E. We have thus:

$$\frac{de}{dt} = j_E^A - j_E^C - re = j_E^A - h_E e \text{ with } j_E^C = j_E^G + j_E^M \qquad (1.A.5)$$

Assumption 4: maintenance has priority over growth Mobilised reserve is first used for maintenance; the rest is used for growth.

As reserve and structure are conditioned by the strong homeostasis assumption, the structure production becomes proportional to the flux that is allocated to growth:

$$j_V^G = y_{VE} j_E^G \qquad (1.A.6)$$

where y_{EV} is the yield coefficient that is assumed to be constant.

The specific maintenance costs are assumed to be constant. The first case, developed by Kooijman (2000), is when maintenance is realised only from reserve:

$$r = j_V^G \text{ and } j_E^M = y_{EP} k_M \tag{1.A.7}$$

where k_M is known (since Pirt, 1965) as the maintenance rate coefficient and y_{EP} a yield coefficient.

By replacing Eqs. 1.A.6 and 1.A.7 in Eq. 1.A.5, we obtain the following specific growth rate (Kooijman, 2000):

$$r = j_V^G = \frac{h_E e - y_{EP} k_M}{y_{EV} + e} \tag{1.A.8}$$

From the previous assumptions (Eqs. 1.A.5 to 1.A.7), we have:

$$\frac{d}{dt} E = J_E^A - J_E^C = J_E^A - y_{EP} k_M V - y_{EV} r V$$

This formulation leads to a flux of matter back to reserve, when the specific growth rate becomes negative, so that it can only be used as long as growth is positive. This formulation also has a thermodynamic problem: the maintenance costs from reserve and from structure are identical, while payment via structure has an extra step in synthesis.

Appendix 1.B. the specific growth rate improved by accounting for the shrinking process.

If $e < k_M / h_E$, the specific growth rate becomes negative and structure starts to shrink. Formally this should involve a second maintenance parameter, namely the amount of structure that is required for maintenance. To improve the DEB theory and adapt it to starvation conditions we propose in Chapter 4 another specific growth rate with the condition that maintenance is realised from reserve in favourable conditions and from structure in starvation conditions. The specific growth rate is thus:

$$r = j_V^G - j_V^M \text{ where } y_{PE} j_E^M + y_{PV} j_V^M = k_M \qquad (1.B.1)$$

where j_V^G and j_V^M are respectively the specific flux associated to the growth and the maintenance processes and y_{PE} and y_{PV} the yield coefficients in the maintenance process.

By replacing Eqs. 1.A.6 and 1.B.1 in Eq. 1.A.5, we obtain:

$$j_V^G = \frac{h_E e - j_E^M}{y_{EV} + e} + j_V^M \frac{e}{y_{EV} + e} \text{ thus } r = \frac{h_E e - j_E^M}{y_{EV} + e} - \frac{y_{EV}}{y_{EV} + e} j_V^M \qquad (1.B.2)$$

The reserve and structure fluxes allocated to maintenance are described in Chapter 4.

In this case, there is no back of matter in reserve when the specific growth rate becomes negative (assumptions Eqs. 1.A.5, 1.A.6, 1.B.1, 1.B.2):

$$\frac{d}{dt} E = J_E^A - J_E^C = J_E^A - \frac{\left(y_{EV} h_E + j_E^M + y_{EV} j_V^M \right)}{y_{EV} + e} eV$$

2

Relations between bacterial biomass and carbon cycle in marine sediments: an early diagenetic model.

Abstract

A new model for early diagenetic processes has been developed that explicitly accounts for microbial population dynamics. Following a mechanistic approach based on enzymatic reactions, a new model has been proposed for oxic mineralization and denitrification. It incorporates the dynamics of bacterial metabolism. We find a general formulation for inhibition processes for which some of other mathematical relations are particular cases. Moreover a fast numerical algorithm has been developed. It allows us to perform simulations of different diagenetic models in non steady states. We use this algorithm to compare our model to a classical one (Soetaert *et al.*, 1996). Dynamic responses on a perturbation of the particulate organic carbon (POC) input are studied for both models. The results are very similar for stationary cases, but with variable inputs, the model that accounts for bacterial biomass dynamics shows noticeable differences, which are discussed.

Keywords: simulation - bacterial dynamics - biogeochemical processes.

2.1 Introduction

Different physical, chemical and biological processes modify the organic matter that is deposited on the sediments. Those acting up to thousand years are called early diagenetic processes. Any estimation of the fluxes of organic matter in the ocean is based on the quantification of the early diagenetic processes. Indeed, when deposited on the sediment, the organic matter can be trapped definitely in the sediment in some cases and its degradation speed depends on the processes involved.

Among the diagenetic processes, the present paper focuses mainly on the modelling of the microbiological ones. In the sediment column, there are some oxic microniches in the anoxic layer. Bacteria degrade the organic matter via a different metabolism that depends on the physical and chemical sediment properties. The rupture of the dioxygen gradient has thus a direct effect on the processes used by bacteria to alter the organic matter, by inducing RedOx oscillations, which in turn will change the total degradation rate. As a consequence, the quantification of these processes and their interactions provides a better understanding of the dynamics of the different chemical compounds in the sediments.

We aim to analyse the dynamics of diagenetic processes in the sediment that is submitted to perturbations. These perturbations may be either natural (phytoplanktonic bloom) or the result of human activities (oil spill). It is the reason why we take the biological compartments into account explicitly since any perturbation should modify living communities, which in turn have different responses in their function with respect to their environment. In this paper:

We present a mechanistic diagenetic model where the formulation of biological processes is based on bacterial metabolism, which involves enzymatic processes. In order to keep the model at the ecosystem level a rather simple, we use quasi-steady state assumptions for the enzymatic processes.

We propose an advanced numerical program (in FORTRAN 90) to perform simulations; this program allows us to make simulations of the diagenetic system of a few months in a few minutes; this implies that we can study the impact of different perturbation scenarios (in non-steady states).

These points provide the basis of the theoretical background for the study of perturbations of the benthic environment. We here only deal with two processes: oxic mineralization and denitrification. This choice is based on the two following reasons: (*i*) we need at least two different electrons acceptors

to analyse the interaction of two types of bacterial metabolism, (*ii*) we want to work with the simplest model and oxic mineralization in combination with denitrification are the main processes at the short time scale (few months) in the first centimetres of sediment. Nitrification is a process that is associated to oxic mineralization and consequently, an extra term is added to describe the effect of nitrification on the amount of nitrate.

In the following section, we recall some generalities about usual diagenetic models in order to explain where our approach is different and why it can be useful. The third section concerns the description of our new model. The fourth section is devoted to the numerical scheme. Finally, we compare two models (with and without bacterial biomass dynamics) and discuss the results.

2.2 Diagenetic models

Early diagenetic models (Berner, 1980; Boudreau, 1996; Boudreau, 1997; Soetaert *et al.*, 1996) provide the quantification of fluxes and reaction rates based on measured profiles in different sediments. Usually based on the Berner's diagenetic equation (1980), they are the most frequently employed models for the benthic system. This equation is applied to dissolved as well as solid chemical species, and is a partial differential equation (PDE) incorporating physical transport processes and biogeochemical reactions. Its mathematical formulation appears under the following general shape:

$$\frac{\partial C}{\partial t} = D\frac{\partial^2 C}{\partial z^2} - W\frac{\partial C}{\partial z} - \Sigma R \qquad (2.1)$$

Time variation = Diffusion + Advection + Reaction;

with C the tracer concentration, D the diffusion coefficient, W the advection velocity and ΣR the biogeochemical reactions rates.

- Diffusion process allows local transport of matter from one point to another one with random motion (Crank, 1976). The diffusion coefficient includes biodiffusion, bioirrigation and molecular diffusion effects.
- Advection is an environmental bulk transport with the velocity W; it is the expression of different physical processes like (*i*) burial linked with particles sedimentation at the sediment interface (W is the sedimentation velocity) (Aller and De Master, 1984; Benninger *et al.*, 1979; Fisher *et al.*, 1980; Goldberg and Koide, 1962; Guinasso and Schink, 1975), (*ii*) compaction which corresponds to a reduction of sediment volume under the action of overlying sedimentary column weights (W is then the

particle or interstitial water movement resulting of this phenomenon) (Berner, 1980; Boudreau, 1997), (*iii*) advection phenomena linked to benthic organisms activity like the one gathered in "non-local" transport of "conveyor-belt" organisms (Boudreau, 1997; Fisher *et al.*, 1980; Rice *et al.*, 1986; Robbins, 1986).

- The reaction terms *R* describe (*i*) the kinetics of the different compounds (organic matter, dioxygen, nitrate, manganese, etc.) via biochemical reactions, (*ii*) the sinks and sources of "non-local" transport model as sediment ingestion by conveyor-belt organisms or as irrigation (Boudreau, 1997).

Berner's equation is the basis of more complex and more realistic models. For instance, Soetaert *et al*. (1996) proposes a model with two types of organic matter (with different labilities) which are subjected to transport (diffusive and advective) and biochemical reactions (oxic mineralization, denitrification, etc.). This model is applied to different types of marine sediments, such as deep and coastal environments. In this kind of model, attention is paid to the sequence of different biochemical reactions in the sediment according to a gradient of decreasing dioxygen concentration with respect to depth.

However, in many papers, the impact of microbial organisms is not sufficiently taken into account. More precisely, only few models investigate the relations between bacterial biomass and organic carbon in biogeochemical models (in the column water: Anderson and Williams, 1999; in the sediments: Boudreau, 1999). Generally, the models do not explicitly take into account the dynamics of bacterial community. The assumption of steady state for bacterial populations densities is implicitly made, which supposes that bacteria are always present. It leads to relative simple biochemical terms in the models, which is very useful according to the complexity induced by the large number of involved processes.

Classically, the biochemical processes have the following form (Boudreau, 1996; Rabouille and Gaillard, 1991; Soetaert *et al.*, 1996):

$$OxMin = \frac{R_{\text{minox}} O_2 C}{K_{\text{minox},s} + O_2} \quad \text{for oxic mineralization} \tag{2.2}$$

$$Denit_S = \frac{R_{\text{denit}} NO_3 C}{K_{\text{denit},s} + NO_3} \left(1 - \frac{O_2}{O_2 + K_{\text{inhib,denit}}} \right) \quad \text{for denitrification} \tag{2.3}$$

with $\begin{cases} R_{\text{denit}}, R_{\text{minox}} & \text{: Maximum degradation rate for organic carbon} \\ K_{\text{denit},s} & \text{: Half-Saturation Constant (HSC) for nitrate limitation in denitrification} \\ K_{\text{minox},s} & \text{: HSC for oxygen limitation in oxic mineralization} \\ K_{\text{inhib,denit}} & \text{: HSC for oxygen inhibition in denitrification} \end{cases}$

The inhibition of denitrification induced by dioxygen is described by means of a decreasing function with respect to the dioxygen concentration. This function is based on empirical arguments which formulation depends on the authors. For instance, Rabouille *et al.* (2001) has drawn up denitrification process on the following way:

$$Denit_R = \frac{R_{\max}^{NO_3} NO_3 C}{K_{m\,NO_3} + NO_3} \exp\left[-\left(\frac{O_2}{K_{m\,O_2}} \right)^2 \right] \tag{2.4}$$

with $\begin{cases} R_{\max}^{NO_3} & \text{: Maximum oxidation rate of the organic mater by NO3} \\ K_{m\,O_2} & \text{: Monod constant for oxygen diminution} \\ K_{m\,NO_3} & \text{: Monod constant for nitrate consumption} \end{cases}$

These examples show that the biochemical part is usually based on Michaelis-Menten kinetics, possibly associated to an inhibition factor in case of competition between different electrons acceptors. For both denitrification process formulations, $Denit_S$ and $Denit_R$, it can be noted that the inhibition term is large when the dioxygen concentration increases, keeping the denitrification rate low.

The stationary state assumption for bacterial biomass leads to some theoretical limitations. Natural (phytoplanktonic bloom) or anthropic (hydrocarbon layer) perturbations of the environment will cause disturbances in living communities governing diagenetic processes; dynamical mineralization will be modified in return. Moreover, some bioturbation processes (Boudreau, 1986) lead to the creation of aerobic microniches in the anaerobic sediment (Fenchel, 1996). These oxygenation modifications lead to a transfer between RedOx area, a re-oxidation process and RedOx oscillations increase, inducing a recombination of bacterial communities and thus a modification of bacterial metabolism. Modelling microbial dynamics in relation with bioturbation is then important to understand the environment evolution.

2.3 Microbial activity modelling

2.3.1 Degradation rates

We here propose a new mathematical model for the sedimentary diagenetic processes, based on Berner's diagenetic equation (1980). Our formulation incorporates physical processes and biogeochemical reactions realised by bacteria. It takes bacterial dynamics into account explicitly. We will describe differences between a classical model composed of biogeochemical reactions developed by Soetaert *et al*. (1996) and our new model. This comparison will be made in the section on numerical results.

Our interest concerns the vertical distribution of dissolved dioxygen, solid organic carbon (POC), dissolved nitrate and bacterial biomass in the first centimetres of sediment column. The reaction terms of our model are obtained from enzymatic mechanisms of oxic mineralization and denitrification chemical reactions.

Concerning the nitrification process, we only deal with the nitrification that is associated with oxic mineralization, resulting from the transformation of produced ammonium to nitrate. For the sake of simplicity, we have decided to avoid inserting the extra variable corresponding to the concentration of ammonium. Indeed, it supposes a complete and instantaneous transformation of ammonium produced by oxic mineralization. Thus, in order to remain rather close to the real set of processes, we took the nitrification kinetics proportional to mineralization. The proportionality coefficient is denoted γ_N and we will explain this part more precisely later on.

The way we use to build the oxic mineralization rate is a common way in biochemistry, but it is rarely applied in biogeochemistry. Since we use the same way for building the denitrification rate, we recall the method here.

The chemical reaction associated to oxic mineralization can be described schematically by:

$$C_{org} + O_2 + \theta_{\cdot} \xrightarrow[k]{} C\theta_O \xrightarrow[k']{} C_{min} + P_1 + \theta_{\cdot} \tag{2.5}$$

Organic carbon C_{org} can be transformed into mineral carbon C_{min}. Available enzymes can belong to two states free or used. The fraction of free enzymes is denoted $\theta_{\cdot}$ and the fraction of enzymes bound to a dioxygen molecule is denoted θ_O. A temporary enzymatic complex $C\theta_O$ is formed during the reaction. P_1 symbolises the reduced oxic mineralization products

released by enzymes at the end of degradation sequence. k and k' are the reactivity rates.

The dioxygen kinetics, which gives the oxic mineralization rate, is given by:

$$\frac{dO_2}{dt} = -kO_2 C\theta_{\cdot} \tag{2.6}$$

according to the Mass Action Law. The equation of temporal evolution for $\theta_{\cdot}$ resulting of Eq. 2.6 can be written as:

$$\frac{d\theta_{\cdot}}{dt} = -kO_2 C\theta_{\cdot} + k'C\theta_O \tag{2.7}$$

Let $\Theta = \theta_{\cdot} + \theta_O$, Eq. 2.7 becomes:

$$\frac{d\theta_{\cdot}}{dt} = -kO_2 C\theta_{\cdot} + k'C\left(\Theta - \theta_O\right) \tag{2.8}$$

Given difference in the time scale between enzymatic processes and biogeochemical processes, we can assume that the total number of enzyme is constant at the short time scale. It means that, at the geochemical time scale, $d\theta_{\cdot} / dt = 0$ (Quasi Steady State assumption), and thus:

$$\theta_{\cdot}^{*} = \frac{k'\Theta}{k' + kO_2} \tag{2.9}$$

where θ^{*} is the SU at steady state. Entering Eq. 2.9 in Eq. 2.6, we find:

$$\frac{dO_2}{dt} = -\frac{k'\Theta kO_2}{k' + kO_2} C = -\frac{k'\Theta O_2}{\frac{k'}{k} + O_2} C = -\frac{R_{\text{minox}} O_2}{K_{\text{minox},s} + O_2} C \tag{2.10}$$

It is the classical form of Michaelis model of the Eq. 2.2 with $R_{\text{minox}} = k$' Θ and $K_{\text{minox,s}} = k$' / k.

As for the oxic mineralization, we now consider the enzymatic reaction for denitrification process. In this case, enzymes react preferentially with dioxygen. A system of two reactions is needed to describe the complete enzymatic reaction of the organic carbon degradation:

$$C_{org} + NO_3 + \theta_{\cdot} \xrightarrow[k_1]{} C\theta_{NO} \xrightarrow[k_1']{} C_{min} + P_2 + \theta_{\cdot} \tag{2.11}$$

$$C\theta_{NO} + O_2 \xrightarrow[k_2]{} NO_3 + C_{org} + \theta_{\cdot} + O_2 \tag{2.12}$$

This set of reactions could be described by the following system of differential equations:

$$\frac{dNO_3}{dt} = -k_1\, NO_3\, C\, \theta_{\cdot} + k_2\, C\, O_2\, \theta_{NO} \tag{2.13}$$

$$\frac{d\theta_{\cdot}}{dt} = -k_1\, NO_3\, C\, \theta_{\cdot} + k_1'\, C\, \theta_{NO} + k_2\, C\, \theta_{NO} O_2 \tag{2.14}$$

Assuming a constant total concentration of enzymes $\Theta = \theta_{\cdot} + \theta_{NO}$ at the short time scale (Quasi Steady State Assumption) the stationary state of Eq. 2.14 is given by:

$$\theta_{\cdot}^{*} = \Theta \frac{k_1' + k_2\ O_2}{k_1\ NO_3\ + k_1' + k_2\ O_2} \tag{2.15}$$

Entering this result in Eq. 2.13:

$$\begin{aligned}\frac{dNO_3}{dt} &= -k_1\, NO_3\, C\, \Theta \frac{k_1' + k_2\ O_2}{k_1\ NO_3\ + k_1' + k_2\ O_2} + k_2\, C\, O_2 \Theta \left(1 - \frac{k_1' + k_2\ O_2}{k_1\ NO_3\ + k_1' + k_2\ O_2}\right) \\ &= C\,\Theta\left(-k_1\, NO_3 \frac{k_1' + k_2\ O_2}{k_1\ NO_3\ + k_1' + k_2\ O_2} + k_2\ O_2 \frac{k_1\ NO_3}{k_1\ NO_3\ + k_1' + k_2\ O_2}\right) \\ &= C\,\Theta k_1\ NO_3 \frac{-k_1'}{k_1\ NO_3\ + k_1' + k_2\ O_2}\end{aligned} \tag{2.16}$$

The inhibition role of dioxygen can be seen in the denominator. To compare this result to Soetaert *et al.* (1996) (Eq. 2.3) – a classical Michaelian form with an inhibition factor – Eq. 2.16 can be written as:

$$\begin{aligned}\frac{dNO_3}{dt} &= -C\Theta \frac{k_1' NO_3}{\frac{k_1'}{k_1} + NO_3} \left(1 - \frac{O_2}{\frac{k_1}{k_2} NO_3 + \frac{k_1'}{k_2} + O_2}\right) \\ &= -C \frac{R_{\text{denit}}\, NO_3}{K_{\text{denit},s} + NO_3} \left(1 - \frac{O_2}{K_{\text{inhib,denit}} + O_2}\right)\end{aligned} \tag{2.17}$$

$K_{\text{inhib,denit}}$ is no more a constant but a linear function of NO_3.

$$K_{\text{inhib,denit}} = \frac{k_1}{k_2} NO_3 + \frac{k_1'}{k_2} \text{ and } \begin{cases} R_{\text{denit}} = k_1' \Theta \\ K_{\text{denit},s} = \dfrac{k_1'}{k_1} \end{cases} \tag{2.18}$$

In conclusion, we find a denitrification rate that is rather close to that used by Soetaert *et al*. (1996) in which the inhibition 'constant' is no longer constant but is nitrate dependent. This method provides a mechanistic basis for the denitrification rate used in our biogeochemical model and for the role of biota in the diagenetic processes.

2.3.2 Bacterial Biomass

We add a variable for the bacterial biomass, which should be related to the amount of available enzymes Θ. For the sake of simplicity, we here assume that the total amount of available enzymes is proportional to bacterial biomass *B*:

$$\Theta = EB \tag{2.19}$$

Indeed a good description of the bacterial growth rate should use an energy budget model to get a relationship between metabolic activities and bacterial population growth (Kooijman, 1993). This is the topic of future work. We here assume a logistic growth of the bacterial population, with the intrinsic growth rate and the carrying capacity being functions of substrates (carbon, dioxygen and nitrate). Indeed, we assume that the intrinsic growth rate is proportional to consumed substrate: the more bacteria are active, the more they duplicate. The carrying capacity is supposed to be proportional to the available carbon resource, qualifying substrate availability and its accessibility by the biomass density. A simple differential equation based on these assumptions is:

$$\begin{cases} \dfrac{dB}{dt} = \alpha_{Bac} \left(OxMin + Denit \right) B \left(1 - \dfrac{B}{K_B} \right) \\ K_B = \gamma_B C \end{cases} \tag{2.20}$$

The coefficient α_{Bac} traduces the bacteria population production rate according to the resource. When $\alpha_{Bac} = 1$, this production rate is maximal and the bacteria profile will be almost proportional to that of POC (with γ_B as proportionality coefficient). We choose $\alpha_{Bac} = 0.3$ (see Tab. 2.I and Fig. 2.3) because this value seems to be realistic (Goldman and Dennett, 2000).

2.3.3 The complete model

We propose a model, which extends usual ones in the sense that it describes the bacterial biomass explicitly. If the bacterial biomass is maintained to a constant value then we get a usual formulation. In other words, if:

$$B(t,z)=1 \tag{2.21}$$

then our reaction terms are identical to Soetaert *et al*. (1996).

The reaction part depends on the number of bacteria; so without bacteria, the organic components will not be degraded. Moreover, bacteria do not move by themselves; adsorbed to sediment particles, they will be moved with the sediment.

In our case, porosity is considered to be constant. This relation is used to link dissolved and particulate elements:

$$\frac{\text{vol particle}}{\text{vol dissolved}}=\frac{1-\phi}{\phi} \tag{2.22}$$

where ϕ is porosity.

A model with four state variables based on Berner's equation and describing particulate organic carbon (noted *C*), dioxygen, nitrate and bacteria mass, can now be formulated, given dynamic spatial variation:

$$\begin{cases} \dfrac{\partial C}{\partial t}=-\dfrac{\partial w_C C}{\partial z}+\dfrac{\partial}{\partial z}\left(D_C\dfrac{\partial C}{\partial z}\right)-\dfrac{R_{\text{minox}}O_2}{K_{\text{minox},s}+O_2}BC-\dfrac{R_{\text{denit}}NO_3}{K_{\text{denit},s}+NO_3}\left(1-\dfrac{O_2}{K_{\text{inhib,denit}}+O_2}\right)BC \\ \dfrac{\partial O_2}{\partial t}=-\dfrac{\partial w_{O_2}O_2}{\partial z}+\dfrac{\partial}{\partial z}\left(D_O\dfrac{\partial O_2}{\partial z}\right)-y_C^{O_2}\left(\dfrac{1-\phi}{\phi}\right)\dfrac{R_{\text{minox}}O_2}{K_{\text{minox},s}+O_2}BC \\ \dfrac{\partial NO_3}{\partial t}=-\dfrac{\partial w_{NO_3}NO_3}{\partial z}+\dfrac{\partial}{\partial z}\left(D_{NO}\dfrac{\partial NO_3}{\partial z}\right)+\left(\dfrac{1-\phi}{\phi}\right)\left(y_{O_2}^{NO_3}\dfrac{R_{\text{minox}}O_2}{K_{\text{minox},s}+O_2}-y_C^{NO_3}\dfrac{R_{\text{denit}}NO_3}{K_{\text{denit},s}+NO_3}\left(1-\dfrac{O_2}{K_{\text{inhib,denit}}+O_2}\right)\right)BC \\ \dfrac{\partial B}{\partial t}=-\dfrac{\partial w_B B}{\partial z}+\dfrac{\partial}{\partial z}\left(D_B\dfrac{\partial B}{\partial z}\right)+\alpha_{Bac}B\left(1-\dfrac{B}{K_B}\right)\left(\dfrac{R_{\text{minox}}O_2}{K_{\text{minox},s}+O_2}+\dfrac{R_{\text{denit}}NO_3}{K_{\text{denit},s}+NO_3}\left(1-\dfrac{O_2}{K_{\text{inhib,denit}}+O_2}\right)\right)C \end{cases} \tag{2.23}$$

where $R_{\text{minox}} = k'$, $R_{\text{denit}} = k_1'$, $K_{\text{inhib,denit}}$ is a linear function of nitrate, K_B a linear function of POC and α_{Bac} is the transformation rate of POC in bacterial biomass (the growth efficiency). In this study, we consider a spontaneous nitrification reaction of the ammonium, produced by the oxic mineralization process. The transformation of ammonium induces an increase of nitrate with rate $y_{O_2}^{NO_3}$ linked to the nitrification process.

2.4 Numerical schemes

In order to study the numerical solution of our mathematical model, we choose the finite volume method. The set of equations is integrated for a small volume CV (control volume) where the computed values are supposed to be constant. With Ostogradsky's theorem, volume integrals can be changed into surface integrals on the CV faces (Ferzinger and Peric, 1999) and system becomes of the type:

$$\int_V \frac{\partial C}{\partial t} dv + \int_S (Cwz) n ds - \int_S \left(\beta D_z \frac{\partial C}{\partial z} z \right) n ds - \sum \int_V R(C) dv = 0 \qquad (2.24)$$

where n is the outer-oriented normal vector; the CVs are based on a Cartesian 2D mesh (node centred) with irregular steps. Each CV face is labelled with its cardinal direction (just North and South in our 1D case).

This efficient computation method also adds the benefit to integrate the mass conservation equation naturally.

For spatial discretisation, the simplest but accurate method of the midpoint rule is used for the approximation of surface integrals. For example, the integral of the value f at a North cell face is:

$$F_n = \int_{Sn} f dS = \overline{f_n} S_n \approx f_n S_n \qquad (2.25)$$

The same low-level approximation is used for the volume integrals and the value of the integral of q is Vq_p where V is the control volume (C and q_p the value of q at the CV centre. To approximate the values at the CV faces, we use linear interpolation between the two nearest nodes.

The interpolation for the diffusive flux is also based on the assumption of a linear profile between two consecutive CV centres and, for example, the spatial gradient of C at the North face is:

$$\left(\frac{\partial C}{\partial z} \right)_n \approx \frac{C_N - C_P}{z_N - z_P} \qquad (2.26)$$

P represents the node; lowercase is used for faces and uppercase for nodes.

The boundary conditions are the particular values given to each equation of the system at the borders of modelled space. These conditions must be well defined; the solutions must exist and be unique. If the concentration is given at the boundary, it is a Dirichlet condition; if the spatial concentration

gradient is given at the boundary, it is a Neumann condition. To the represent POC input, mostly dominated by bioturbation effects, a Neumann condition is used. For dissolved elements (dioxygen and nitrate), the concentration at the water-sediment interface is defined by a Dirichlet condition.

If the boundary of the modelled space expresses a physical impermeability for an element, it is not necessary to define a boundary condition (advection and diffusion fluxes are null). For bacteria populations, we choose to consider no sink or source from the surface, so the fluxes for the surface-face of the CV are zero.

For numerical diffusion, instability problems or computational costs, it is sometimes interesting to compute each different term of the convection-diffusion equation separately with an appropriate temporal scheme. Douglas and Rachford (1956), Peaceman and Rachford (1955) proposed this splitting-up for the first time. An explicit method is used for the non-linear reaction terms while a more accuracy implicit method is used for the transport equation. This splitting-up method can only be used for small disturbances, which means that dynamical fields have small local variations in time and space.

For the Eq. 2.24, we have:

$$\begin{cases} \int_V \frac{\partial C}{\partial t} dv + \int_S (Cwz) nds - \int_S \left(\beta D_z \frac{\partial C}{\partial z} z \right) nds = 0 \\ \int_V \frac{\partial C}{\partial t} dv - \sum \int_V R(C) dv = 0 \end{cases} \tag{2.27}$$

Consequently, we consider the transport terms and the reactions terms in the equations system separately. The time dependent equations of reaction terms are calculated first and then, this partial result is applied for the transport terms to find the result for the next time-step. We obtain for the explicit and implicit Euler method:

$$\begin{cases} C^{n+1*} = \frac{\Delta t}{V} \sum \int_V R\left(C^n\right) dv + C^n \\ C^{n+1} = \frac{\Delta t}{V} \left[\int_S \left(\beta D_z \frac{\partial C^{n+1}}{\partial z} z \right) nds - \int_S \left(C^{n+1} wz \right) nds \right] + C^{n+1*} \end{cases} \tag{2.28}$$

where we used the shorthand notation $C_{n+1} = C\ (t_n + \Delta t)$ and the * indicates that is not the final value of the solution at t_{n+1}.

To avoid instability and excessive numerical diffusion problems, we choose an implicit method to solve the system of linear equations for transport. However, given the large number of required computations, we need to use the accuracy of iterative methods like GMRES or bi-CGSTAB as proposed van den Vorst (1992). We used the Fortran 90 library "smlib v1.1" for sparse matrix calculations created by Meese (1998), which has routines for these iterative methods. Based on these tools, which compute only non-zero elements, we have written accurate routines for products of sparse matrices, the solution of systems of linear equations and for matrix inversions.

2.5 Simulations and Numerical results

2.5.1 Steady State

One-dimensional simulations are realised in a sedimentary column of 30 centimetres. We used a 200 nodes grid with constant steps of 0.5 millimetres for the first 8 centimetres and increasing for the rest.

We consider sediment porosity (ϕ) and temperature (T) to be constant throughout the sedimentary column ($\phi = 0.8$, $T = 15°C$). Dissolved dioxygen and nitrate diffusion coefficients (respectively D_O and D_{NO}) - corresponding to molecular diffusion and bioirrigation, depending on biodiffusion - are also constant in the surface layer of sedimentary column (6 first centimetres). Their values are calculated by Soetaert *et al*. (1996) from sediment temperature and porosity, coefficient for temperature dependency of diffusion coefficient and molecular diffusion coefficient at 0°C of these compounds. We assume the bulk of sediment to be constant. The particles sedimentation rate is considered constant during time and throughout the sedimentary column ($W = 1cm/10years$).

All the compound values, their dynamical fields and associated reactions are described in the following Tab. 2.I.

Tab. 2.I. Initial value of state variables and parameters used in the MODELS I and II.

Notation	value
State Variables at the surface	
C	9000 μmol.l^{-1}d^{-1}
O_2	130 μmol.l^{-1}
NO_3	20μmol.l^{-1}
Parameters	
Physical and numerical geometry	
z_{max}	30 cm
N	300
Δz	0.05 cm
Δt	0.001 d
Physical fields and constants	
W	1cm/10 yr.
D_{O2}	3.0 cm^2.d^{-1}
D_{NO3}	2.7 cm^2.d^{-1}
$D_{M\,O2}$	1.0 cm^2.d^{-1}
$D_{M\,NO3}$	0.9 cm^2.d^{-1}
ϕ	0.8 %
Biological	
D_B D_C	0.05 cm^2.d^{-1}
α_{Bac}	0.3 l.(μmol C)$^{-1}$
γ_B	2.52E-04 %.(μmol C)$^{-1}$
Biogeochemical	
R_{minox}, R_{denit}	0.04 d^{-1}
$K_{\text{minox, }s}$	3 μmol O_2.l^{-1}
$K_{\text{denit, }s}$	30 μmol NO_3.l^{-1}
$K_{\text{inhib, denit}}$	10 μmol O_2.l^{-1}
$y_C^{O_2}$	1 mol O_2.(mol C)$^{-1}$
$y_C^{NO_3}$	0.8 mol NO_3.(mol C)$^{-1}$
$y_{O_2}^{NO_3}$	14 mol NO_3.(mol O_2)$^{-1}$

Our study consists in a comparison of two models. The first one, the so-called MODEL I, does not take bacterial biomass explicitly into account and is obtained from Eq. 2.23 where the bacterial biomass is maintained fixed at a unit value $B(z,t) \equiv 1$. It corresponds to usual type of models. The second model (MODEL II) is the one we developed in this paper and is actually given by Eq. 2.23. We start from a steady state configuration where almost all compounds are degraded and simulate a perturbation. Then we analyse the impact of taking the bacterial biomass explicitly into account via the responses of the different dissolved compounds to the perturbations. As a consequence, we first study a stationary state with constant input of chemical compounds (POC, O_2 and NO_3) at the surface. Even if only a few parts of early diagenetic processes are modelled here, realistic numerical values are used.

The coefficient K_B, which defines the maximum bacteria number locally present in the sedimentary column, depends linearly on POC concentration (Eq. 2.20). The larger the proportionality coefficient γ_B, the more the bacteria number in the environment will grow and the more mineralization processes become important. An analysis of the effect of this parameter γ_B on the bacterial biomass at steady state and on the POC quantity is presented on Fig. 2.1. The value of γ_B is chosen such that both models have the same quantity of POC in the sedimentary column in steady state.

In order to have a reference for the comparison between MODEL I and MODEL II, we started with the same total mass of POC for both models at steady state, which is obtained by putting γ_B = 2.52E-04 (Fig. 2.2).

Vertical profiles at steady state are shown on Fig. 2.2 for both models. Starting from the water-sediment interface, POC is degraded by O_2 and an exponential decreasing of these compounds could be observed. The NO_3 concentration is increased by the nitrification at the surface. The most important differences can be seen for dioxygen and nitrate profiles. MODEL II uses, on the whole, a smaller quantity of electron acceptors for degrading the same amount of POC.

Given, the inputs of compounds at the surface and the bacteria growth coefficients, steady vertical profiles are obtained where almost compounds disappear (see Fig. 2.3). The differences between both models are coming from the vertical repartition of bacteria. Since MODEL I is similar to MODEL II if state variable B is fixed at 1, comparisons between models are possible. At this steady state, the profile for bacteria is almost proportional to that of POC for MODEL II. This repartition, mostly important in the surface layer, activates oxic mineralization effects. With a low quantity of biomass, MODEL I and II lead to similar results.

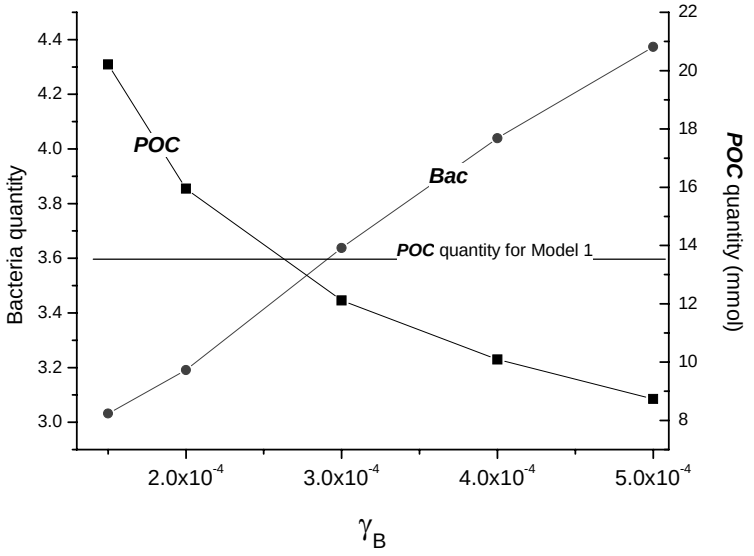

Fig. 2.1. Analysis of the effect of proportionality coefficient γ_B, included in the expression of the carrying capacity $\boldsymbol{K_B}$ (Eq. 2.20), on the bacterial biomass at steady state and on the POC quantity.

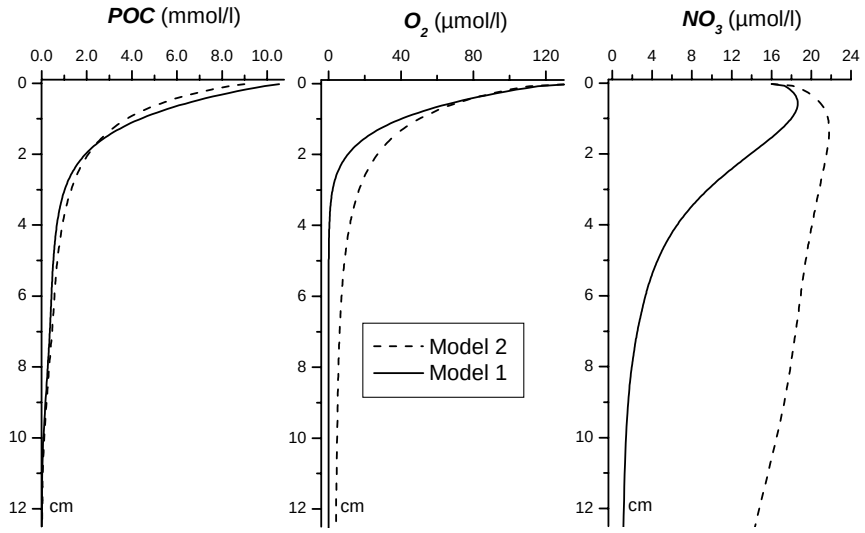

Fig. 2.2. Vertical steady state profiles comparison of POC, O_2 and NO_3 between the MODEL I (solid line) and the MODEL II (dashed line) with the same total mass of POC ($\gamma_B = 0.024$).

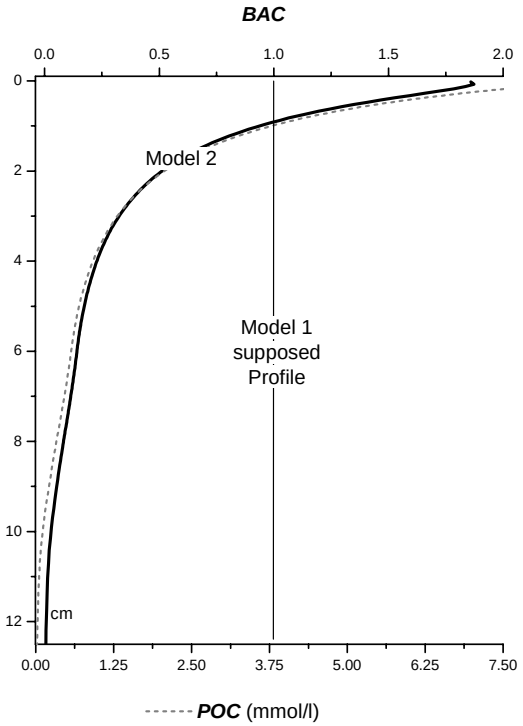

Fig. 2.3. The vertical bacterial biomass profile with MODEL II (dashed line) compared with the POC profile (solid line). At steady state, both profiles are proportional. As a reference, a vertical straight line indicates the value of bacterial biomass assumed by MODEL I.

2.5.2 Perturbations

Starting from the precedent stationary state, a perturbation in POC input is applied. This is a theoretical perturbation where the amount of available carbon flux at the water-sediment interface is doubled. We aim to understand the bacterial response to an increased input at the surface. Fig. 2.4 shows the dynamics for both models simultaneously; the simulation resulting from the MODEL I is represented in solid lines while that obtained with MODEL II is in dashed lines. The number of each simulation corresponds to the days since the initial perturbation. The large differences for POC concentrations are the consequence of the response of bacterial biomass to the increase of the POC flux.

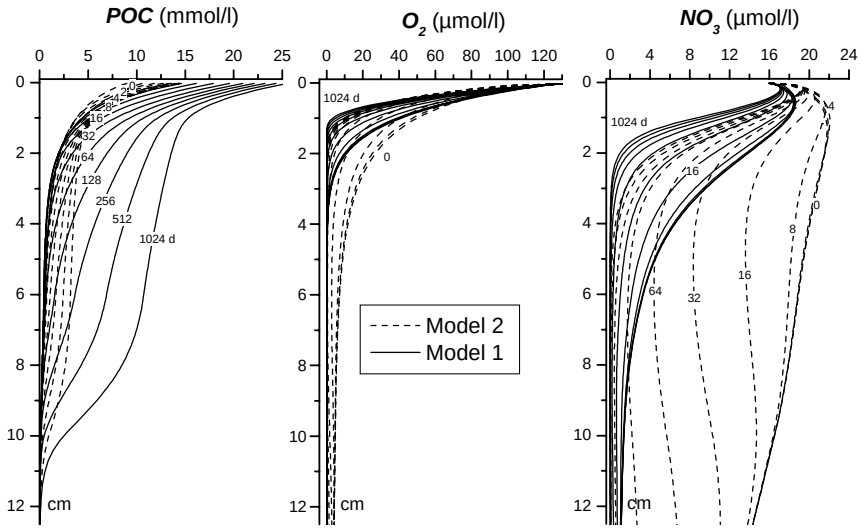

Fig. 2.4. Profiles evolution comparison of POC, O2 and NO3 concentrations between both models. The outline, resulting from the MODEL I simulation, is represented in solid line and in dashed line the profile evolutions of MODEL II. The number associated to each outline corresponds to the number of evolution day since the initial perturbation.

The POC is half-degraded in the first centimetres of sediment. The system needs a long time to come back to a steady state, which is not yet reached after more than 1000 days for the MODEL I. The dioxygen concentration decreases fast and anoxic conditions reach the 2 centimetres layer after a month. When the new equilibrium state is approached, the sediment is anoxic after the depth of 1 centimetre. The nitrate concentration starts to vanish in both models only after a few days when POC penetrates in a weakly oxic layer. The nitrate peak concentration comes near the surface to settle down at a depth of 2 millimetres.

Although, both models have similar trends, the burying of POC for MODEL II, is very limited and a new equilibrium seems to be reached faster (Fig. 2.5).

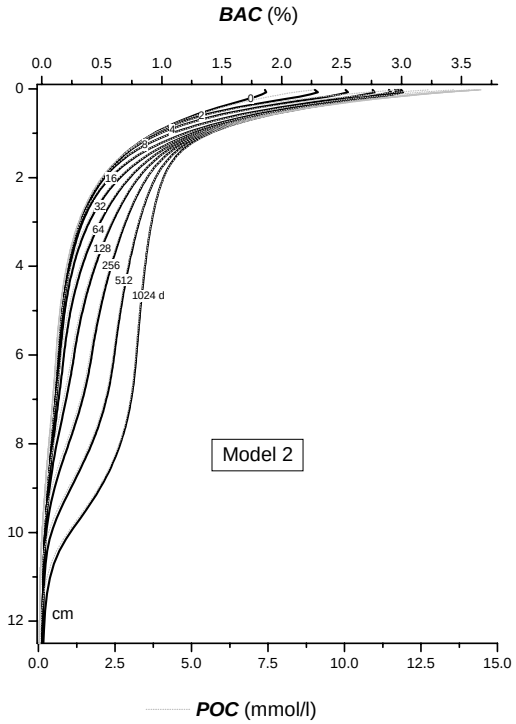

Fig. 2.5. The profiles of bacteria for MODEL II compared with POC profiles evolution

The bacterial biomass dynamics follows that of the POC concentration. This increasing biomass has an important influence on the disappearance of POC. These simulations show a problem with our mathematical model since bacterial biomass is still important, even when there are no electron acceptors (see Fig. 2.4). This artefact can be avoided by adding terms corresponding to biomass loss (maintenance, mortality). This will be done in future work.

Fig. 2.6 presents the rates of the biogeochemical processes, oxic mineralization and denitrification, that are taken into account in the models presented in this paper. Both models are presented in the same figure for comparison. Once again, we can see the role of the extra variable associated to bacterial biomass. Indeed, it can be seen that the oxic mineralization is intensified and the denitrification is reduced in MODEL II with respect to MODEL I. The deposition of organic matter leads to an intense bacterial production, which in turn translates into higher biogeochemical activities. This mineralization activity leads to a nitrate production and an activity peak of denitrification at a depth of 2 millimetres.

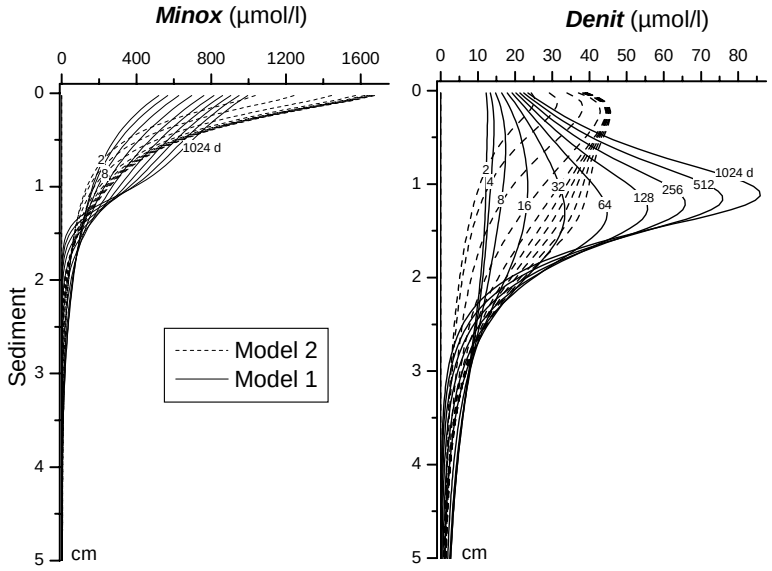

Fig. 2.6. Intensity comparison of the biogeochemical processes (oxic mineralization and denitrification) between the MODELS I (solid line) and II (dashed line). The number associated to each outline corresponds to the number of evolution day since the initial perturbation.

Finally, we compare the matter assessment in the whole sediment column. This step should be important in practice since it concerns the role of modelling. Indeed, this type of models is often used to calculate assessment in order to know, for instance, if the sediment is a source or a sink of carbon, nitrogen, and so on. The results are presented in Fig. 2.7. We can see that the POC quantities are very different for both models. However, we also note that the significant differences for dioxygen and nitrate concentrations at the start of the perturbation vanish with the disappearance of compounds. The bacterial biomass increased proportional to the burying of POC.

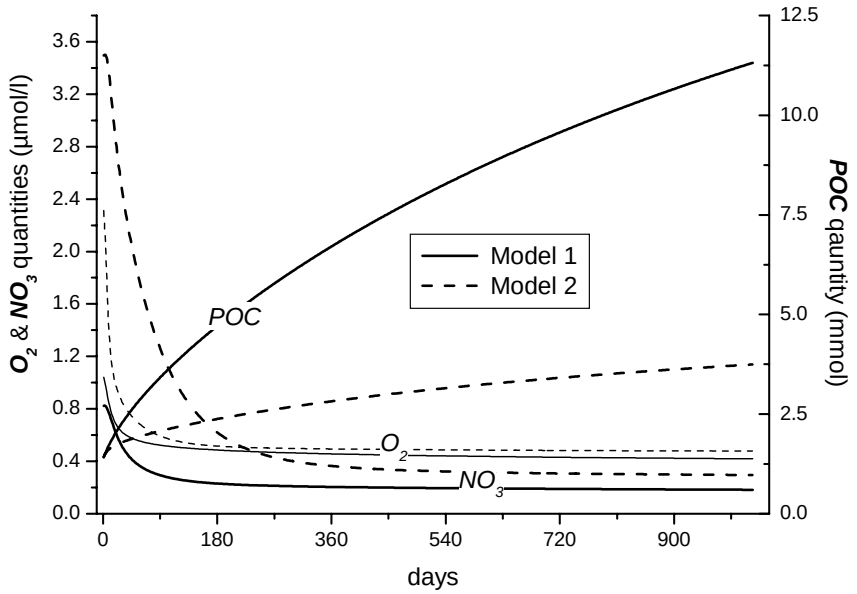

Fig. 2.7. The temporal evolution comparison of POC, O_2 and NO_3 amounts in the whole sedimentary column between the MODELS I (solid line) and II (dashed line). The bacterial biomass of the MODEL II has been multiplied by 4 to adjust its outline to the POC one's.

2.6 Conclusion

We presented a diagenetic model where the bacterial biomass is explicitly taken into account. We built the model for microbial activity on a mechanism based on enzymatic processes. We then obtained the model for the column of sediment by using time scale separation and the quasi-steady state assumption. Dilão and Domingos (2000) suggested this method to build trophic chains; we show here that this approach is even more powerful and is useful to build general ecosystem models on mechanistic arguments. This method is a particular case of the aggregation of variables method described in Auger and Poggiale (1998).

We have shown that the model without explicit bacterial biomass gives significant differences in the dynamics of the profiles as well as in the assessments. We shall sum up three points, which we consider as important in our approach.

First of all, we note that the added particulate organic carbon is rapidly degraded when bacteria are taken into account: when the environment is

enriched, the bacterial biomass is enhanced in the upper sediment layer. This phenomenon cannot be simulated by MODEL I which exhibits an organic matter burial in deeper layers.

The second point concerns the process intensities (oxic mineralization and denitrification). Simulations show that the oxic mineralization is enhanced at the sediment surface with MODEL II while the denitrification is reduced. This can be the result of the strong activity of the large bacterial biomass in the oxic zone. Since the POC is rapidly consumed, the deeper layer is poorer with respect to organic matter and thus the denitrification intensity is smaller. In MODEL I, where the bacterial biomass is constant, the added carbon is buried and transported in the anoxic zone where it is denitrified. This can also be seen in the nitrate profiles for both models: MODEL I exhibits a low profile for nitrate concentrations with respect to MODEL II.

The last point deals with the simulation of the assessment: we see that the POC amount in the sediment is much larger in MODEL I than in MODEL II. This is the result of the previous points. However, we must say that there is no bacterial biomass loss in our model. This loss should in fact be a source of POC and a more complete model should give a lower difference in the assessment.

From a numerical point of view, the use of an implicit temporal scheme was not necessary for the diffusion and convection rates, but it allowed the testing of the computational speed and the quality of results relatively to time and space steps. The finite volume method seems to be appropriate for this kind of modelling. The program was written of all models based on the equation of Berner; it turns to be effective. The program can be used for 2D simulations too, and simulations of dynamical response to macrobenthos perturbation will be tested. The chosen numerical discretisation was found to be efficient.

3

Comparison of the classical models analysing the bacterial dynamics

Abstract

A comparison of classical models analysing the bacterial dynamics (as Monod and Droop) and a DEB based model has been realised through an application to a set of data. For each model, we took an interest in the quantitative and the qualitative fitting but also in the parameter variation with the increase of the dioxygen concentration. For the Monod model, the bacterial growth ceases as soon as the substrate disappeared from the environment. The two other models which are very close qualitatively offer a good fit to this set of data. In this case, the maintenance doesn't play an important role and the Droop model, which takes reserve into account, is enough. Moreover, the model complexification decreases the mean distance between simulations and data but it clearly increases the variability from initial parameter value. Indeed, the model complexity in terms of numbers of parameters and variables must match the availability of data. Furthermore, all the parameters show a strong dependence on the increase of the dioxygen concentration. In simplified model, this strong variability in parameter values can come from some essential processes not taken into account. Although too complex for this particular data set, the DEB model obtains parameter values that are useful for perturbation studies.

Keywords: Droop - Marr-Pirt – Monod - DEB theory - fitting.

3.1 Introduction

Monod, Marr-Pirt and Droop are classical models of microbial growth in the chemostat, formulated at the population level. These models are not structured which means that all the individuals of the population are assumed to be identical (Kooi and Kooijman, 1994b). They link substrates and microbial biomass and they offer a good description of population growth for high substrates concentrations (Kooijman *et al.*, 1991).

This paper compares the classical models for the bacterial dynamics and a new mechanistic model based on the DEB theory, through an application to a set of data (Bonin *et al.*, 1992). The Appendix A, at the end of the manuscript, offers a detailed description of all the parameters and variables used in this manuscript.

3.2 Model descriptions

3.2.1 The DEB model for V1-morphs

The DEB theory has parameters at the individual level. Hanegraaf and Muller (2001) have developed a DEB model for V1-morphs and applied it to bacterial communities. They showed that this model explains the changes in the composition of bacterial biomass as a result of the change in growth rate. We propose here a mechanistic model, based on the DEB theory, describing the bacterial dynamics at the individual level and processes from enzymatic kinetics. From the DEB theory for the V1-morphs (Kooijman, 2000), we have:

$$\begin{cases} \dfrac{d}{dt}X = I_X - j_X^A V \\ \dfrac{d}{dt}E = \left(j_E^A + j_E^G + j_E^M\right)V \\ \dfrac{d}{dt}V = j_V^G V \end{cases} \tag{3.1}$$

where X represents the substrate concentration, e the reserve density (unit of reserve by unit of structure), V the structural biomass density. I_X represents the substrate supply, j_*^{Π} is the specific flux of compound * associated to the

process Π (with here A: assimilation, G: growth and M: maintenance) and can be determined from enzyme kinetics.

The specific flux associated to the assimilation process

The assimilated substrate is converted to reserve. We can write the following enzymatic kinetics:

$$\alpha_{\cdot} + X \xrightarrow{a_X} \alpha_X \xrightarrow{a_X'} \alpha_{\cdot} + y_{EX} E$$

where y_{EX} is the yield coefficient of reserve on substrate in the assimilation process, $\alpha_{\cdot}$ is the free fraction of the synthesizing units (SUs) associated to assimilation process, α_X the fraction of SUs that is bound to the substrate X; we have $\alpha_{\cdot} + \alpha_X = 1$; a_X and a_X' are respectively the binding and the dissociation rates. Refer to Appendix A for more description of parameters and variables.

From the previous enzymatic kinetics, we obtain the following system:

$$\alpha = \begin{pmatrix} \alpha_{\cdot} \\ \alpha_X \end{pmatrix} \text{ and } A = \begin{pmatrix} -\rho_X j_X & a_X' \\ \rho_X j_X & -a_X' \end{pmatrix}$$

where ρ_X is the binding probability of X, $\rho_X j_X = a_X X$ is the specific flux of X or the substrate availability for the assimilation process, such as:

$$\frac{d}{dt}\alpha = A\alpha$$

By assuming a different time-space scale for the processes at the enzymatic and at the population levels, we solve the previous system at quasi steady state. Thus:

$$\begin{cases} j_X^A = -\rho_X j_X \alpha_{\cdot}^* \\ j_E^A = y_{EX} a_X' \alpha_X^* \end{cases} \quad \text{with} \quad \alpha_X^* = 1 - \alpha_{\cdot}^* \text{ and } \alpha_{\cdot}^* = \frac{a_X'}{a_X' + a_X X}$$

where $\alpha_{\cdot}^*$ and α_X^* are the SU fractions at steady state free and bound to substrate X bound respectively. For the assimilation process, we have:

$$j_X^A = j_{XAm} \frac{X}{X + K_X} \tag{3.2}$$

This is similar to the Michaelis-Menten kinetics with:

$$j_{XAm} = a'_X \text{ and } K_X = \frac{a'_X}{a_X}$$

where j_{XAm} the maximal specific absorption flux of the substrate, *f(X)* a Michaelis-Menten function with K_X the half saturation constant.

The cell will use the mobilized reserve for maintenance first and then the rest for growth.

The specific maintenance flux

If the maintenance is realised only from reserve, it is not necessary to describe the kinetics. Indeed, the maintenance cost (k_M) is supposed to be constant for a given cell size, i.e. by unit of structure. The specific flux of reserve allocated to maintenance is:

$$j_E^M = y_{EP} k_M \tag{3.3}$$

The specific growth rate

The corresponding kinetics for growth can be written as follows for an enzyme molecule γ:

$$\gamma_. + E \xrightarrow{g_E} \gamma_E \xrightarrow{g'_E} \gamma_. + y_{EV} V$$

The use of reserves in the DEB theory follows from two conditions: (*i*) the reserve dynamics is partitionable; (*ii*) the reserve dynamics is weak homeostatic (refer to Appendix 1.A). We obtain:

$$\frac{de}{dt} = j_E^A - h_E e \text{ and } j_V^G = \frac{h_E e - y_{EP} k_M}{y_{EV} + e} \tag{3.4}$$

where $h_E\ e$ is the flux from reserve, $y_{EP}\ k_M$ is the maintenance cost realised from reserve, $e + y_{EV}$ is the total energy costs for biomass (reserve plus structure).

By replacing Eqs. 3.2 to 3.4 in Eq. 3.1, we finally obtain the following ordinary differential equations:

$$\begin{cases} \dfrac{dX}{dt} = I_X - j_{XAm} f(X) V \\ \dfrac{de}{dt} = \nu f(X) - h_E e \\ \dfrac{dV}{dt} = \dfrac{h_E e - y_{EP} k_M}{y_{EV} + e} V \end{cases} \qquad \begin{cases} f(X) = \dfrac{X}{X + K_X} \\ \nu = y_{EX} j_{XAm} \end{cases} \tag{3.5}$$

This model gives a biological interpretation of the parameters j_{XAm} and K_X, but it also has one more parameter h_E.

We have the following cases:

If $h_E\, e > y_{EP}\, k_M \rightarrow r > 0$: part of the reserve flux is used for the maintenance (thus maintenance is only realised from reserve).

If $h_E\, e < y_{EP}\, k_M \rightarrow r < 0$: there is not enough reserve to realise maintenance, part of the structure is used which leads to the shrinking phenomenon. But in starvation conditions, this formulation leads to a return flux in reserve E and to a thermodynamic problem (see Appendix 1.A).

3.2.2 The classical models

The classical models are particular cases of the DEB model (Kooi and Kooijman, 1994b).

The Monod model is frequently used for the growth if only one substrate is limiting growth. It assumes that the growth rate is proportional to the substrate assimilation rate. Biomass growth ceases as soon as the substrate disappears. The Monod model is a particular case of the DEB theory under the following conditions:

$$\boxed{y_{EV} \rightarrow \infty \text{ and } h_E \rightarrow \infty \text{ and } k_M = 0} \;\Rightarrow\; r = \frac{h_E}{y_{EV}} e \text{ and } e = f(X)$$
$$\text{if } f(X) = 1 \rightarrow r = r_{\max} = \frac{h_E}{y_{EV}} \tag{3.6}$$

Marr and Pirt introduce the maintenance notion which gives some stability to the model. This group of processes is realised from the structure in the Marr-Pirt model and is not differentiable from death. But both losses lead to different products that don't have the same role in the ecosystem functioning. Like the Monod model, it presupposes a constant composition of the bacterial biomass. The Marr-Pirt model is a particular case of the DEB theory with the following conditions:

$$\boxed{y_{EV} \to \infty \text{ and } y_{EP} \to \infty \text{ and } h_E \to \infty} \Rightarrow r = \frac{h_E}{y_{EV}} e - \frac{y_{EP}}{y_{EV}} k_M \text{ and } e = f\left(X\right)$$

$$\text{if } h_E e < y_{EP} k_M \to r < 0$$

$$\text{if } f\left(X\right) = 1 \to r = r_{\max} = \frac{h_E - y_{EP} k_M}{y_{EV}}$$

(3.7)

The Droop model assumes that the growth rate is a function of the limiting nutrients inside the cell. There is no direct relation between the growth rate and the extra-cellular nutrient concentrations. This is the notion of reserve or quota allowing the growth process to continue for a while after the disappearance of substrate.

The Droop model was initially formulated with the number of individuals (N) and a quota that represents the overall nutrient (i.e. chemical element) in an individual (Q in $mol\ X.N^{-1}$). A transformed Droop model, considering an amount of structural biomass instead of an individual number and reserve instead of quota can be obtained from the DEB model with the following conditions.

$$\boxed{k_M = 0} \Rightarrow r = \frac{h_E e}{e + y_{EV}} \geq 0 \Rightarrow \begin{cases} \text{if } e >> y_{EV} \to r = r_{\max} = h_E \\ \text{if } e << y_{EV} \to r = r_{\min} = \dfrac{h_E e}{y_{EV}} \to 0 \end{cases} \quad (3.8)$$

However, the Transformed Droop model conserves the same dynamical properties than the initial Droop model and allows the mass conservation law.

The Tab. 3.I, proposed by Kooijman (1993), gives a classification of the previously described models, from their construction assumptions. Kooi and Kooijman (1994b) show that classical models have a less efficient fit to data than the DEB model. The introduction of both reserve and maintenance to the Monod model is necessary to describe the microbial dynamics that they studied. The introduction of only reserve leads to a bad fit compared to the Monod model.

Tab. 3.I. Classification of the present models analysing the bacterial dynamics, according to their construction assumptions.

		Reserve	
		$e = 0$	$e > 0$
Maintenance	m = 0	Monod	Droop
	m > 0	Marr-Pirt	DEB

3.3 Models comparison through an application

3.3.1 Data and fitting assumptions

The studied bacterial strain has been isolated from coastal marine sediment. It has been identified as being *Pseudomonas nautica* with the reference *Pseudomonas nautica n° 617 / 1.85*. It is a facultative aerobic strain which means by definition that it is able to fulfil both the oxic mineralization and the denitrification processes and thus to use independently dioxygen, nitrate, nitrite and nitrous oxide as electron acceptor for its respiratory functioning. This characteristic allows us to study the competition between the different electron acceptors.

The experimental study by Bonin *et al*. (1992) aimed to determine the effect of oxygenation on the enzymatic activity associated to the oxic mineralization and the denitrification processes. It consists of following the bacterial growth of *Ps nautica* in a batch culture. The cells were cultivated under aerobic and anaerobic conditions, and in presence and absence of nitrate. For each experiment, they applied an initial concentration of nitrate, carbonated substrate (sodium lactate: $C_3H_5O_3Na$) and dioxygen in percentage. From one experiment to another one, they applied different dioxygen concentrations at steady state (0, 10 %). The nitrogen, necessary to construct its living material, can be obtained either from the substrate (complex organic matter) or from the dissolved ammonium or nitrate present in the environment. But to be used in metabolism, the nitrate will have to be previously transformed into ammonium first.

As the N_2, N_2O and NO compounds are in gaseous form, Bonin *et al*. (1992) measured (*i*) the respiratory activities through the consumption and/or the production kinetics of the different denitrification step and more particularly the nitrate and nitrite concentrations, (*ii*) the amount of carbonated substrate that remained at the end of the experiment and (*iii*) the

optical density (O.D.) which is an indicator of bacterial biomass (number of cell) with the following relation for *Pseudomonas nautica* (*Marinobacter*):

$$1\ \text{O.D.} \longrightarrow 6.78\ 10^{6}\ \text{cells.ml}^{-1}$$

As the model can be very complex relative to the amount of data and of measured parameters, we made some assumptions:

(i) We neglect the nitrification process which constitutes a nitrate supply by means of the transformation of ammonium. In that way, we assume that the bacterial strain is unable to realise this process.

(ii) We also neglect the mortality term which is important at a larger space time scale than the experimental one.

(iii) The carbon and the dioxygen concentrations are assumed to be constant as the experimental results only provide the initial carbon value and consider dioxygen at steady state during each experiment.

(iv) The terminal oxydase, responsible for the oxic mineralization, is always present in the environment and its concentration is supposed to be constant.

3.3.2 Fitting method

To justify the mechanistic model, we compared the different models (Monod, Droop and DEB) through the parameter values that minimize the Euclidian distance between model simulations and experimental results via the simplex method (Matlab, *fminsearch*). For each model, we took an interest in the quantitative and the qualitative fitting but also in the parameter variation with the increase in the dioxygen concentration.

Distance

We first calculated the weighted Euclidian distance between experimental data and the model simulations (the biomass and the dissolved nitrate concentrations) under the different environmental conditions (different dioxygen concentrations at steady state). The distance for the compound X is:

$$D_X^2 = \sum_{i=1}^{m} \left[\hat{y}_{Xi} - y_{Xi}\left(p_1,...,p_n\right) \right]^2$$

where $\hat{y}_{Xi}$ is the observed concentration of X and y_{Xi} the concentration of X obtained from simulations with parameters (p_1, ..., p_n) at time step i ($1 < i < m$).

We have two elements: the biomass (D_B) and the nitrate (D_{NO_3}) that are not comparable in terms of units. To normalise and give significance to the sum of the distances, we weight by the following stoichiometric coefficient:

$$\gamma = \frac{\left[B_{obs}\right]_{\max}}{\left[NO_{3obs}\right]_{\max}} \text{ such that } D = \sqrt{D_B^2 + \gamma^2 D_{NO_3}^2} \tag{3.9}$$

where $[B_{obs}]_{\max}$ and $[NO_{3obs}]_{\max}$ are the maximal observed biomass and dissolved nitrate concentrations. Thus the overall distance D is expressed by unit of biomass.

We then minimize this function D of several variables (p_1, ..., p_n) by the simplex method (function *fminsearch* in Matlab).

Local or global minimum

We want to know if a minimum obtained for a set of parameters is local or global, by searching the form of the least square distance curve. This study can be realised by varying the initial parameter values of the fit. In this way, we could see if the fitted parameter values are optimal and independent of the initial parameter values. For example, if the curve is flat in its minimum, we will find a lot of parameter values for a same distance.

From the different simulations, we measure the mean (M) and the variability (V) of the parameter p. Contrary to the classical standard deviation, the variability of the p parameter is without dimension and must be comparable from one model to another one or from one parameter to another one:

$$V(p) = \sum_{i=1}^{n} \left(\frac{p_i - \overline{p}}{p_i} \right)^2 \tag{3.10}$$

where p_i is the value of the parameter p obtained after the fit i, n the total number of numerical simulations with different initial parameter values for the same data set, and $\overline{p}$ the mean of all the fit on the same data set.

3.3.3 Results

Reserve as a part of the total volume

Kooijman (2000) showed that the contribution of the reserve in the total cell volume is negligible. Consequently, the living biomass volume comes essentially from the structure compartment. Indeed, in the equation $B = V + \varepsilon Ve$, after the fit of B, the ε value is estimated between 10^{-1} and 10^{-16}. Moreover, there is a significant change of the parameter values if the reserve would contribute to the total volume of the bacterial biomass but without changing significantly the distance D. In this study, we will neglect the contribution of the reserve in the total volume of the bacteria.

Qualitative and quantitative study

We study qualitatively which model and which parameter set has the minimal curved shape (sigmoïdality) compared to the data, quantitatively we measure the Euclidian distance between the experimental data and the different model simulations.

Then, to compare the different approaches and to determine which process takes an important place in this data, we fix some parameter values:

(*i*) in the Droop model from the Monod one,

(*ii*) in the DEB model from the Droop and Monod ones.

The Fig. 3.1 shows the Monod, Droop and DEB model fits to the data from Bonin *et al.* (1992) with all the parameter values variable and the Fig. 3.2 with some parameter values fixed.

The Tab. 3.II describes the correspondent distance (Eq. 3.9), the mean parameter values and their variability (Eq. 3.10) of the Monod, Droop and DEB models for different steady state dioxygen concentrations (0% and 10%), in black without any parameters fixed and in grey the fit with some parameters fixed (in bold).

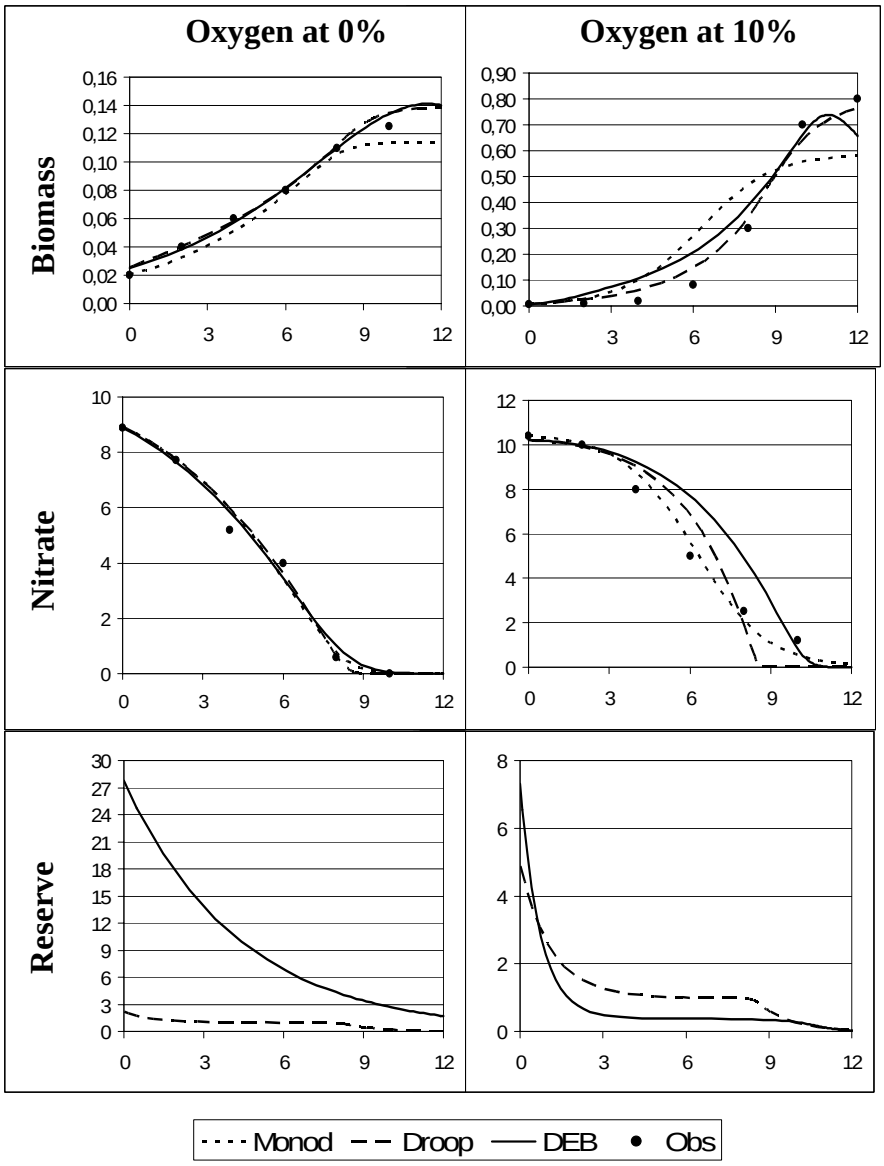

Fig. 3.1. Models fit with variable parameter values: Monod (dot line), Droop (dashed line) and DEB (line) to the data set from Bonin *et al.* (1992, dots): for dioxygen at 0 and 10%. The corresponding Euclidian weighted distances and the set of parameter values are presented in Tab. 3.II.

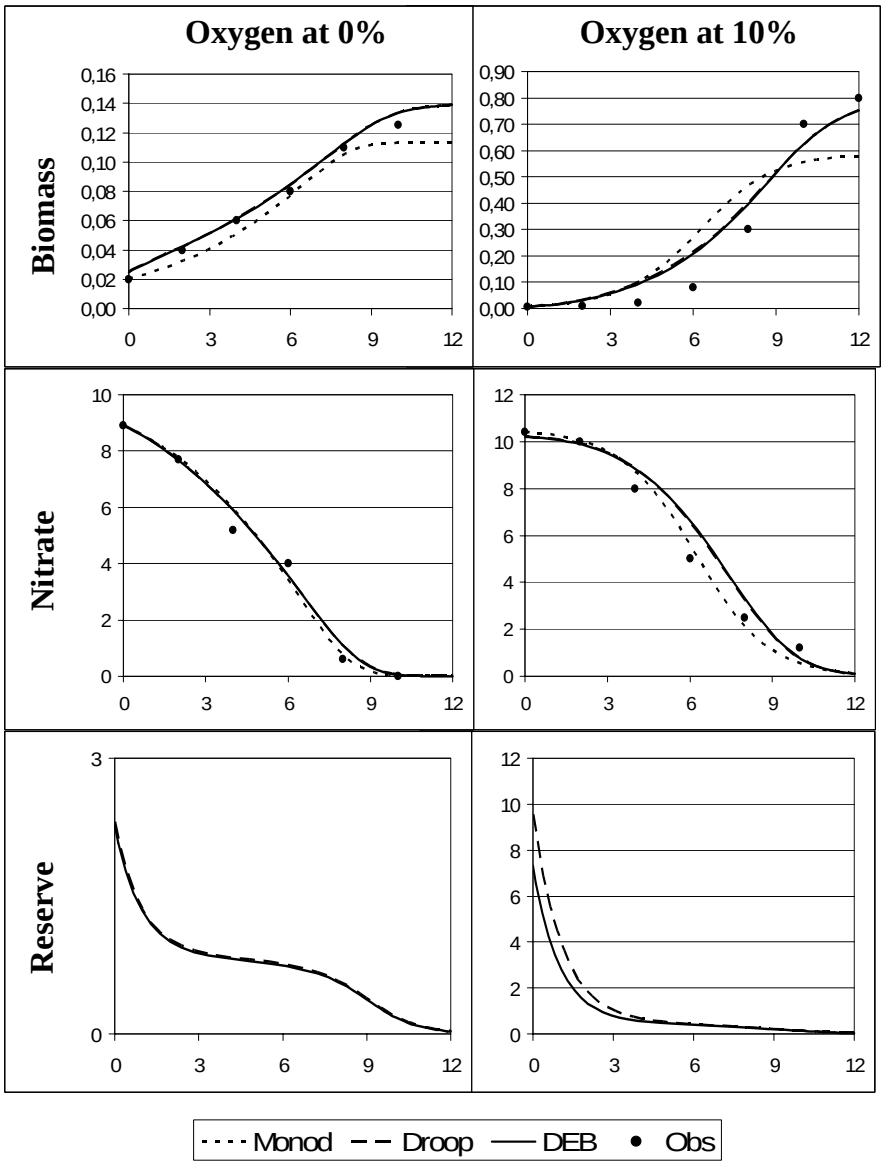

Fig. 3.2. Models fit with some parameter values fixed: Monod (dot line), Droop (dashed line) and DEB (line) to the data set from Bonin *et al*. (1992, dots): for dioxygen at 0 and 10%. The corresponding Euclidian weighted distances and the set of parameter values are presented in Tab. 3.II.

Tab. 3.II. Parameter values of the Monod, Droop and DEB models for different steady state dioxygen concentrations (0% and 10%). In black without any parameters fixed, in grey the fit with some parameters fixed (bold). Indeed, some parameter values of the Droop model are fixed from the Monod one, and for the DEB model from Droop and Monod ones. *M* is the mean parameter value obtained after the fit from different initial parameter values and *V* its variability (Eq. 3.10). *D* is the mean of Euclidian weighted distance between the experimental data (nitrate and biomass) and the model simulations (Eq. 3.9). j_{NAm} is the maximal assimilation rate of nitrate and K_N the half saturation constant. The extreme results are not taken into account.

	O_2 = 0%				**O_2 = 10%**			
	M		***V***		***M***		***V***	
	Monod							
j_{NAm}	21,24		4,48E-10		20,24		1,11E-10	
K_N	1,48		5,89E-9		12,6		3,02E-10	
h_E/y_{EV}	0,26		3,37E-11		1,34		1,1E-10	
D	0,022		7,3E-10		0,31		0	
	Droop							
j_{NAm}	21	**21,24**	0,03	**0**	12,71	**20,24**	0,3	**0**
K_N	1,2	**1,48**	7,2	**0**	0,31	**12,6**	24598	**0**
$v = h_E$	3,7	1,05	8	0,25	1,37	1,028	0,352	0,075
y_{EV}	14,4	4,3	5,11	0,21	1,18	0,72	0,975	0,023
e_0	1,4	2,27	560	3,4E-2	3,08	7,31	20,2	0,848
D	1,8E-2	1,6E-2	0,08	0	0,24	0,25	0,015	0,001
	DEB							
j_{NAm}	23,98	**21,24**	0,66	**0**	10,49	**20,24**	0,09	**0**
K_N	1,74	**1,48**	20	**0**	1,8	**12,6**	2264	**0**
v	1,9E-5	**1,05**	101	**0**	0,25	**1,028**	6,5	**0**
e_0	27,72	**2,27**	1354	**0**	0,1	**7,31**	1E+11	**0**
y_{EV}	3,7E-2	**4,3**	6,9E+5	**0**	0,59	**0,72**	5	**0**
$y_{EP}\, k_M$	0,4474	5E-4	65,8	∞	0,58	1,8E-11	7,6	24,5
h_E	0,23	1,03	963	2E-3	0,8	1	0,17	3,41
D	1,5E-2	1,4E-2	5,3E-3	Div / 0	0,19	0,2	Div / 0	Div / 0

The Monod model fit at 0% and 10% of dioxygen is efficient for the nitrate but the biomass growth stopped earlier than the experimental data. Indeed, the bacterial growth ceases as soon as the substrate disappeared from the environment. This result is intrinsic to the model formulation.

The two other models offer a good fit to this set of data. They are very close qualitatively, except for the case of 10% of dioxygen with variable parameter values (Fig. 3.1). Indeed, the DEB model, that takes into account the reserve and the maintenance notions, indicates a possible fit of the biomass data, while the Droop model shows a nitrate disappearance sooner than the set of data.

The corresponding mean distance (Tab. 3.II) between observations and numerical simulations is higher for the Monod model than for the two other models which are really close. Indeed, the model complexification decreases the mean distance between simulations and data but it clearly increases the variability from initial parameter value: it is much more difficult to find a global minimum. More particularly, the maintenance parameter (in the DEB model) doesn't change the qualitative behaviour or improve the distance. Indeed, the maintenance may not play an important role in this data set.

Parameters evolution with the dioxygen increase

Among the other results, all the parameters show a strong dependence on the increase of the dioxygen concentration (Tab. 3.II). The numerical experiments suggest a variability of the value of the half saturation constant of nitrate K_N, from one dioxygen concentration to another one, weaker for the models that account for reserve and maintenance than for the Monod model. Indeed, in simplified model, this strong variability in parameter values, from one dioxygen concentration to the other one, can come from some essential processes not taken into account.

The half saturation constant K_N and the initial amount of reserve (e_0) show the highest variabilities (V).

The maximum assimilation rate of nitrate j_{NAm} decreases with the increase in dioxygen concentration. Indeed, in oxic conditions, the nitrate is no more the substrate use as electron acceptor. Furthermore, with variable parameter values, the maintenance cost is higher for 0% of dioxygen than for 10%.

For the Monod model, the parameters variability compared to the initial values is negligible for 0%. For a 10% oxygenation, we obtain two possible sets of parameter values, that correspond to two local minima and for which the distance between model and data is small. We have represented the set

with the smallest distance. Note that the ratio between j_{NAm} and K_N is constant when we started from different initial values.

For the Droop model, the ratio between j_{NAm} and K_N is not longer constant, but the ratio between v and g doesn't vary in this model. Then, we fixed some of the parameter values from the Monod model (mean values of j_{NAm} and K_N obtained from the Monod fit, the bold numbers in Tab. 3.II) and we estimated the others ($v = h_E$, y_{EV} and E_0).

The parameter variability (V), when we started from different initial values, is higher for the more complex models than for the Monod one, whatever the dioxygen concentration is. This strong variability can come from an over-parameterisation. To avoid this, we fixed some of the parameter values (the bold numbers in Tab. 3.II) and we estimated the others.

The variability with the change of the initial parameter value is smaller with equivalent distances. This technique improved the fit of the Droop and DEB models (Fig. 3.2).

The over-parameterisation problem increases with the number of parameters. This phenomenon inevitably resulted from our methodology. Indeed, the data only provides the nitrate and bacterial biomass evolutions at the surface while the model specifies the intrinsic processes to these curves.

3.3.3 Discussion - conclusion

In conclusion, it is not necessary to make classical models more complex for this kind of data which are at constant environmental conditions and which involve only few measured variables. Indeed, in this case, the Droop model, which takes reserve into account, is enough. Present empirical models allow to reproduce a particular ecosystem under constant conditions, but in case of environmental change, the parameter values change and the reproducibility gets lost. The mechanistic model, which is close to the biological processes, needs more data to be parameterised and analysed. Indeed, the model complexity in terms of numbers of parameters and variables must match the availability of data. It has been constructed to study the effect of variable environmental conditions as produced by the bioturbation activity of the macrobenthos. Although too complex for this particular data set, our model obtained parameter values that are useful for perturbation studies.

Kooijman (2000, p321) showed that two different models can pass by the same points with different parameter values, when they are more complex that the data. In our case, for example, measurements of the carbonated substrate would have completed this study. The half saturation constant value

equals to zero for the Droop model, but is different from zero for the Monod model. The parameter values depend on the studied environment but also on the considered species, characterizing a special ecosystem. Its evaluation is important but to find the correct value we have to get enough data and also have to select the correct predominant processes of the considered ecosystem.

As the dioxygen concentration has an important impact on the parameter values, it would be necessary to introduce the concentration of dioxygen as a variable, in order to compare the constant parameters previously obtained. The next step to validate and complete the model is to set up new experiments and measure more variables. Moreover, it would be interesting to study the effect of parameter values on model predictions by simulations.

4

A kinetic inhibition mechanism for maintenance.

Abstract

To fulfil their maintenance costs, most species use mobile pools of metabolites (reserve) in favourable conditions, but can also use less mobile pools (structure) under food-limiting conditions. While the Marr-Pirt model always pays maintenance costs from structure, the presence of reserve inhibits the use of structure for maintenance purposes. The standard Dynamic Energy Budgets (DEB) model captures this by simply supplementing all costs that could not be paid from reserve with structure. This is less realistic at the biochemical level, and involves a sudden use of structure that can complicate the analysis of the model properties. We here propose a new inhibition formulation for the preferential use of reserve above structure in maintenance that avoids sudden changes in the metabolites use. It is based on the application of the DEB theory for synthesizing units, which can easily become rather complex for demand processes, such as the maintenance. We found, however, a simple explicit expression for the use of reserve and structure for maintenance purposes and compared the numerical behaviour with that of the Marr-Pirt model in oscillating conditions, by using parameter values from a fit of the models to data on yeasts in a batch culture. We conclude that our model can better handle variable environments. This new inhibition formulation has a wide applicability in modelling metabolic processes.

Keywords: maintenance - inhibition formulation - DEB theory - Synthesizing Units.

4.1 Introduction

Many applications of models for population dynamics require a tight link between the properties of individuals and that of populations. The Dynamic Energy Budget (DEB) theory for the metabolic organisation of individuals has been designed specifically for this purpose. Generally, the evaluation of population consequences involves the theory of structured population dynamics, but for V1 morphs (i.e. individuals that change in shape during growth such that their surface area is proportional to their volume), the structured dynamics collapses to a rather simple set of ODE's. The population dynamics of dividing organisms (such as most unicellulars) can be well approximated by that of V1-morphs. DEB theory delineates reserve apart from structure, and it has the nice property that the single reserve-single structure system for V1-morphs reduces to the Droop model (Droop, 1968) in the case of neglectably small maintenance costs, to the Marr-Pirt model (Pirt, 1965) in the case of neglectably small reserve capacity, and to the Monod model (Monod, 1942) if both maintenance costs and reserve capacity are neglectably small. Applications to the transient state of food chains (where wild oscillations occur) showed, however, that these quantities cannot be ignored (Kooi and Kooijman, 1994b).

The reduction of the DEB model to the Marr-Pirt model (as discussed in Brandt *et al.*, 2003; Brandt *et al.*, 2004; Evers, 1991a; Kooijman *et al.*, 1991) involves an intriguing problem around the payment of maintenance costs, that is the focus of this paper. Maintenance is the collection of processes to stay alive, excluding net production (growth and reproduction). It comprises the turnover of structure, the activity (transport and movement), the maintenance of concentration gradients and of defence systems. The maintenance costs are taken to be proportional to the amount of structure. The present standard formulation in the DEB model (Kooijman, 2000) is that maintenance is paid from reserve; payment is supplemented with structure if the mobilized reserve flux is too small. This involves a metabolic switch (see Eq. 4.1 for the specification of the switch (S) model), that can become a problem if starvation periods are common, as frequently happens in the field (Gurney *et al.*, 2003). Switches can easily give rise to inaccuracies in numerical simulations to the extent that they can dominate the result. This especially applies to individual-based population models (IBM's), where the number of switches is proportional to the number of individuals in the population. An accurate numerical scheme requires the evaluation of the exact moments at which point events occur, which can be computationally quite intensive if the number of events is large.

The Marr-Pirt model (Harvey *et al.*, 1967; Marr and Ingraham, 1962; Marr *et al.*, 1963; Pirt, 1965) has no reserve and maintenance is always paid from structure. This shrinking is biochemically unrealistic. The difference becomes important as soon as product formation is involved, such as ammonia, which is used as substrate by many organisms. By accounting for reserve(s), the DEB model can handle growth rate related to changes in the chemical composition of biomass, and reserve is typically enriched in nitrogen. In many applications, it is also essential to distinguish maintenance from death, as the products of maintenance are mostly simple minerals (carbon dioxide, ammonia), and that of death is organic matter that might serve as energy substrate for other organisms.

Gurney *et al*. (2003) and Gurney and Nisbet (2004) studied, by means of the DEB theory, the impact of starvation on the resource allocation and the adaptation to poor nutritional conditions. In contexts like these, the details on how maintenance is actually paid do matter and the outcome is quite sensitive to the possible use of structure under starvation conditions and the inhibition of the use of structure by the reserve in non-limiting conditions.

Section 2 of this paper presents a model, based on the DEB theory, for the preferential use of reserve to pay maintenance costs that does not suffer from switches. We call this model the preference (P) model. It turns out to be rather complex for applications in population dynamics; so, we provide a simplified version (SP model) which conserves the same properties.

Section 3 compares the SP and S models and implements the maintenance modules in a population model. We then compare the previous population models with the Marr-Pirt (MP) model using the parameter values of a batch culture of yeast (Evers, 1991b; Ratledge *et al.*, 1984). Finally, we present a numerical study of the properties of the complete SP and the MP models, under varying environmental conditions. Our results are discussed in the last section.

4.2 Models description

4.2.1 Biological processes and general assumptions

In the DEB theory, biomass is partitioned in reserve and structure. Their amounts characterize the individual's state. We here focus on unicellulars, and don't pay attention to maturation and reproduction for reasons given in Kooijman (2000, p118). Reserve is the available material for the metabolic use defined as a temporary biomass; it is a generalised compound, a mixture

of different kinds of protein, lipid, etc. The reserve notion allows for the growth to be dependent on the internal state of the organism and not directly on the external concentrations of nutrients and substrates. Structure represents the part built from reserve and that cannot be remobilized. Resources are taken up from the environment and converted to reserve (assimilation); mobilized reserve that is not allocated to maintenance is converted to structure (growth); see Fig. 4.1. The DEB theory assumes that only the structure needs to be maintained, and the turnover of structure comprises a substantial part of the maintenance costs (Fig. 4.1). The maintenance rate is taken to be proportional to the amount of structure.

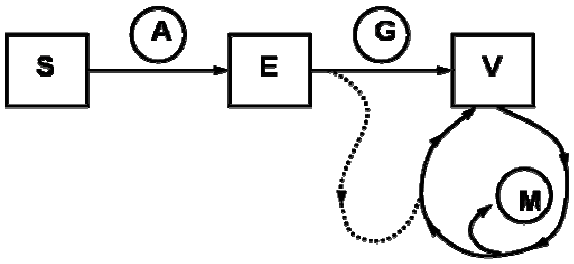

Fig. 4.1. Scheme of the mechanistic assumptions for the uptake and the use of resources in the DEB theory. The processes are *A*: assimilation, *M*: maintenance and *G*: growth, with the state variables *S*: substrates, *E*: reserve compartment and *V*: structural biomass. Maintenance is a part of the structure turnover (the loop). It is paid preferentially by reserve (dashed line) but if reserve is not enough it is paid by structure. The MP model is a particular case of the DEB model considering that A is proportional to G and the dashed line equals to 0.

The rate at which reserve is mobilized only depends on the amounts of reserve and structure and the amount of reserve decreases during starvation. At low reserve levels, allocation rules to the different processes can change to increase the survival period of the individual (Dawes, 1985). Growth usually continues in the first part of the starvation period. Some organisms are able to cease reproduction process. Moreover, when the reserve density drops below a threshold value (prolonged starvation), a variety of possible biological behaviours can occur, such as dormancy (Archuleta *et al.*, 2005) or migration, depending on the species and the environmental factors. Some bacteria can survive starving for many years (Morita, 1985; Postgate, 1990). Many species can, to some extent, shrink in structural mass during starvation, as a way to pay their somatic maintenance costs (Dawes, 1976). Such a shrinking process has been observed in bacteria (Barcina *et al.*, 1997) as well as in invertebrates (molluscs, Downing and Downing, 1993) and vertebrates (shrews, Genoud, 1988) or even humans (Lumey *et al.*, 1995). Maintenance

is preferentially paid from reserve, rather than from structure for efficiency reasons. Since structure is synthesized from reserve as well, payment via structure involves an extra step that comes with overhead costs. Consequently, maintenance costs are paid from reserve when the environmental conditions are good or from structure when the reserve is exhausted (Fig. 4.1).

4.2.2 Mathematical formulations

The preferential use of reserve to pay maintenance costs can be modelled as an inhibition process: the reserve inhibits the use of structure for the maintenance. Indeed, structure will be used for maintenance only when reserve will not be enough. We first recall the switch model and then derive a smooth preference model. A description of variables and parameters is given in the Appendix A, at the end of the manuscript.

The Switch (S) model

The S model (Kooijman, 2000) assumes that reserve allocation to maintenance has absolute priority above growth. If the flux of mobilized reserve is not sufficient to pay maintenance, the rest is paid from structure. The required flux of maintenance is $k_M y_{EP}$ if paid from reserve or $k_M y_{VP}$ if paid from structure. So, the specific loss-fluxes to maintenance are:

$$j_E^M = \min\left(j_E, k_M y_{EP}\right) \text{ and } j_V^M = \left(k_M - j_E^M / y_{EP}\right) y_{VP} \qquad (4.1)$$

where j_E^M is the specific flux of reserve allocated to maintenance, j_V^M the specific flux of structure allocated in maintenance and j_E the specific flux of mobilized reserve that is the reserve flux per unit of structure.

From Eq. 4.1, if j_E is larger than or equal to the maximum maintenance cost paid from reserve, all the maintenance costs are paid from reserve; if j_E is smaller, part of the maintenance costs are paid from structure. Note that if $j_E = 0$, all of the maintenance costs are paid from structure.

The preference (P) model and its simplification (SP)

From the enzymatic point of view, we can consider structure and reserve as substitutable substrates for the maintenance process (Brandt *et al.*, 2004). Each has its own set of products that is released in the environment. Fig. 4.2(A) illustrates our implementation of inhibition based on the concept of Synthesizing Units (SU, Kooijman, 1998, 2000) dealing with fluxes rather than concentrations. In this formulation, the SU can bind both *E* (reserve) and

V (structure) but it can bind *V* only if *E* is not bound. *V* does not affect the binding or transformation of *E*. However, *E* affects also the use of *V* if the last one is already bound; it leads to a release of *V*. *P* is the product of the reaction. Appendix 4.A gives the mathematical formulation of the P model.

Since the P model is rather complex, there is a practical need for simplification. Fig. 4.2(B) and Appendix 4.B present the simplified preference (SP) model, where the two dissociation rates k_E and k_{EV} are equal. This allows for rather simple explicit expressions for the use of reserve and structure for maintenance purposes under the various nutritional conditions, with just a single parameter for the inhibition quantification.

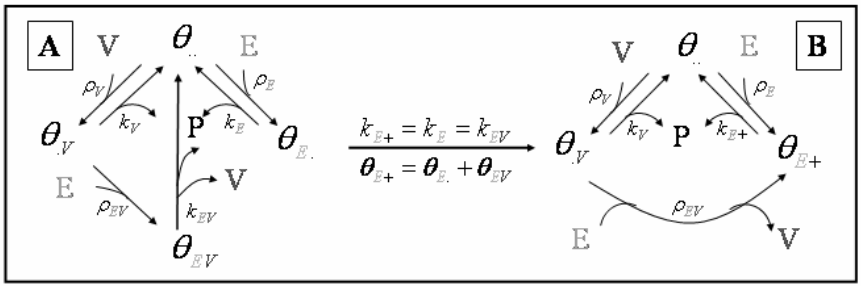

Fig. 4.2. Scheme of the SU states in the P model (A) and the SP model (B). Both models describe the interaction between transformations of reserve (*E*) in product (*P*) and structure (*V*) in product (*P*) for maintenance, with a preference for the first one. The Appendix A describes parameters and variables. The arrow between A and B indicates the transformations to obtain the SP model from the P model.

4.3 Results

4.3.1 Comparison of fluxes

We here compare the fluxes of reserve and structure allocated to maintenance for the S and the SP models, using a time scale separation argument to motivate that the binding fractions of SUs vary in pseudo-equilibrium. Fig. 4.3 illustrates the specific fluxes allocated to maintenance of reserve j_E^M (grey) and structure j_V^M (black) as functions of the available reserve flux j_E. Since turnover is a main part of the maintenance costs, we assume that the specific flux of mobilized structure, j_V is also constant ($\rho_V j_V = k_M y_{VP}$, Appendix 4.B); the part that is not used returns to the structure.

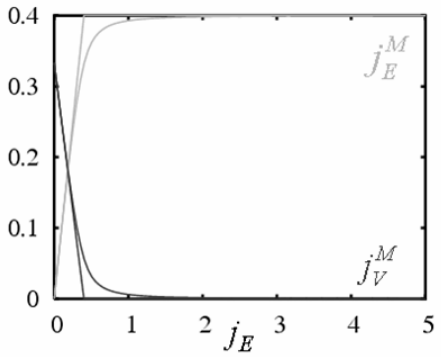

Fig. 4.3. Comparison between the S (lines) and the SP (curves) models through a simulation of the specific reserve (grey) and structure (black) fluxes allocated to maintenance as function of the available reserve with α = 0.1, k_M = 0.04 t^{-1}, y_{PV} = 0.12, y_{PE} = 0.1 and $\rho_E = \rho_{EV} = 1$.

The behaviour of the SP model is controlled by the parameter α: the proportionality ratio between dissociation rates of the SU-structure and the SU-reserve complexes; see Appendix 4.A. When α decreases to zero, the product release from the SU-structure complex is stopped, as long as there is some reserve used for the maintenance. So, α quantifies the ability of the organism to use a minimal structure amount. For vanishing α, the SP model reduces to the S model and the switch appears. The variation of the binding probabilities, ρ_E and ρ_{EV}, affects the threshold value of the reserve density at which the switch occurs. If ρ_{EV} <1, the switch of the SP model is at higher reserve mobilization rates than the S model. The S model is a particular case of the SP model, and the SP model a particular case of the P model.

4.3.2 Parameters estimation in constant environment

We now incorporate the SP and the S modules in a DEB-based population model in a varying environment and compare them with the Marr-Pirt (MP) model, using parameter values that we obtained from fitting the models to a set of data.

Appendix 4.C shows how the SP and the S modules can be implemented in the DEB growth model, and also presents the MP model. We use data from Ratledge *et al*. (1984), on a nitrogen limited yeast, *Apiotrichum curvatum*, growing in a batch culture for the parameter settings that are given in Tab. 4.I. Fig. 4.4 shows the fits of the SP and the MP models. We assume that y_{PV} and k_M are identical for the SP and the MP models. In Fig. 4.4, the S model is also simulated using the parameter values of the SP model.

Contrary to the MP model, the SP model fits the data perfectly. Growth ceases in the MP model as soon as substrate is exhausted, while in fact it continues for a while, due to the use of reserve. The biomass-trajectory of the

MP model is below that of the S and SP models, for the same substrate-trajectory. This observation comes from the condition that $y_{PV} < y_{PE}\, y_{EV}$ meaning that it is more expensive to pay maintenance via structure than via reserve. This is consistent, since the MP model assumes that maintenance is paid from structure only.

As long as there is some reserve, the fraction of SU-reserve complex is positive, but if the reserve is fully depleted, the SU-structure complex becomes dominant. The behaviour of SUs in the SP model is very sensitive for the values of ρ_{EV} and α, while there is hardly an effect at the population level. This is illustrated in Fig. 4.4. We conclude that the values of α and ρ_{EV} are very important at the molecular level, but not at the population level. The implication is also that we need data at the molecular level to estimate these parameters appropriately.

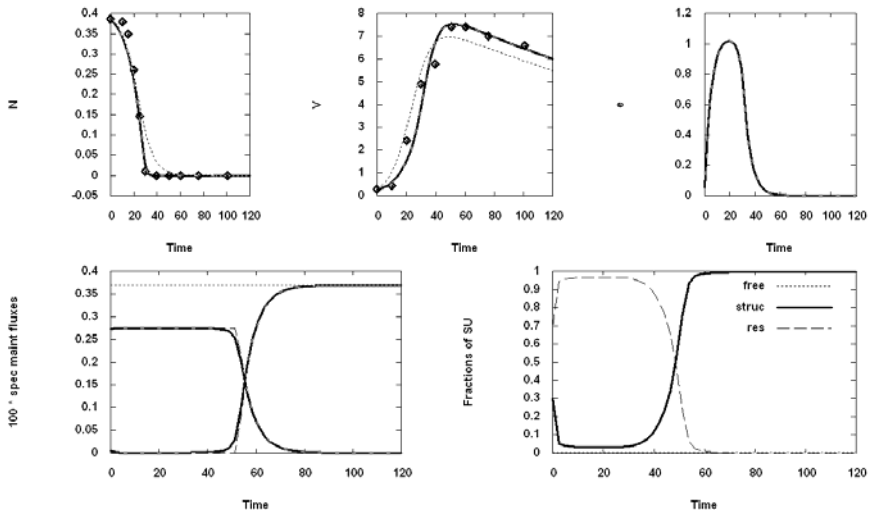

Fig. 4.4. Data (dots) from Ratledge *et al.* (1984) on the growth of the yeast *Apiotrichum curvatum* on nitrate in a batch culture versus time (h). The dotted curve is the fit of the MP model; the line is the fit of the SP modules and the dashed line the simulation of the S model, both implemented in a DEB-based model for V1 morphs. The S and the SP models are superimposed. See Tab. 4.I for parameter values and Appendix 4.C for more details on models formulation. N is the substrate amount in the culture (g$N.l^{-1}$), e the reserve density (g$N.gV^{-1}$), V the structural biomass (g$V.l^{-1}$) and *spec. maint. fluxes* represents j_E^M (g$N.gV^{-1}.h^{-1}$) and j_V^M (h^{-1}).

Tab. 4.I. Estimated parameter values of the SP and the MP models from the set of data from Ratledge *et al.* (1984). See Appendix A, at the end of the manuscript, and Appendix 4.C for the definition of parameters. Here, *E* represents the nitrogen reserve and *gV* the gram of structural biomass. The S model simulations are realised from the SP model parameter values.

Parameters	Unit	Value	Origin
$N\ (t=0)$	$gN.l^{-1}$	0.387	Ratledge *et al.*, 1984
$V\ (t=0)$	$gV.l^{-1}$	0.28	Ratledge *et al.*, 1984
k_M	h^{-1}	$3.25\ 10^{-3}$	Hanegraaf and Muller, 2001
y_{PV}	$gP.gV^{-1}$	$0.9\ y_{PE}\ y_{EV}$	Estimated
The SP model parameters			
$e\ (t=0)$	$gN.gV^{-1}$	0.051	Evers, 1991b
j_{NAm}	$gN.gV^{-1}.h^{-1}$	0.013	Evers, 1991b
K_N	$gN.l^{-1}$	0.05	Evers, 1991b
y_{EV}	$gN.gV^{-1}$	0.829	Kooijman, 2000
y_{EN}	-	17.1637	Estimated
h_E	h^{-1}	0.1821	Estimated
y_{PE}	$gP.gN^{-1}$	1.1797	Estimated
α	-	0.035	Estimated
$j_V' = \rho_V j_V$	h^{-1}	1	Estimated
$\rho_E = \rho_{EV}$	-	1	Estimated
The MP model parameters			
j_{NAm}	$gN.gV^{-1}.h^{-1}$	0.0703	Estimated
K_N	$gN.l^{-1}$	3.48	Estimated
y_{VN}	$gV.gN^{-1}$	19.57	Estimated

4.3.3 Simulations in varying environments

In this section, we compare the MP with the SP model in varying environments. The initial values of structure and reserve and the parameter values are the same as in the previous fit (Tab. 4.I).

We simulate systems with a substrate supply given in $gN.l^{-1}.h^{-1}$ by:

$$I_N(t) = A\exp\left[D\left(\cos(Pt)-1\right)\right] \tag{4.2}$$

where A is the amplitude of the oscillations, D the dispersion of the input peak and P its pulsation.

We have the following cases: (*i*) a batch culture as previously (Eq. 4.2, A= 0 so that $I_N(t)$ = 0, Figs. 4.4 and 4.5); (*ii*) a fed-batch culture with a constant substrate supply (Eq. 4.2, P = 0 so that I_N is a constant, Fig. 4.6); and (*iii*) with a periodically oscillating substrate supply (Fig. 4.7).

In order to study the influence of the supply quality, the total amount of supplied substrate in cases (*ii*) and (*iii*) is taken to be the same and such that the cumulative amount of supplied substrate during the "experiment" equals the initial amount in case (*i*): $N_{\text{int}} = \int_0^{t_{\max}} I_N \, dt = 0.387\ gN.l^{-1}$. Some amplitude variations of N_{int} will be compared.

The comparison of Figs. 4.4 and 4.5 shows that the distance between the MP and SP models increases with the amount of substrate. The biomass in the MP model tends to grow faster than in the SP model because of the absence of reserve (Fig. 4.5). Similarly, the structural biomass in the MP model decreases as soon as substrate is exhausted, while the decrease is delayed if reserve is present (as in the SP model).

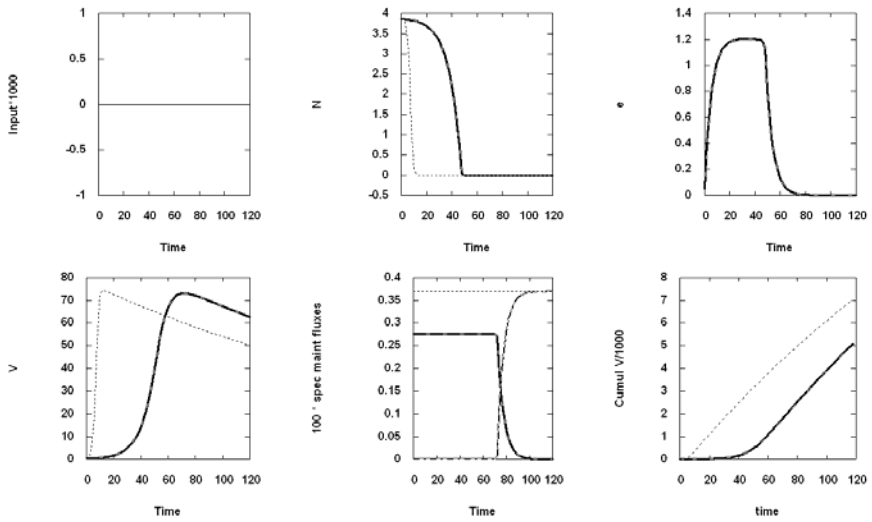

Fig. 4.5. Simulation of the SP (line), S (dash line) and the MP (dot line) models in a batch culture ($I_N = 0$) with initial substrate amount of 3.87 $gN.l^{-1}$ versus time (h). The S and SP models are superimposed. See Tab. 4.I for parameter values. N is the substrate amount in the culture (g$N.l^{-1}$), e the reserve density (g$N.gV^{-1}$), V the structural biomass (g$V.l^{-1}$) and *spec. maint. fluxes* represents j_E^M (g$N.gV^{-1}.h^{-1}$) and j_V^M (h^{-1}), *Input* is I_N ($gN.l^{-1}.h^{-1}$), *Cumul V* the cumulative structural biomass (g$V.l^{-1}$).

Biomass in the MP model grows more slowly at low substrate levels (Figs. 4.6 and 4.7); this model underestimates the cumulative structure and overestimates the substrate. Indeed, for low substrate amounts ($N << K_N$), we have:

$$j_{NAm} \frac{N}{N + K_N} \cong \frac{j_{NAm}}{K_N} N \tag{4.3}$$

For the MP model j_{Nam} / K_N equals 0.02 ($l.gV^{-1}.h^{-1}$), while it equals 0.26 for the SP model. This is the reason for the time delay of the structure dynamics of the MP model in varying environments (Fig. 4.7).

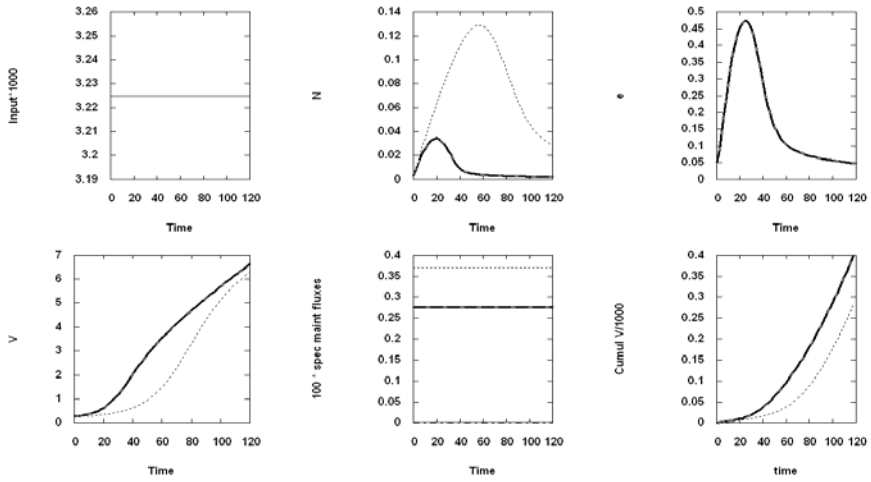

Fig. 4.6. Simulation of the SP (line), S (dash line) and the MP (dot line) models in a fed-batch culture with a constant substrate supply versus time (h). The integrated supply is equal to 0.387 $gN.l^{-1}$. The S and SP models are superimposed. See Tab. 4.I for parameter values. *N* is the substrate amount in the culture, *e* the reserve density, *V* the structural biomass and *spec. maint. fluxes* represents j_E^M and j_V^M, *Cumul V* the cumulative structural biomass and *Input* = I_N.

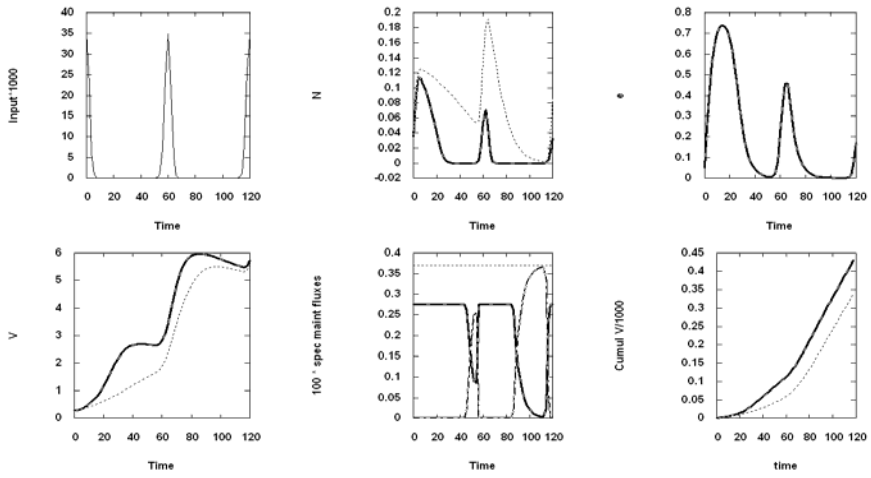

Fig. 4.7. Simulation of the SP (line), S (dash line) and the MP (dot line) models in a fed-batch culture with an oscillating substrate supply versus time (h). The integrated supply equals 0.387 $gN.l^{-1}$. The S and SP models are superimposed. See Tab. 4.I for parameter values. *N* is the substrate amount in the culture, *e* the reserve density, *V* the structural biomass and *spec. maint. fluxes* j_E^M and j_V^M, *Cumul V* the cumulative structural biomass and *Input* = I_N.

Figs 4.5 to 4.7 also show when the cells make the switch of using structure for maintenance.

The MP and SP models can have a similar behaviour in constant environments at low substrate levels, with the same parameter set (results not shown), but they become different in varying environments.

Figs. 4.6 and 4.7 show that the amount of structure at the end of the experiment increases with the amplitude of the oscillations, while the cumulative amount of supplied substrate is the same.

4.5 Discussion - conclusion

Although the P model has the best link up with the underlying processes at the molecular level, it is complex in terms of non-linearity and contains many variables and parameters. The SP and S models turned out to behave very similar, and with the "cost" of a single parameter we could remove a switch and still preserve the link with underlying processes. Indeed, the SP model allows a better understanding of the internal dynamics in variable environment and makes it easier to link the individual level to phenomena at the molecular level and the population or the ecosystem levels. The SP and MP models turned out to be rather different, especially in varying environments. When fitted to the same data, parameters that have the same interpretation can result in different values (see Fig. 4.4 and Tab. 4.I). Furthermore, models that give similar predictions under one set of conditions, can give different predictions under other conditions (Fig. 4.4 compared to Fig. 4.5). These fact arise a problem in the comparison of different models.

Brandt *et al*. (2004) modelled the diauxic growth of microorganisms that live on two substitutable substrates. Diauxic growth patterns arise from the expression if one type of carrier suppresses the expression of the other type. Although applied in a very different context, this module is, in retrospection, identical to the one that we developed here, but then applied to supply systems (substrate controlled), while we had to use demand systems (product controlled). Assimilation (the key process in the study of Brandt) is a supply process, while maintenance is a demand process. Although the concept is the same, the resulting equations look very different. Demand systems are much more complex to model, as is further demonstrated by the study of Kuijper *et al*. (2004) on the use of carbohydrate versus protein reserves for maintenance purposes in zooplankton, assuming that these reserves are partly substitutable. Furthermore, by applying the Brandt *et al*. (2004) formulation

in the flux comparison study, we observe that it doesn't allow the absolute priority of reserve above structure in maintenance (result not shown).

Not all organisms can use structure for maintenance, and die if shrinking is too fast or too far. Muller and Nisbet (2000) implemented death due to starvation when somatic maintenance requirements cannot be met from reserve. They showed that organisms grow bigger at varying food density, rather than constant density with similar average level. We also found that the biomass increases with the amplitude of the substrate supply rate, for reasons that are very similar to the hyperphagia in animals as reported by Gurney *et al*. (2003). Food fluctuations may lead to death by starvation, the likelihood of which increases with the strength and duration of the bleak periods. Like Kooijman (1993, p132-134), Muller and Nisbet suggested that organisms become bigger with increasing latitude (Bermann's law) due to an increasing seasonal variability in food. The results of these different studies are consistent.

Appendix 4.A. Specification of the P model

The change in the fractions of SU that are unbound and bound to one or two substrates in the P model (see Fig. 4.2(A)) is given by:

$$\frac{d}{dt}\begin{pmatrix}\theta_{..}\\ \theta_{E.}\\ \theta_{.V}\\ \theta_{EV}\end{pmatrix}=\begin{pmatrix}-\rho_V j_V-\rho_E j_E & k_E & k_V & k_{EV}\\ \rho_E j_E & -k_E & 0 & 0\\ \rho_V j_V & 0 & -\rho_{EV} j_E-k_V & 0\\ 0 & 0 & \rho_{EV} j_E & -k_{EV}\end{pmatrix}\begin{pmatrix}\theta_{..}\\ \theta_{E.}\\ \theta_{.V}\\ \theta_{EV}\end{pmatrix} \qquad (4.A.1)$$

where j_V and j_E are the specific binding flux for structure and reserve (t^{-1}), respectively. The Appendix A, at the end of the manuscript, describes variables and parameters. The flux of mobilized structure j_V is taken to be constant, because the turnover of structure represents a substantial part of the maintenance costs and $j_E = e\ (h_E - r)$ with r the specific growth rate (Appendix 4.C).

Here, j_*^{Π} is the specific flux, which means by unit of structure, of the compound * (i.e. *S*, *E*, *V* and *P*), associated to the process Π (*A*: assimilation, *M*: maintenance and *G*: growth). Let $J_*^{\Pi} = j_*^{\Pi} V$ be the absolute flux of compound *, associated to the process Π. As enzymatic kinetics is at a lower time-space scale than population dynamics, j_*^{Π} is obtained from the steady state fractions of SU. The absolute reserve and structure fluxes allocated to maintenance are:

$$\begin{cases} J_V^M = j_V^M V = \left(-\rho_V j_V \theta_{..}^* + k_{EV} \theta_{EV}^*\right) V \\ J_E^M = j_E^M V = -y_{EV} j_E \left(\rho_E \theta_{..}^* + \rho_{EV} \theta_{.V}^*\right) V \end{cases} \quad (4.A.2)$$

where θ_{ij}^* is the steady state fraction of SU at the binding state i and j and y_{EV} the yield coefficient of reserve on structure (i.e. cost for structure in terms of reserve).

The release of product in association with maintenance amounts to:

$$\frac{d}{dt} P = y_{PE} \left(k_E \theta_{E.}^* + k_{EV} \theta_{EV}^*\right) V + y_{PV} k_V \theta_{.V}^* V \quad (4.A.3)$$

and simpler as: $\frac{d}{dt} P = J_P^M = j_P^M V$ with $j_P^M = y_{PE} j_E^M + y_{PV} j_V^M$ (4.A.4)

The specific maintenance flux is taken to be constant (output controlled system), so we require that j_P^M is constant ($j_P^M = k_M$) by allowing k_E, k_{EV} and k_V to depend on θ_{ij}^*. We define unequal dissociation rates:

$$\begin{cases} k_V = \alpha k_M / \theta \\ k_E = \beta k_M / \theta \\ k_{EV} = \gamma k_M / \theta \end{cases} \quad \text{with} \quad \theta = \alpha y_{PV} \theta_{.V}^* + y_{PE} (\beta \theta_{E.}^* + \gamma \theta_{EV}^*)$$

Appendix 4.B. Specification of the SP model

We simplify the P model by imposing $k_{E+} = k_E = k_{EV} = k_M / \theta$ and $\theta_{E+} = \theta_E + \theta_{EV}$, where $\theta = \alpha y_{PV} \theta_{.V}^* + y_{PE} \theta_{E+}^*$ (Fig. 4.2(B)). Eq. 4.A.1 then reduces to:

$$\frac{d}{dt} \begin{pmatrix} \theta_{..} \\ \theta_{.V} \\ \theta_{E+} \end{pmatrix} = \begin{pmatrix} -\left(\rho_V j_V + \rho_E j_E\right) & \alpha k_M / \theta & k_M / \theta \\ \rho_V j_V & -\alpha k_M / \theta - \rho_{EV} j_E & 0 \\ \rho_E j_E & \rho_{EV} j_E & -k_M / \theta \end{pmatrix} \begin{pmatrix} \theta_{..} \\ \theta_{.V} \\ \theta_{E+} \end{pmatrix} \quad (4.B.1)$$

The specific fluxes of reserve and structure that are allocated to maintenance are:

$$\begin{cases} j_V^M = \alpha \theta_{.V}^* k_M / \theta^* \\ j_E^M = \left(k_M - y_{PV} j_V^M\right) y_{EP} \end{cases} \quad (4.B.2)$$

Note that, since the specific maintenance costs are constant, and the turnover of structure comprises a substantial part of these costs, it is natural to give at j_V, the specific mobilisation rate of structure, a value just enough to pay maintenance costs in the worst case. The worst case is without reserve ($j_E = 0$); all must be paid from structure. This gives $\rho_V j_V \geq k_M y_{VP}$. Indeed, if $\rho_V j_V < k_M y_{VP}$, it can only pay maintenance costs if there is some reserve left over; and if $e < e_S$, it should die because it can no longer pay maintenance costs. If we want to minimise payment of maintenance costs from structure, the particular case $\rho_V j_V = k_M y_{VP}$ corresponds to a structure flux just enough to pay maintenance costs. But, when $j_E = 0$, this equality fixes the steady state solutions at $\theta_{..}^* = 1$ and $\theta_{.V}^* = 1 - \theta_{..}^* = 0$. Thus, the chosen value of $\rho_V j_V$ influences the evolution of the steady state fractions of SU.

The steady state solutions are explicit, but complicated. For $\rho_E = \rho_{EV}$, $\rho_E j_E = j_E'$ and $\rho_V j_V = j_V'$, the steady state solutions simplify considerably and the specific structure flux allocated to maintenance is:

$$j_V^M = \frac{2Ak_M / y_{PV}}{2A + y_{PE}\left(\sqrt{B^2 - 4AC} - B\right)} \tag{4.B.3}$$

with:

$$\begin{cases} A = \alpha j_V' k_M y_{PV} \\ B = y_{PE} C + \left((1-\alpha) j_E' + j_V'\right) k_M \\ C = -j_E'\left(j_E' + j_V'\right) \end{cases}$$

Appendix 4.C. Implementation of the maintenance modules in the DEB model

We will now implement the SP module in the DEB model of standard V1-morphs, which accounts for assimilation and growth:

$$\begin{aligned} &\frac{d}{dt}S = I_S - j_S^A V \\ &\frac{d}{dt}e = j_E^A - h_E e \\ &\frac{d}{dt}V = rV \end{aligned} \quad \text{with} \quad \begin{aligned} &j_S^A = j_{SAm} f(S) \\ &j_E^A = y_{ES} j_S^A \\ &f(S) = S/(S + K_S) \end{aligned} \tag{4.C.1}$$

Substrate S is, in the example that we use here, the nitrogen compound is represented by N (g$N.l^{-1}$). I_S is the input of substrate (g$N.l^{-1}.h^{-1}$), $f(S)$ is a Michaelis-Menten function with the half saturation constant K_S (g$N.l^{-1}$), y_{ES} is the yield of reserve on substrate and r is the specific growth rate. According to the DEB theory, the specific growth rate is:

$$r = \left(\frac{h_E e - j_E^M}{e + y_{EV}} \right) - j_V^M \left(\frac{y_{EV}}{e + y_{EV}} \right) \tag{4.C.2}$$

The first part of the Eq. 4.C.2 corresponds to the sum of growth and maintenance processes from reserve; the second part corresponds to the maintenance costs that are covered by structure (shrinking). The maintenance costs are no longer constant, due the varying way the costs are covered;

$$j_P^M = y_{PE} j_E^M + y_{PV} j_V^M = k_M \quad \Rightarrow \quad j_E^M + y_{EP} y_{PV} j_V^M = y_{EP} k_M$$

Thus, if $y_{EP}y_{PV} = y_{EV}$, the last equation is equivalent to the standard specific growth rate of the DEB theory:

$$r = \left(\frac{h_E e - y_{EP} k_M}{e + y_{EV}} \right) \tag{4.C.3}$$

In this specific growth rate (Eq. 4.C.2), reserve kinetics doesn't change during shrinking with the implication that growth continues as long as there is some reserve.

We replace j_E^M and j_V^M by the expression of S (Eq. 4.1) or SP (Appendix 4.B) models. Note that j_V^M is a function of $j_E = (h_E - r)\, e$ (Eq. 4.B.3), and so of r; we indicate this with $j_V^M(r)$. This implies that the specific growth rate is only given implicitly. This does not give much practical problems, however, since the sequence:

$$r_{i+1} = \frac{h_E e - k_M / y_{PE} + (y_{PV} / y_{PE} - y_{EV})\, j_V^M(r_i)}{e + y_{EV}} \tag{4.C.4}$$

rapidly converges, $r_i \to r$, in a few steps, starting from $r_0 = 0$.

By replacing the S module (Eq. 4.1) in the Eq. 4.C.2, as long as $j_E > k_M y_{EP}$, the specific growth rate amounts to Eq. 4.C.3.

Payment of maintenance from structure starts when $j_E = k_M y_{EP} = j_E^M$; $j_V^M = 0$; $r = 0$ and $e = y_{EP}\, k_M / h_E = e_S$ is at the threshold value. The growth

rate after this moment switches to $r = -j_V^M$ with $j_V^M = \left(k_M - y_{PE} j_E^M\right) y_{VP}$ and $j_E^M = j_E = \left(h_E - r\right) e$ (all the mobilize resource is used for maintenance). Thus in the S model, the specific growth rate after the switch is:

$$r = \frac{h_E e - y_{EP} k_M}{e + y_{EP} / y_{VP}} \tag{4.C.5}$$

Since $\lim_{e \uparrow e_S} r = \lim_{e \downarrow e_S} r = 0$, the growth rate is continuous around the switch, but not differentiable for $y_{PV} \neq y_{PE} y_{EV}$. This also applies to *de* / *dt*.

In MP model, we have (see Eq. 4.C.1 for the description of j_S^A):

$$r = y_{VS} j_S^A - y_{VP} k_M \tag{4.C.6}$$

Appendix 4.D. Other formulations

In this appendix, we describe and compare other formulations, through the comparison of the specific structure and reserve fluxes allocated to the maintenance, as function of the amount of reserve.

1. SP model with equal dissociation rates (SP-EDR)

Suppose that the dissociation rates are equal: $k_E = k_V = k_{EV} = k_M / \theta$ with k_M is the maintenance cost (t^{-1}), $\theta = y_{PV}\, \theta_V^* + y_{PE}\, \theta_{E+}^*$ and $\theta_{E+} = \theta_{E.} + \theta_{EV}$.

As the Appendix 4.B, we obtain for the SP-EDR model the following specific reserve and structure fluxes allocated to the maintenance:

$$j_V^M = \theta_V^* k_M / \theta^*$$
$$j_E^M = \left(k_M - y_{PV} j_V^M\right) y_{EP}$$

From the condition $\rho_V j_V = k_M y_{VP}$, we also represent the specific fluxes as function of the reserve availability (Fig. 4.D.1).

The switch of this model, given absolute priority of reserve above structure in maintenance, occurs at a higher reserve mobilisation rate than the S model and the SP model.

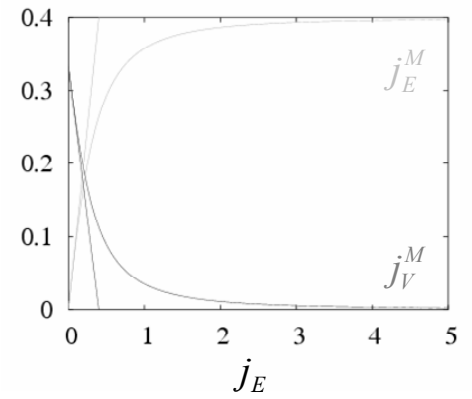

Fig. 4.D.1. Comparison between the S (lines) and the SP models with equal dissociation rates (curves) through a simulation of the specific reserve (grey) and structure (black) fluxes allocated to maintenance as function of the available reserve (j_E) with k_M = 0.04 t^{-1}, y_{PV} = 0.12, y_{PE} = 0.1 and $\rho_E = \rho_{EV} = 1$.

2. Unilateral Binding Inhibition (UBI, Brandt *et al.*, 2004)

Brandt *et al*. (2004) have defined the kinetics represented in Fig. 4.D.2 for the inhibition of one substrate above another. In this model, the reaction $y_{VP}V \rightarrow P$ (structure transformation) is inhibited by the E compound (reserve). The SU can bind both E and V but it can bind V only when E is not bound. And contrary to the P and SP models, E doesn't affect the P production from the V transformation if V is already bound.

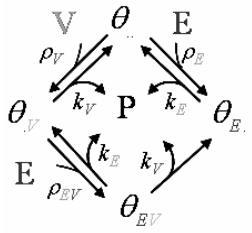

Fig. 4.D.2. Enzymatic kinetics of the UBI model (Brandt *et al.*, 2004). Interaction between the transformations $E \rightarrow P$ and $V \rightarrow P$, with a preference for the first one. A substrate (E) can prevent the use of another one (V) but not *vice et versa*.

As the Appendix 4.B, we obtain for the UBI model the following specific reserve and structure fluxes allocated to the maintenance:

$$j_V^M = \alpha\left(\theta_V^* + \theta_{EV}^*\right)k_M / \theta^*$$

$$j_E^M = \left(k_M - y_{PV}\, j_V^M\right)y_{EP}$$

The numerical study of the UBI model (Fig. 4.D.3) shows, just like the SP model, a smoother switch. This formulation avoids numerical problems and underlines the role of α in the absolute priority of reserve above structure. However, this formulation implies a continuous use of structure whatever the parameter values are.

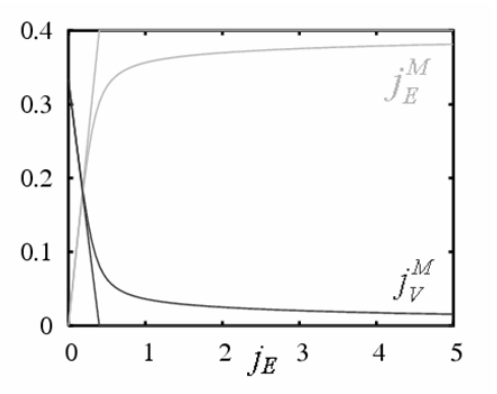

Fig. 4.D.3. Comparison between the S (lines) and the UBI (curves) models through a simulation of the specific reserve (grey) and structure (black) fluxes allocated to maintenance as function of the available reserve (j_E) with $k_M = 0.04\ t^{-1}$, $y_{PV} = 0.12$, $y_{PE} = 0.1$ and $\rho_E = \rho_{EV} = 1$.

3. Other simplifications of the P model

We can also study two other simplifications of the P model (Fig. 4.D.4).

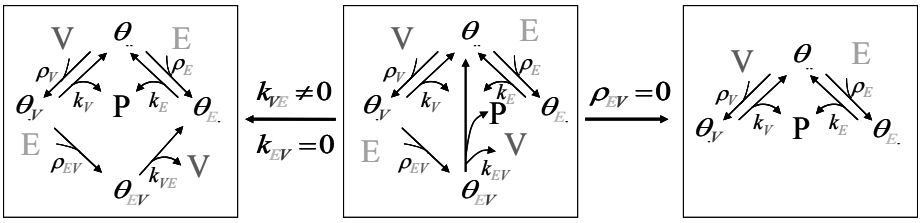

Fig. 4.D.4. Scheme of two other simplifications of the P model (at the centre) - Interaction between $E \rightarrow P$ and $V \rightarrow P$ transformations, with a preference for the first one: at the right, the indirect model (I model) without any direct interference and at the left the direct model (D model) where a substrate (E) can prevent the use of another one (V) but not *vice et versa*. On the arrows are described the assumptions to obtain the new simplified formulations from the P model.

Indirect (I model)

The first simplification (right part of the Fig. 4.D.4) is obtained from $\rho_{EV} = 0$; It is the simplest formulation commonly used in models, where the inhibition is passive and operative through the difference between the binding probabilities of the two compounds. It describes an indirect interaction (SU availability) between conversions $E \rightarrow P$ and $V \rightarrow P$, but without any direct interference contrary the previous formulations. That's why we call it the indirect model (I model).

For the I model, the reasoning is presented in Appendix 4.B, we obtain the following specific reserve and structure fluxes allocated to maintenance:

$$j_V^M = \alpha\theta_{.V}^* k_M / \theta^*$$
$$j_E^M = \left(k_M - y_{PV} j_V^M\right) y_{EP}$$

The numerical study of this first simplification (Fig. 4.D.5) shows insensitivity for variations in the value of α and a strong sensitivity for the ρ_E value variations (binding probability for the SU fraction to be bound with a reserve molecule). Indeed, the more this parameter value decreases, the farer is the I model from the S model. We present here the numerical solution obtained for the maximal probability (ρ_E = 1). The I model curves are very far from the S model whatever the parameter values are.

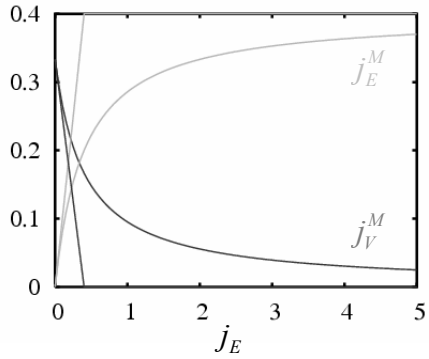

Fig. 4.D.5. Comparison between the S (lines) and the I (curves) models through a simulation of the specific reserve (grey) and structure (black) fluxes allocated to maintenance as function of the available reserve (j_E) with α = 0.1, k_M = 0.04 t^{-1}, y_{PV} = 0.12, y_{PE} = 0.1 and ρ_E = 1.

Direct formulation (D model)

Compared to the P model, the second simplification neglects the direct link of the maintenance production from θ_{EV}, defining a link between θ_{EV} and $\theta_{E.}$. (Fig. 4.D.4). It is called the direct model (D model). It defines a new parameter k_{VE}, the releasing rate of the structure when a reserve molecule is bound on $\theta_{.V}$) different from the dissociation rate for reserve.

From the reasoning presented in Appendix 4.B, the specific reserve and structure fluxes allocated to maintenance for the D model are:

$$j_V^M = \alpha\theta_{.V}^* k_M / \theta^*$$
$$j_E^M = \left(k_M - y_{PV} j_V^M\right) y_{EP}$$

It leads to the same numerical solutions, compared to the SP model, concerning the variations in the α parameter and the new parameter k_{VE} doesn't bring it closer to the S model. Indeed, when this parameter value decreases, the preference for using reserves for maintenance becomes less absolute. (Fig. 4.D.6).

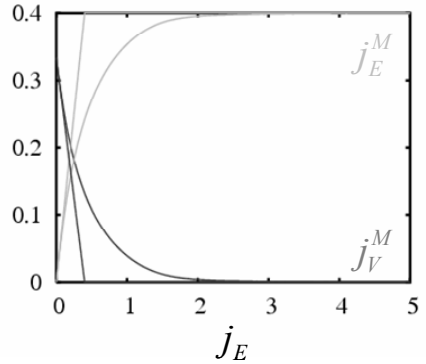

Fig. 4.D.6. Comparison between the S (lines) and the D (curves) models through a simulation of the specific reserve (grey) and structure (black) fluxes allocated to maintenance as function of the available reserve (j_E) with α = 0.1, k_M = 0.04 t^{-1}, y_{PV} = 0.12, y_{PE} = 0.1, ρ_E = ρ_{EV} = 1 and k_{VE} = 0.1.

5

Benthic nitrogen mineralization and RedOx oscillations: a modelling approach

Abstract

Gilbert *et al*. (in preparation) observed that the oscillating environment increases the total mineralised matter compared to the oxic one. To explain this non-expected result, we develop a new mechanistic model (M-model), based on the Dynamic Energy Budget theory, which takes into account the bacterial dynamics, and improves the description of substrate interactions in biogeochemical models. We compare, through a theoretical and a numerical analysis, the usual model based on Michaelis-Menten formulations (Ph-model) with the M-model. The fit of the Ph-model to the oxic and anoxic data allows to obtain parameter values. Simulating oxygen oscillations, the Ph-model suggests that the empirical construction is not suitable for perturbed environments. Furthermore, it doesn't support the non-expected result. The theoretical analysis shows that the phenomenological and the mechanistic approaches lead to different results in the case of environmental perturbations. Contrary to the Ph-model, in the M-model all the supplied matter will be absorbed by the structural biomass which has already been observed experimentally. Moreover, the M-model is much more stable than the Ph-model. We prove that the quality of the dioxygen supply has its importance on the stability, and consequently on the evolution of the compound concentrations. Thus this study demonstrates that the non-expected result is possible.

Keywords: perturbations - Michaelis-Menten kinetics - mechanistic formulations - Synthesizing Units.

5.1 Introduction

Marine sediments are characterised by the dynamic coexistence of oxic and anoxic areas. These RedOx-oscillations (temporal and spatial) come partly from the mixing activity of macrobenthic organisms which represents one of the major processes in the aquatic ecosystem functioning. Among others, this bioturbation activity allows the supply of reduced material at the surface of the sediment and of oxidised matter in depth; it leads to the creation of anaerobic microniches in aerobic sediment (and inversely).

5.1.1 The biogeochemical models

Many biogeochemical models for sediments (Berner, 1980; Boudreau, 1996; Boudreau, 1997; Soetaert *et al.*, 1996) take the bioturbation processes into account by means of a "biodiffusion" term. The associated biodiffusion coefficient D_B is a measure of the reworking induced by the macrofauna. However, some authors have proposed various approaches in order to give a better description of the macrobenthic activities by considering more precise displacements of particles and solutes (Boudreau, 1997; Choi *et al.*, 2002; François-Carcaillet *et al.*, 1997; Meysman *et al.*, 2003). Although, they often consider non-local transport and transformation, they do not explicitly account for bacterial population dynamics.

Bacterial dynamics problem

Bacterial populations are responsible for the degradation processes and the bioturbation activity is known to have a quantitative impact on the microbial activities. Indeed, the oxygenation modifications, linked to bioturbation, affect the bacterial metabolism and lead to a restructuration and a recomposition of bacterial communities. However, all the previous early diagenetic models consider dynamics of bacterial communities to be in steady state. And, the Chapter 2 indicated that a better understanding of the dynamics of the organic matter in models requires an appropriate knowledge of the dynamics of the bacterial community.

Phenomenological problem

Some biogeochemical models describe the interaction between organic matter and bacteria but include other processes such as carbon production, the transfer of matter to higher trophic levels and the different carbon pools (Anderson and Williams, 1998; Anderson and Williams, 1999; Anderson and

Ducklow, 2001; Baretta-Bekker *et al.*, 1995; Blackburn *et al.*, 1996; Dearman *et al.*, 2003; Lancelot *et al.*, 2002; Spitz *et al.*, 2001). Furthermore, in these models, carbon uptake by bacteria is generally computed from Monod kinetics, and the interactions between the various substrates are often of the Michaelis-Menten type.

These phenomenological formulations (early diagenetic and biogeochemical models) do not necessarily represent the intrinsic mechanism. Indeed, empirical formulations are based on experiments with fixed environmental conditions. However, in the natural environment, substrate is rarely in equilibrium and is subjected to spatial or temporal variability of substrate supplies. Moreover, as they don't describe precisely the intrinsic mechanism of the processes and the relations between the different compounds, they do not describe appropriately the interactions between substrates and the concerned communities, in the case of environmental perturbations.

5.1.2 Objectives

In the present work, we aimed to understand the impact of macrobenthic activity on the nitrogen cycle. We give a better description of the biological processes in order to be able to simulate the response of living organisms to perturbations. This improvement of biogeochemical models is required to provide a better estimate of the nitrogen fluxes in marine sediments. The work proposes a trade-off between a more detailed description of biological processes, and a rather simple formulation of model at the ecosystem level. More precisely, we have focused in this work on improving the description of substrate interactions in biogeochemical models, and the relation with the bacterial communities. For this, we developed a new mechanistic model, based on the Dynamic Energy Budget theory (DEB, Kooijman, 2000), which takes into account the bacterial dynamics, and the mechanisms of substrate and biogeochemical processes interactions. In this paper, the different analyses are based on the experiment described in Gilbert *et al*. (in preparation) in order to understand their following non-expected result: the oscillating environment increases the respiration rates, compared to an oxic environment.

5.1.3 Forcing dioxygen as a bioturbation impact

In this experiment (Gilbert *et al.*, in preparation), bioturbation is considered as a forcing factor inducing changes in the dioxygen concentration. Three cases are analysed: a constant oxic environment, a constant anoxic environment and RedOx oscillations (see Fig. 5.1).

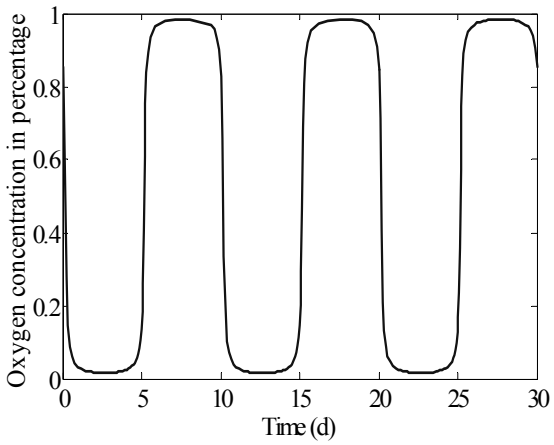

Fig. 5.1. Dioxygen concentration variations in percentage during the experiment. These oscillations are supposed to be induced by macrobenthic activities.

The dioxygen oscillations are obtained from the following formulation:

$$O_2(t) = \left[M + \mathrm{Atan}\left(C * \cos\left(Ft + P \right) \right) / D \right] A \tag{5.1}$$

where *A/D* is the amplitude of the oscillation, *MA* the mean, *C* controls the curved shape, *F* the frequency and *P* the oscillations start.

Compared to the Gilbert *et al*. (in preparation) data, we neglect the transport processes between the overlying water and the porewater environments, assuming that all the activities are achieved in the sediment compartment. Thus, in this study, we underestimate the process rate and concentrations of compound (nitrogen mineralised), focusing on the process ratio and their qualitative behaviour in the different environments (oxic, anoxic and oscillating).

5.1.4 Nitrogen cycle

In this paper, we will focus on the main processes taking place in the nitrogen cycle in the marine sediments, which have been measured in the experiment (Gilbert *et al.*, in preparation): mineralization of organic nitrogen, ammonification, nitrification and denitrification. Indeed, the different reactions rates and the amount of nitrate and ammonium have been measured in the different dioxygen conditions. And, as the ammonification rate was very low in the experiment whatever the oxygenation conditions, we have

neglected it. Furthermore, the nitrogen cycle could be simplified by using the observation that nitrite is always constant in the experiments (see Fig. 5.2).

$$N_{org} \xrightarrow[\text{Mineralisation}]{} NH_4 \xrightarrow[\text{Nitrification}]{} NO_3 \xrightarrow[\text{Denitrification}]{} N_2$$

Fig. 5.2. Processes taken into account in the nitrogen cycle model.

All the respiration processes have regulation rules, depending on the environmental conditions.

5.1.5 Relationships between substrates - process regulations

The first regulation we define concerns the substrates used for the various processes (dioxygen in the oxic mineralization for example). In this case, we can define two modes of transformation of two substrates (X_1 and X_2) into one product (p), as functions of the relative role of each substrate in the process (Brandt *et al.*, 2003).

Firstly, some substrates are complementary: the product formation needs several substrates simultaneously; such that the lack of one substrate prevents the use of the other one (example: dioxygen and organic matter in the oxic mineralization process).

Others are substitutable: the product formation can be from each substrate separately (example: dioxygen and nitrate in the organic matter degradation through respectively the oxic mineralization and the denitrification processes).

If both substrates interact in the binding process, we can have a competition interaction. Indeed, at the level of the enzyme activity, there is the preferential use of one terminal electron acceptor (X_1) with respect to another one (X_2). Thus, the use of X_2 will depend indirectly on the presence of X_1. This interaction is described in the model by enzymatic binding velocities that are greater for one substrate than for the other one. According to the degree of preference, we can observe a continuous weak use of X_2, in presence of the preferential substrate X_1. For example, denitrification and oxic mineralization are in competition concerning the organic matter degradation. But the oxic mineralization is energetically more favourable.

As a second process regulation, the transformation of substrate X_1 can be affected by the presence of substrate X_2. The inhibition can be at the enzyme synthesis level or the enzyme activity level. Indeed, the enzyme synthesis takes place under particular environmental conditions. The inhibition takes

place at the transcription or translation level of the gene coding for the enzyme synthesis (Madigan *et al.*, 2003, p208) Furthermore, X_2 can block a particular step of the process: the enzyme becomes inactive either by X_2 fixation or being partly degraded by the presence of X_2. This transformation will change the enzyme's shape or its composition and will prevent an efficient binding of the initial substrate X_1. As an example, dioxygen inhibits the denitrification process but not totally. The presence of this factor creates a complex impact on the denitrification process. Indeed, the different enzymes occurring in this metabolic way haven't the same sensibility to the dioxygen.

The differences between the competition and the inhibition processes are difficult to define. One of them is that when the inhibiting substrate X_2 disappears, the use of X_1 is delayed because of the damage, contrary to the competition interaction. In our formulations, we considered the same generalized enzyme called Synthesis Unit (SU) in the competition interaction and different SUs in the inhibition interaction.

In the following part, we will compare, through a mathematical and a numerical study, the usual model based on Michaelis-Menten formulations (Berner, 1980; Soetaert *et al.*, 1996) called the phenomenological model (Ph-model) with a new mechanistic model (M-model) based on the DEB theory. We first describe the different models. Then, in order to get parameter values, we fit the Ph-model to the experiment described in Gilbert *et al*. (in preparation). And finally, in order to understand their dynamical differences, we apprehend a theoretical and a numerical analysis.

5.2 The process formulations

5.2.1 The biogeochemical processes

The different experimental measurements (Gilbert *et al.*, in preparation) are dioxygen, nitrate, nitrite and ammonium and the denitrification, nitrification and ammonification rates. Oxic mineralization and nitrification are realised in presence of dioxygen while denitrification and anoxic mineralization are inhibited by the presence of dioxygen. In this study, we will assume that the non-measured organic nitrogen is not saturating, focusing only on the respiration regulation by the presence of dioxygen. The carbon substrate is not measured and assumed to be not-limiting. There are three dioxygen environments: oxic (O_2 = 100%), anoxic (O_2 = 0%) and oscillating (Eq. 5.1) which schematically represents an environment with bioturbation activity, forcing factor inducing changes in the dioxygen concentration (see above). In the following part, NO_3, NH_4 and N_{org} are

respectively the nitrate, ammonium and organic nitrogen concentrations. Furthermore, let us remind that $J_{P,M}$ represents the absolute flux of the process considered P linked to model M. It is linked to the specific process flux $j_{P,M}$ (flux by unit of structure V) by: $J_{P,M} = j_{P,M} V$. As said before, the Ph-model considers bacterial population dynamics at steady state, thus V is a constant. Appendix A presents a description of variables and parameters.

Oxic mineralization

Oxic mineralization needs dioxygen and organic nitrogen. The absolute oxic mineralization rate of the Ph-model is:

$$J_{\min ox,Ph} = R_{\min ox,Ph} \frac{O_2}{K_{\min ox,Ph} + O_2} N_{org} \tag{5.2}$$

where $R_{minox,Ph}$ is the maximum mineralization rate and $K_{minox,Ph}$ the half-saturation constant for dioxygen. In Chapter 2, we proposed for this process the enzymatic kinetics presented in Fig. 5.3.

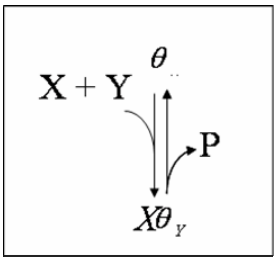

Fig. 5.3. Scheme of two complementary substrates X and Y with X not saturating (Talin *et al.*, 2003). θ. is the free SU and $X\theta_Y$ is the complex formed with the substrate Y fixed and X transformed, P the products of the reaction. In the oxic mineralization, X is the organic nitrogen, Y the dioxygen and P the whole product of the reaction i.e. ammonium, carbon dioxide, water and the mineralised organic matter.

From the general scheme (Fig. 5.3), we obtain for the oxic mineralization the following enzymatic kinetics:

$$O_2 + N_{org} + \mu_{\cdot} \xrightarrow{m_O} N\mu_O \xrightarrow{m'} NH_4 + P_{\text{minox}} + \mu_{\cdot}$$

with $\mu_{\cdot}$ the free SU linked to the oxic mineralization, $N\mu_O$ the complex formed with dioxygen and organic nitrogen and P_{minox} the set of products associated to the process (i.e. carbon dioxide, water and the mineralised organic matter). m_O and m' are the binding and the dissociation rates.

From this kinetics, we obtain the following specific reaction rates (see Chapter 2 for more reasoning behind this description) for the M-model:

$$j_{\min ox,M} = r_{\min ox,M} \frac{O_2}{K_{\min ox,M} + O_2} N_{org} \tag{5.3}$$

It is the usual form of the Michaelis-Menten model (Eq. 5.2) with $r_{\text{minox},M} = m'$ and $K_{\text{minox},M} = m'/m_O$ where m' is the product releasing rate and m_O the binding rate of dioxygen and organic nitrogen.

Nitrification

Nitrification needs ammonium and dioxygen. When the reaction needs two complementary substrates (X and Y) that can be saturating, the usual formulations often use products of Michaelis-Menten terms (Berner, 1980). This is the case of the nitrification process (X: ammonium and Y: dioxygen). The Ph-model amounts to the following formula, with a maximum nitrification rate ($R_{\text{nit},Ph}$), a half-saturation constant for dioxygen ($K_{\text{nit},O,Ph}$) and a half-saturation constant for ammonium ($K_{\text{nit},N,Ph}$).

$$J_{\text{nit},Ph} = R_{\text{nit},Ph} \frac{O_2}{K_{\text{nit},O,Ph} + O_2} \frac{NH_4}{K_{\text{nit},N,Ph} + NH_4} \tag{5.4}$$

The previous formulation fulfils the following limiting constraints: (*i*) if one of the two substrates tends to zero, the transformation rate tends to zero; (*ii*) if one of the limiting factors tends to infinity, the formulation reads as a simple Michaelis-Menten one with respect to the other limiting factor; (*iii*) if the two substrates tend to infinity, the reaction rate is constant and maximal: $J_{\text{nit},Ph} = R_{\text{nit},Ph}$.

The mechanistic formulation proposes a complementarity between NH_4 and O_2 in the nitrification process. Furthermore, the SUs can independently bind first X or Y; the two compounds do not interfere in the binding process: they are parallel (Brandt *et al.*, 2003, Fig. 5.4).

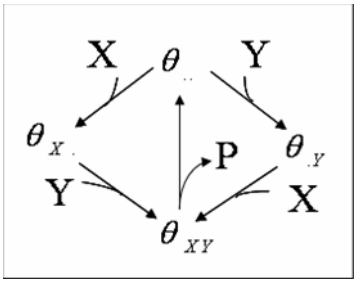

Fig. 5.4. Scheme of two complementary substrates X and Y which can be saturating. Their binding interaction is parallel (Brandt *et al.*, 2003). θ_{**} is the SU at different binding state, P the product of the reaction. In the nitrification case, X could be the dioxygen, Y the ammonium and P the whole products i.e. nitrate and water.

From the general scheme (Fig. 5.4), we obtain for the nitrification the following enzymatic kinetics:

$$O_2 + \nu_{..} \xrightarrow{n_O} \nu_{O.} + NH_4 \xrightarrow{n_{NH}} \nu_{ONH}$$
$$NH_4 + \nu_{..} \xrightarrow{n_{NH}} \nu_{.NH} + O_2 \xrightarrow{n_O} \nu_{ONH}$$
$$\nu_{ONH} \xrightarrow{n'} \nu_{..} + P_{\text{nit}} + NO_3$$

with $\nu_{..}$ the fraction of free SU linked to the nitrification, ν_{**} the fraction of SU's in different binding states, P_{nit} the product associated to the process and not taken into account (i.e. water), n_* the binding rate of compound * and n' the dissociation rate.

From this kinetics, we obtain the following specific nitrification rate:

$$j_{\text{nit},M} = \frac{n' n_O n_{NH} O_2 NH_4 \left(n_O O_2 + n_{NH} NH_4\right)}{n' n_O n_{NH} O_2 NH_4 + n' \left(n_O O_2\right)^2 + n' \left(n_{NH} NH_4\right)^2 + n_O n_{NH} O_2 NH_4 \left(n_O O_2 + n_{NH} NH_4\right)} \tag{5.5}$$

where n' is the production rate associated to the nitrification process, n_O the binding rate of dioxygen and n_{NH} the binding rate of ammonium.

We try to find a link between the Ph-model and the M-model (between Eqs. 5.4 and 5.5) from the limiting constraints. Indeed, the mechanistic formulation fulfils all these constraints, with:

$$\text{If } NH_4 \to \infty \quad \Rightarrow \quad K_{\text{nit},O,M} = n' / n_O$$
$$\text{If } O_2 \to \infty \quad \Rightarrow \quad K_{\text{nit},N,M} = n' / n_{NH}$$
$$\text{If } O_2 \to \infty \text{ and } NH_4 \to \infty \quad \Rightarrow \quad r_{\text{nit},M} = n'$$

We could not find the exact link between both formulations but we have an exact link between the mechanistic formulation and this Michaelis-Menten form:

$$J_{\text{nit}} = R_{\text{nit}} \frac{O_2 NH_4}{K_{\text{nit}} + K_{\text{nit},N} O_2 + K_{\text{nit},O} NH_4 + O_2 NH_4}$$

with $K_{\text{nit}} = K_{\text{nit},N,Ph}\, K_{\text{nit},O,Ph}$ in the Ph-model (Eq. 5.4).

So let us define the following link:

$$r_{\text{nit},M} = n', \; K_{\text{nit},O,M} = \frac{n'}{n_O}, \; K_{\text{nit},N,M} = \frac{n'}{n_{NH}} \text{ and}$$
$$K_{\text{nit},M}\left(O_2, NH_4\right) = -\frac{n' O_2 NH_4}{\left(n_{NH} NH_4 + n_O O_2\right)}$$

In the M-model, K_{nit} is no more a constant but a function of dioxygen and ammonium concentrations and we have:

If one of the two substrates tends to 0, $K_{\text{nit},M} \to 0$

If $O_2 \to \infty$ then $K_{\text{nit},M} = -\dfrac{n' NH_4}{n_O} = -K_{\text{nit},O,M}\, NH_4$

If $NH_4 \to \infty$ then $K_{\text{nit},M} = -\dfrac{n' O_2}{n_{NH_4}} = -K_{\text{nit},N,M}\, O_2$

Denitrification

This reaction needs nitrate and organic nitrogen, and is inhibited by dioxygen. But there is also a competition process between oxic mineralization and denitrification, as described above. The classical models do not distinguish both interactions. Indeed, the Ph-model amounts to the formula:

$$J_{\text{denit},Ph} = R_{\text{denit},Ph} \frac{NO_3}{K_{\text{denit},Ph} + NO_3} \left(1 - \frac{O_2}{K_{\text{inhib,denit},Ph} + O_2}\right) N_{org} \qquad (5.6)$$

with $R_{\text{denit},Ph}$ the maximum denitrification rate, $K_{\text{denit},Ph}$ the half-saturation constant for nitrate and $K_{\text{inhib,denit},Ph}$ the inhibition constant linked to the presence of dioxygen.

In this work, we will only consider the inhibition interaction, but we could then compare it to a competition formulation. For the mechanistic denitrification inhibition, we proposed in Chapter 2 the kinetics presented in Fig. 5.5.

From the general scheme (Fig. 5.5), we obtain for the denitrification the following enzymatic kinetics:

$$NO_3 + N_{org} + \delta_{\cdot} \xrightarrow{d_{NO}} N\delta_{NO} \xrightarrow{d'} P_{\text{denit}} + \delta_{\cdot}$$
$$N\delta_{NO} + O_2 \xrightarrow{d_O} N_{org} + NO_3 + \delta_{\cdot} + O_2$$

with $\delta_{\cdot}$ the free SU linked to the denitrification, $N\delta_{NO}$ the complex formed with nitrate and organic nitrogen, P_{denit} all products associated to the process and not taken into account (i.e. molecular nitrogen, carbon dioxide, water and the mineralised organic matter), d_* and d' are respectively the binding rate of compound * and the dissociation rate. The second line describes the denitrification inhibition by dioxygen.

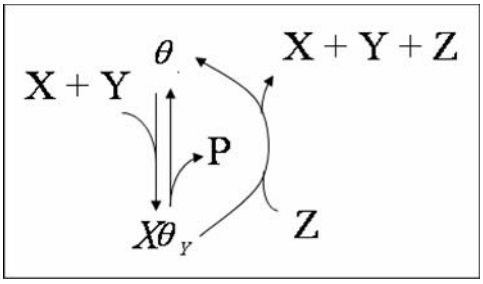

Fig. 5.5. Scheme of two complementary substrates *X* and *Y* where the reaction is inhibited by *Z* (Talin *et al.*, 2003). θ is the free SU and $X\theta_Y$ is the complex formed with the substrate *Y* fixed and *X* transformed, *P* the products of the reaction. In the denitrification, *X* is the organic nitrogen, *Y* the nitrate, *Z* the dioxygen and *P* the whole products i.e. molecular nitrogen, ammonium, carbon dioxide, water and the mineralized organic matter.

From this kinetics, we obtain, for the M-model, the following specific reaction rates (see Chapter 2 for the reasoning behind this description).

$$j_{\text{denit},M} = r_{\text{denit},M} \frac{NO_3}{K_{\text{denit},M} + NO_3}\left(1 - \frac{O_2}{K_{\text{inhib,denit,M}}\left(NO_3\right) + O_2}\right) N_{org} \qquad (5.7)$$

$K_{\text{inhib,denit}}$ is no longer a constant but a linear function of NO_3.

$$K_{\text{inhib,denit},M}\left(NO_3\right) = \frac{d_{NO}}{d_O} NO_3 + \frac{d'}{d_O} \text{ and } \begin{cases} r_{\text{denit},M} = d' \\ K_{\text{denit},M} = \dfrac{d'}{d_{NO}} \end{cases}$$

This result can be explained by the meeting probabilities. Indeed, for a given constant dioxygen concentration, the more the nitrate concentration increases, the more the enzyme will meet a nitrate molecule, the less the inhibition process will take place.

Anoxic mineralization

This reaction needs organic nitrogen and an electron acceptor (as *Mn*, *Fe*, SO_4). To simplify, let us assume that the non-specified electron acceptor is present in a high and constant concentration, so that we do not take it into account. This process is inhibited by dioxygen, like the denitrification process. Moreover, its interaction with the nitrate is not well known. Indeed, the anoxic mineralization, as it is less favourable than the denitrification process (which consumes nitrate) from an energy point of view. It occurs in

the layer below the denitrification zone. But some papers (Scholten *et al.*, 2002) show that the accumulating products of denitrification process inhibit some steps of the anoxic mineralization. The usual models do not distinguish both interactions. Indeed, there is a maximum mineralization rate (R_{mananox}) and two inhibition constants linked to nitrate ($K_{\text{inhib,min},N}$) and dioxygen ($K_{\text{inhib,min},O}$). The Ph-model amounts to the formula:

$$J_{\text{minanox},Ph} = R_{\text{minanox},Ph}\left(1-\frac{O_2}{K_{\text{inhib,min},O,Ph}+O_2}\right)\left(1-\frac{NO_3}{K_{\text{inhib,min},N,Ph}+NO_3}\right)N_{org} \quad (5.8)$$

We formulate both really different interactions using the M-model.

1- Inhibition of the anoxic mineralization by nitrate compound - the M-model

We propose the mechanistic kinetics for this inhibition interaction, presented in Fig. 5.6.

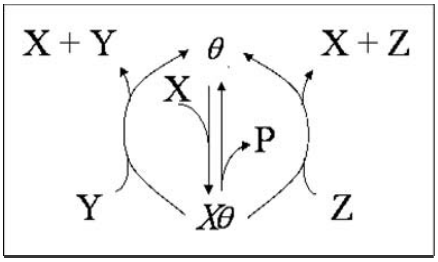

Fig. 5.6. Scheme of a reaction realised from substrate X and inhibited by two other substrates (Y and Z) θ is the free SU and $X\theta$ is the complex formed with the substrate X bound, P the products of the reaction. In the anoxic mineralization, X is the organic nitrogen, Y the dioxygen, Z the nitrate and P the whole products i.e. ammonium, carbon dioxide, water and the mineralized organic matter.

From the general scheme (Fig. 5.6), we obtain, for the anoxic mineralization inhibition, the following enzymatic kinetics:

$$N_{org} + \alpha_{..} \xrightarrow{a} N\alpha \xrightarrow{a'} P_{\text{minanox}} + NH_4 + \alpha_{..}$$
$$N\alpha + O_2 \xrightarrow{a_O} N_{org} + O_2 + \alpha_{..}$$
$$N\alpha + NO_3 \xrightarrow{a_{NO}} N_{org} + NO_3 + \alpha_{..}$$

with $\alpha_{..}$ the free SU linked to the anoxic mineralization, $N\alpha$ the complex formed with the organic nitrogen and the corresponding electron acceptor, P_{minanox} all products associated to the process and not taken into account (i.e. i.e. carbon dioxide, water and the mineralized organic matter), a_* the binding

rate of compound * and *a*' the releasing rate. The second line describes the anoxic mineralization inhibition by dioxygen and the third line by nitrate.

The solution of the system of two equations at steady state gives the following anoxic mineralization rate:

$$\begin{aligned} j_{\text{minanox},M} &= \frac{aa^{'}N_{org}}{a+a^{'}+a_O O_2 + a_{NO}NO_3} \\ &= N_{org}\left(\frac{aa^{'}}{a+a^{'}}\right)\left(1-\frac{a_O O_2}{a+a^{'}+a_O O_2}\right)\left(1-\frac{a_{NO}NO_3}{a+a^{'}+a_O O_2+a_{NO}NO_3}\right) \end{aligned}$$

$$j_{\text{minanox},M} = r_{\text{minanox},M}\left(1-\frac{O_2}{K_{\text{inhib,min},O,M}+O_2}\right)\left(1-\frac{NO_3}{K_{\text{inhib,min},N,M}(O_2)+NO_3}\right)N_{org}$$

(5.9)

For the M-model, we obtain the same formulation than the Ph-model with $K_{\text{inhib,min},N}$ that is no longer constant but the following linear function of dioxygen concentration:

$$K_{\text{inhib,min},N,M}(O_2) = \frac{a+a^{'}+a_O O_2}{a_{NO}} \text{ and } r_{\text{minanox},M} = \frac{aa^{'}}{a+a^{'}},$$

$$K_{\text{inhib,min},O,M} = \frac{a+a^{'}}{a_O}$$

There is as a priority in the inhibition by dioxygen above the inhibition by nitrate which is quite normal as dioxygen is chemically more reactive than nitrate and as there is no denitrification in oxic environment. But, in absence of dioxygen, denitrification will perform the anoxic mineralization inhibition, by the accumulation of its product.

Thus in the case of inhibition interactions, the specific disappearance flux of nitrate and appearance flux of ammonium linked to denitrification and anoxic mineralization processes are:

$$\begin{cases} j_{NO_3,M} = j_{\text{denit},M} \\ j_{NH_4,M} = j_{\text{denit},M} + j_{\text{minanox},M} \end{cases} \quad (5.10)$$

2- Competition between denitrification and anoxic mineralization - the M-model

To express this competition, we can define the enzymatic kinetics described in the Fig. 5.7.

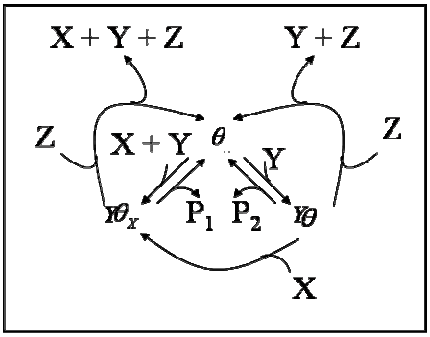

Fig. 5.7. Scheme of two reactions in competition: the first one is realised from substrates *X* and *Y* and the second one is realised only from substrate *Y*, both are inhibited by a third substrate (*Z*). $\theta^{\cdot}$ is the free SU and $Y\theta_*$ is the complex formed at different binding state, *P* the products of the reactions. The first reaction represents the denitrification process and the second one, the anoxic mineralization. Where *X* is the nitrate, *Y* is the organic nitrogen, *Z* the dioxygen and P_1 and P_2 the whole products of the reactions.

From the general scheme (Fig. 5.7), we obtain, for the anoxic mineralization and the denitrification competition, the following enzymatic kinetics:

$$NO_3 + N_{org} + \theta^{\cdot} \xrightarrow{d_{NO}} N\theta_{NO} \xrightarrow{d'} P_{\text{denit}} + \theta^{\cdot}$$

$$N\theta_{NO} + O_2 \xrightarrow{d_O} N_{org} + NO_3 + \theta^{\cdot} + O_2$$

$$N_{org} + \theta^{\cdot} \xrightarrow{a} N\theta \xrightarrow{a'} P_{\text{minanox}} + NH_4 + \theta^{\cdot}$$

$$N\theta + O_2 \xrightarrow{a_O} N_{org} + O_2 + \theta^{\cdot}$$

$$N\theta + NO_3 \xrightarrow{d_{NO}} N\theta_{NO}$$

with $\theta^{\cdot}$ the free SU linked to the anoxic mineralization and denitrification, $N\theta_{NO}$ the complex formed by denitrification, $N\theta$ the complex formed by anoxic mineralization. The other parameters have the same definition than the previous cases (see above).

The first and the third lines specify the denitrification and the anoxic mineralization, respectively. The competition interaction is performed here by a common SU for both processes. In this kinetics, the generalised enzyme will preferentially realise the denitrification process by a greater binding velocity of nitrate. The second and the fourth lines describe the denitrification and the anoxic mineralization inhibition by dioxygen, respectively. But, there is also an absolute priority of denitrification above anoxic mineralization (the

last line) by the binding of nitrate to the complex formed in the anoxic mineralization. In order to simplify the equations, we assume that the binding rate of nitrate to $N\theta$ (the complex of organic nitrogen and the electron acceptor of the anoxic mineralization) is high and equal to the binding rate of nitrate to the free enzyme (d_{NO}).

From the last kinetics, we obtain the following specific disappearance velocities of nitrate linked to denitrification: $j_{NO_3,M} = j_{\text{denit},M}$ with the same parameters as given in Eq. 5.7. And we obtain the following specific appearance rates of ammonium linked to denitrification and anoxic mineralization:

$$j_{NH_4,M} = \frac{aa'd' + aa'd_O O_2 + d_{NO}d'NO_3\left(a + a' + d_{NO}NO_3 + a_O O_2\right)}{\left(d' + d_{NO}NO_3 + d_O O_2\right)\left(a + a' + d_{NO}NO_3 + a_O O_2\right)} N_{org}$$

$$\Leftrightarrow j_{NH_4,M} = j_{\text{denit},M} + j_{\text{minanox},M} - \frac{aa'd_{NO}NO_3}{\left(d' + d_{NO}NO_3 + d_O O_2\right)\left(a + a' + d_{NO}NO_3 + a_O O_2\right)} \quad (5.11)$$

Thus, there is no change in the specific nitrate flux, by considering inhibition or competition interaction. But concerning the specific ammonium flux, there is one term more in competition process (Eq. 5.11) compared to the inhibition interaction (Eq. 5.10). Since the Ph-model, coming from the classical Michaelis-Menten kinetics, does not have this supplementary term, it indicates inhibition rather than competition. Furthermore, by the comparison of the fits of both formulations to a set of data and of the resulting parameter values, we can determine if the interaction between nitrate and the anoxic mineralization is an inhibition or a competition process in the considered environment.

In the future, we could also describe the interaction between the oxic mineralization, denitrification and anoxic mineralization using only one generalised enzyme. This comprehensive system will underline the competition between the different electron acceptors to mineralise the organic matter. From an energy-gain perspective, the SU will preferentially bind dioxygen for the oxic mineralization, then nitrate for the denitrification process and then the electron acceptor for the anoxic mineralization. The nitrification process is not in competition with the other processes. We have to study the coupled processes, using the acquired knowledge, to better represent the interactions existing in the ecosystem.

5.2.2 The bacterial dynamics

Contrary to the Ph-model, we take explicitly into account the bacterial dynamics in the M-model. Following a mechanistic approach (DEB theory), based on enzymatic reactions, Kooijman (2000) proposed a mechanistic model for dynamics of the individual bacterial metabolism. Individual growth is based on the acquisition and the use of energy. It describes the energy and material aspects of how microorganisms assimilate, store substrates (food, nutrients, light) in the reserve compartment and how they use this for maintenance and growth; the corresponding equations are presented further in the section on complete models.

By this very mechanistic approach, we can determine the underlying cell physiology. Moreover, all these sub-processes (assimilation, growth and maintenance) of the overall bacterial dynamics are associated with respiration processes.

5.2.3 The complete formulations

So the M-model and the Ph-model incorporates oxic mineralization (Eqs. 5.2 and 5.3), nitrification (Eqs. 5.4 and 5.5), denitrification that is inhibited by dioxygen (Eqs. 5.6 and 5.7), and anoxic mineralization that is inhibited by dioxygen and nitrate (Eqs. 5.8 and 5.9). The M-model takes explicitly bacterial dynamics into account. We suppose here that organic nitrogen is at the dissolved state. Contrary to the Ph-model, its parameters are expressed per unit of structure. The structural biomass V and the reserve density e are expressed in units of nitrogen. The M-model delineates maintenance and the growth; the maintenance costs are paid from reserve only. I_N is the organic nitrogen input.

Ph-model

$$\begin{cases} \dfrac{dN_{org}}{dt} = I_N - J_{\text{minox},M} + J_{\text{minanox},M} + J_{\text{denit},M} \\ \dfrac{dNH_4}{dt} = J_{\text{minox},M} + J_{\text{minanox},M} - J_{\text{nit},M} + J_{\text{denit},M} \\ \dfrac{dNO_3}{dt} = J_{\text{nit},M} - y_{N_{org}}^{NO_3} J_{\text{denit},M} \end{cases} \tag{5.12}$$

M-model

$$\begin{cases} \dfrac{dN_{org}}{dt} = I_N - \left(j_{\text{minox},M} + j_{\text{mananox},M} + j_{\text{denit},M} \right) V \\ \dfrac{dNH_4}{dt} = \left(j_{\text{minox},M} + j_{\text{mananox},M} - j_{\text{nit},M} + j_{\text{denit},M} \right) V \\ \dfrac{dNO_3}{dt} = \left(j_{\text{nit},M} - y_{N_{org}}^{NO_3} j_{\text{denit},M} \right) V \\ \dfrac{de}{dt} = y_{EN} \left(j_{\text{minox},M} + j_{\text{mananox},M} + j_{\text{nit},M} + j_{\text{denit},M} \right) - k_E e \\ \dfrac{dV}{dt} = \dfrac{k_E e - k_M}{e + y_{EV}} V \end{cases} \tag{5.13}$$

Since the concentration of dioxygen is considered as a known function of time, we can simplify the biogeochemical processes, see Appendix 5.A.

5.3 Results

5.3.1 Data fit

As the data from Gilbert *et al*. (in preparation) does not include bacterial dynamics, we fit here the Ph-model. As the amount of data is small for the number of parameters, some of the parameters of the Ph-model are fixed at the value of Soetaert *et al*. (1996). The initial value of organic nitrogen is unknown and extracted from the data.

During these experiments, the different dioxygen concentrations are maintained at steady state. We first fit in the anoxic condition as some processes do not occur. We then fix the found parameters and fit the oxic condition to find the inhibition rate and the parameters for the oxic processes. The Tab. 5.I gives the parameter values. Finally, after the fitting step, we simulate the system perturbed by varying dioxygen concentrations as a validation step. Fig. 5.8 shows the oxic and anoxic fits and Fig. 5.9 the simulation in an oscillating environment.

Tab. 5.I. Fitted and fixed parameter values of the Ph-model. See Appendix A at the end of the manuscript for parameters definition. Here, * represents the compared parameter value proposed by Soetaert *et al*. (1996); but not used in this work. The estimated parameters are obtained by fitting the Ph-model to a set of data from Gilbert *et al*. (in preparation) and will be used for the stability analysis of the Ph- and M-models. As the M-model gets more parameters, we have to do some assumptions in order to compare it with the Ph-model.

Symbol	Origin	Value	Assumptions in the M-model
$N_{org}(t=0)$	fitted	113	113
		Denitrification	
$R_{\text{denit},Ph}$	fitted	1.2844	$r_{\text{denit},M}$
$K_{\text{denit},Ph}$	fixed	30	$K_{\text{denit},M}$
$K_{\text{inhib,denit},Ph}$	fitted	0.0072 * = 10	$K_{\text{inhib,denit},M}(NO_3) = \frac{r_{\text{denit},M}}{d_O K_{\text{denit},M}} NO_3 + \frac{r_{\text{denit},M}}{d_O}$ $d_O = \frac{r_{\text{denit},M}}{K_{\text{inhib,denit},Ph} K_{\text{denit},M}} NO_3(t=0) + \frac{r_{\text{denit},M}}{K_{\text{inhib,denit},Ph}}$
$y_{N_{org}}^{O_2}$	fixed	5.71	5.71
		Anoxic mineralization	
$R_{\text{minanox},Ph}$	fitted	0.0049	$r_{\text{minanox},M}$
$K_{\text{inhib,min},O,Ph}$	fitted	0.5 * = 5	$K_{\text{inhib,min},O,M}$
$K_{\text{inhib,min},N,Ph}$	fixed	5	$a' <<< a \Leftrightarrow \begin{cases} r_{\text{minanox},M} = a' \\ K_{\text{inhib,min},O,M} = \frac{a}{a_O} \\ K_{\text{inhib,min},N,M}(O_2) = (a + a_O O_2)/a_{NO} \end{cases}$ $O_2 \to 0 \Leftrightarrow K_{\text{inhib,min},N,M}(O_2) = K_{\text{inhib,min},N,Ph}$ $\boxed{K_{\text{inhib,min},N,M}(O_2) = \frac{K_{\text{inhib,min},N,Ph}}{K_{\text{inhib,min},O,M}}(K_{\text{inhib,min},O,M} + O_2)}$
		Oxic mineralization	
$R_{\text{minox},Ph}$	fitted	0.2753	$r_{\text{minox},M}$
$K_{\text{minox},Ph}$	fixed	3	$K_{\text{minox},M}$
		Nitrification	
$R_{\text{nit},Ph}$	fitted	5.9429 * = 20	$r_{\text{nit},M}$
$K_{\text{nit},O,Ph}$	fixed	1	$K_{\text{nit},O,M}$
$K_{\text{nit},N,Ph}$	fitted	10	$K_{\text{nit},N,M}$

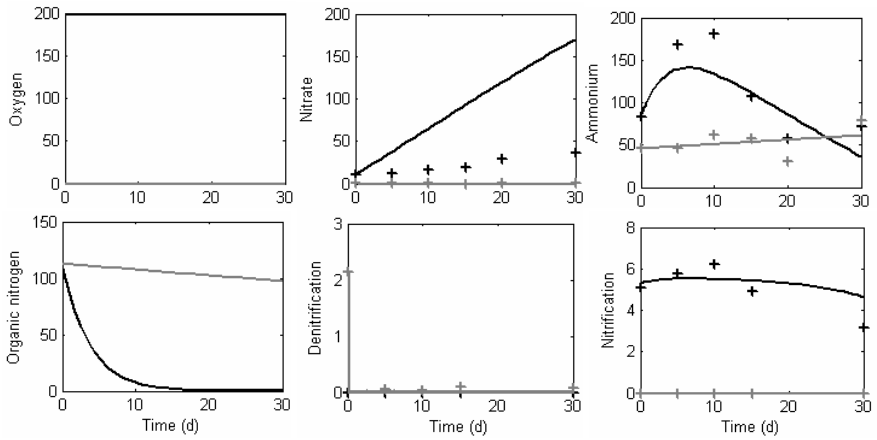

Fig. 5.8. Fit of the Ph-model (lines) on experimental data from Gilbert *et al*. (in preparation, cross), in different oxygenation conditions: dioxygen saturation (black) and anaerobe (grey). See Tab. 5.I for parameter values and Appendix A for unit description.

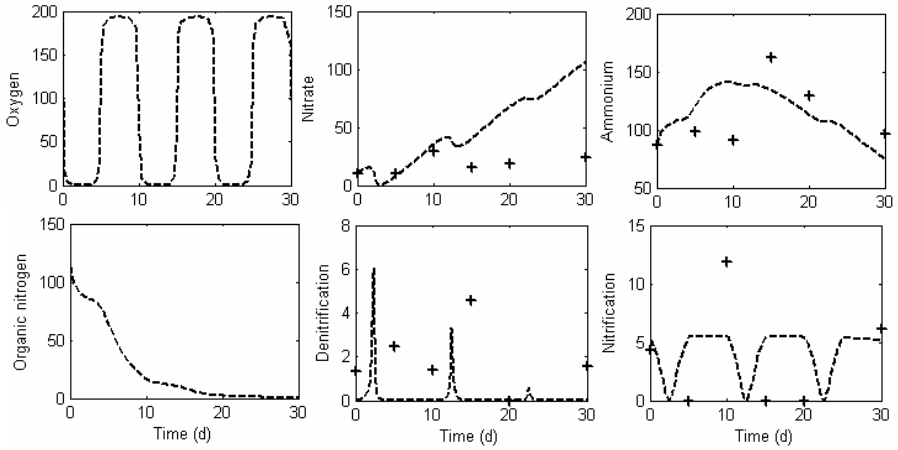

Fig. 5.9. Dynamics of the respiration processes (nitrification and denitrification) and of the nitrate and ammonium concentrations in oscillating oxygenation conditions. The cross are the experimental data from Gilbert *et al*. (in preparation) and the dashed lines the Ph-model simulations. See Tab. 5.I for parameter values and Appendix A for unit description.

However, the data set presents a contradiction. It shows some denitrification while dioxygen is saturating. This unacceptable result can result from: (*i*) the presence of anaerobic microniches, due to a non-homogeneous environment; (*ii*) the aerobic incubation time is not sufficient to obtain the saturation with dioxygen; (*iii*) a very weak inhibition of the denitrification process in the presence of dioxygen, which was not observed in the experimental results that are reported in the literature. We will assume that no denitrification occurs under saturating dioxygen conditions, as it is consistent with the literature.

The reactions rates are extracted from the observed concentrations of compounds. The reaction rates of Ph-model are well determined but we show that there is a bad goodness-of-fit. We can explain this under-estimation of measured nitrate by the diffusion process that occurs from the pore water to the overlying water which is not taken into account in these local models. But this problem can also suggest that the biological dynamics are lacking in the model specification. Now the parameter values are determined; we can use them to simulate the non-measured rates of anoxic and oxic mineralization and the organic nitrogen evolution in strictly oxic and anoxic environments. Concerning the RedOx-oscillation simulation, both reaction rates and compound concentrations are very far from the experimental observations under constant conditions.

An assessment of the mineralized organic nitrogen (during the whole experimental period) has been done, corresponding to:

$$N_{min} = \frac{dN_{org}}{dt} = \frac{dNH_4}{dt} + \frac{dNO_3}{dt} + \frac{dN_2}{dt}$$

Then a comparison between oxic, anoxic and oscillating cases showed that, during the experiment, the complete oxic condition is more efficient for the mineralization and equal to the oscillating case at the end of the simulation. The oscillating and oxic cases are more efficient than the anoxic ones (Fig. 5.10).

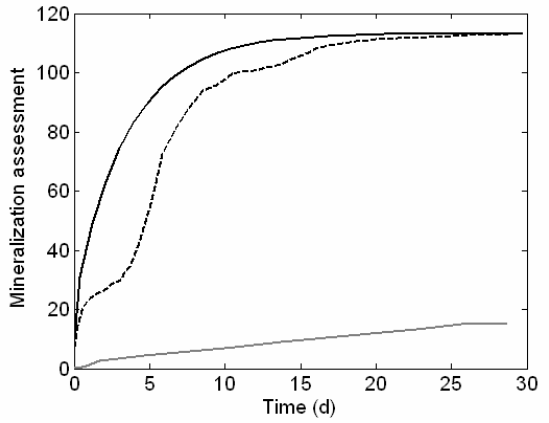

Fig. 5.10. Mineralization assessment for the three dioxygen conditions expressed in $\mu mol\ N.l^{-1}$. The blue curve gives the result for the oscillating dioxygen concentration. The oxic case corresponds to the red curve and the green curve illustrates the anoxic case.

This result is not supported by the experimental observations of Gilbert where the oscillations increased the total mineralization by a factor 4.8. But the model (Fig. 5.8) explains the decrease in ammonium in the oxic case, by the disappearance of organic nitrogen. Thus, the organic nitrogen becomes limiting at 20 days for the oxic case and only at the end of the experiment for the oscillating case. As we look at the total mineralised organic nitrogen, at the end of the experiment, oxic and oscillating environments allow maximal mineralization.

5.3.2 Theoretical analysis

We want to explain the unexpected experimental result: oscillating environment increases the total mineralised matter, compared to an oxic environment. We can see two possibilities. First, we can try to reproduce the observed results with numerical simulations using the mechanistic model. However, this blind method will not reveal the intrinsic properties of the model. Second, we can find the differences between both models analytically, focusing on asymptotic conditions. This method consists of determining the equilibriums and analysing their stability. We have chosen in this second method in our theoretical approach.

To this end, we consider an organic nitrogen input: a system is rarely closed from a biological point of view, even in a batch culture with sediment where a continuous supply of matter invades microniches by diffusion. The organic nitrogen input is assumed to be constant and the organic nitrogen not saturating.

Equilibrium determination

The Ph-model

From Eq. 5.12, we have at steady state:

$$\begin{cases} J_{\text{minox},Ph} + J_{\text{mananox},Ph} + J_{\text{denit},Ph} = I_N \\ J_{\text{minox},Ph} + J_{\text{mananox},Ph} + J_{\text{denit},Ph} = J_{\text{nit},Ph} \\ J_{\text{nit},Ph} = y_{N_{org}}^{NO_3} J_{\text{denit},Ph} \end{cases} \quad \begin{cases} J_{\text{minox},Ph} + J_{\text{mananox},Ph} + J_{\text{denit},Ph} = I_N \\ J_{\text{nit},Ph} = I_N \\ J_{\text{denit},Ph} = I_N \Big/ y_{N_{org}}^{NO_3} \end{cases}$$

The second line of the system gives:

$$R_{\text{NIT},Ph} \frac{NH_4^*}{K_{\text{nit},N,Ph} + NH_4^*} = I_N \Leftrightarrow NH_4^* = \frac{I_N K_{\text{nit},N,Ph}}{R_{\text{NIT},Ph} - I_N}$$

where * indicates the concentration at the equilibrium.

The equilibrium exists if:

$$I_N < R_{\text{NIT},Ph} = R_{\text{nit},Ph} \frac{O_2}{K_{\text{nit},O,Ph} + O_2}$$

As we have verified the biological meaning of the Ph-model (Appendix 5.B), it cannot accept a negative equilibrium value. The negative equilibrium is unstable. This result is not only intuitive but can also be proved mathematically. Indeed, intuitively, it is obvious that if the supply of substrate is too large, it cannot be all consumed and the substrate accumulates. So this negative equilibrium is equivalent to an infinite amount of substrate.

Mathematically, we can easily demonstrate that if $I_N > R_{\text{NIT},Ph} = V_{\text{nit},Ph,MAX}$:

$$\begin{cases} I_N = J_{\text{minox},Ph} + J_{\text{mananox},Ph} + J_{\text{denit},Ph} \\ \dfrac{dNH_4}{dt} = J_{\text{minox},Ph} + J_{\text{mananox},Ph} + J_{\text{denit},Ph} - J_{\text{nit},Ph} \end{cases} \Leftrightarrow \quad \frac{dNH_4}{dt} = I_N - J_{\text{nit},Ph} > \alpha > 0$$

with α a constant. Thus NH_4 is always increasing.

The third line of the system gives:

$$y_{N_{org}}^{NO_3} R_{\text{DENIT},Ph} \frac{NO_3^*}{K_{\text{denit},Ph} + NO_3^*} N_{org}^* = I_N \Leftrightarrow NO_3^* = \frac{I_N K_{\text{denit},Ph}}{y_{N_{org}}^{NO_3} R_{\text{DENIT},Ph} N_{org}^* - I_N}$$

(5.14)

We search N_{org}^{*} (first line of the system):

$$R_{\text{MINOX},Ph}N_{org}^{*} + R_{\text{MINANOX},Ph}\left(1 - \frac{NO_3^{*}}{K_{\text{inhib,min},N,Ph} + NO_3^{*}}\right)N_{org}^{*} + \frac{I_{N_{org}}}{y_{N_{org}}^{NO_3}} = I_{N_{org}}$$

By replacing the Eq. 5.14 in the last equality, we have the following second order polynomial equation:

$$a\left(N_{org}^{*}\right)^2 + b\left(N_{org}^{*}\right) + c = 0$$

with

$$\begin{cases} a = K_{\text{inhib,min},N,Ph}\left(R_{\text{MINOX},Ph} + R_{\text{MINANOX},Ph}\right)y_{N_{org}}^{NO_3}R_{\text{DENIT},Ph} > 0 \\ b = I_N\left(R_{\text{MINOX},Ph}K_{\text{denit},Ph} - K_{\text{inhib,min},N,Ph}\left(R_{\text{MINOX},Ph} + R_{\text{MINANOX},Ph} + \left(y_{N_{org}}^{NO_3} - 1\right)R_{\text{DENIT},Ph}\right)\right) \\ c = {I_N}^2\left(\left(y_{N_{org}}^{NO_3} - 1\right)\Big/ y_{N_{org}}^{NO_3}\right)\left(K_{\text{inhib,min},N,Ph} - K_{\text{denit},Ph}\right) \end{cases}$$

From the parameter values found after the fitting step (Tab. 5.I), we have $c < 0$. Thus:

$$ac < 0 \Leftrightarrow \Delta = b^2 - 4ac > 0 \Leftrightarrow \Delta > b^2 \Leftrightarrow \sqrt{\Delta} > |b|$$

The two solutions of the polynomial equations are real and equal to:

$$N_{org_1} = \frac{-b - \sqrt{\Delta}}{2a} < 0 \text{ and } N_{org_2} = \frac{-b + \sqrt{\Delta}}{2a} > 0\,.$$

As we deal with concentrations, we will only look at the positive solution:

$$N_{org}^{*} = \frac{I_N\left(K_{\text{inhib,min},N,Ph}\left(R_{\text{MINOX},Ph} + R_{\text{MINANOX},Ph} + \left(y_{N_{org}}^{NO_3} - 1\right)R_{\text{DENIT},Ph}\right) - R_{\text{MINOX},Ph}K_{\text{denit},Ph}\right) + \sqrt{\Delta}}{2K_{\text{inhib,min},N,Ph}\left(R_{\text{MINOX},Ph} + R_{\text{MINANOX},Ph}\right)y_{N_{org}}^{NO_3}R_{\text{DENIT},Ph}}$$

with

$$\Delta = {I_N}^2\left(\begin{array}{l}\left(R_{\text{MINOX},Ph}K_{\text{denit},Ph} - K_{\text{inhib,min},N,Ph}\left(R_{\text{MINOX},Ph} + R_{\text{MINANOX},Ph} + \left(y_{N_{org}}^{NO_3} - 1\right)R_{\text{DENIT},Ph}\right)\right)^2 \\ +4K_{\text{inhib,min},N,Ph}R_{\text{DENIT},Ph}\left(R_{\text{MINOX},Ph} + R_{\text{MINANOX},Ph}\right)\left(K_{\text{denit},Ph} - K_{\text{inhib,min},N,Ph}\right)\left(y_{N_{org}}^{NO_3} - 1\right)\end{array}\right)$$

As b and Δ are proportional to I_N, let $N_{\text{org}}^{*} = \sigma I_N$ with σ independent of I_N.

By replacing the N_{org}^{*} in the formulation of NO_3^{*} (Eq. 5.14), we obtain:

$$NO_3^{*} = \frac{K_{\text{denit},Ph}}{y_{N_{org}}^{NO_3} R_{\text{DENIT},Ph}\sigma - 1}$$

So NO_3^{*} doesn't depend on I_N which means that whatever the input of organic nitrogen, there is always the same equilibrium value for nitrate. It can be explained, from a biochemical point of view, by the ceasing of denitrification as soon as there is no more organic nitrogen, leading to an accumulation of nitrate as long as there is some ammonium and dioxygen for the nitrification. Similarly, if ammonium and organic nitrogen tend to zero, nitrate is neither produced nor consumed.

So the unique equilibrium of this trivial system is:

$$\left\{ NH_4^{*} = \frac{I_N K_{\text{nit},N,Ph}}{R_{\text{NIT},Ph} - I_N}, N_{org}^{*} = \sigma I_N, NO_3^{*} = \frac{K_{\text{denit},Ph}}{y_{N_{org}}^{NO_3} R_{\text{DENIT},Ph}\sigma - 1} \right\}$$

With the following existence conditions:

$R_{\text{NIT},Ph} > I_N$ (called Ph1) and $y_{N_{org}}^{NO_3} R_{\text{DENIT},Ph}\sigma > 1$ (called Ph2).

Fig. 5.11 schematically represents the equilibrium as function of the organic nitrogen supply for a constant dioxygen concentration. Indeed, when there is some substrate input, in the chemostat case, there is a stable equilibrium plan, where the input change indicates a curve that increases linearly with I_N for the organic nitrogen.

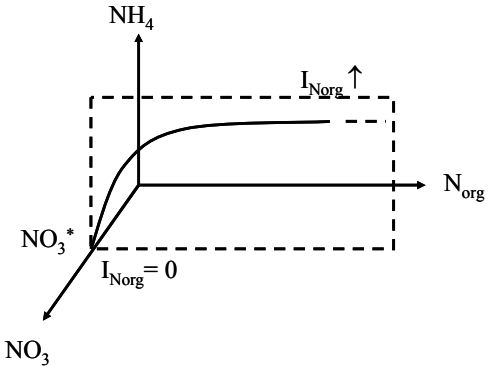

Fig. 5.11. The representation of the equilibrium of the Ph-model as function of the change in the supply of organic nitrogen, for constant dioxygen concentrations.

The M-model

In this case, the bacterial dynamics and the biogeochemical processes are considered at the same space-time scale. This model will help to evaluate the significance of bacterial dynamics. From Eq. 5.13, we have at steady state:

$$\begin{cases} j_{\text{minox},M} + j_{\text{minanox},M} + j_{\text{denit},M} = I_N / V^* \\ j_{\text{nit},M} = I_N / V^* \\ y_{N_{org}}^{NO_3} j_{\text{denit},M} = j_{\text{nit},M} \\ e^* = 2 y_{EN} I_N / k_E V^* \\ e^* = k_M / k_E \end{cases} \Rightarrow \begin{cases} j_{\text{minox},M} + j_{\text{minanox},M} + j_{\text{denit},M} = I_N / V^* \\ j_{\text{nit},M} = I_N / V^* \\ y_{N_{org}}^{NO_3} j_{\text{denit},M} = j_{\text{nit},M} \\ V^* = 2 y_{EN} I_N / k_M \\ e^* = k_M / k_E \end{cases}$$

The second line of the system gives:

$$\Leftrightarrow r_{\text{NIT},M} \frac{NH_4^*}{\frac{K_{\text{NIT},N,M,1} K_{\text{NIT},N,M,2}}{NH_4^* + K_{\text{NIT},N,M,2}} + NH_4^*} = \frac{k_M}{2 y_{EN}}$$

Thus $a\left(NH_4^*\right)^2 + b\left(NH_4^*\right) + c = 0$ with

$$\begin{cases} a = \left(r_{\text{NIT},M} - \dfrac{k_M}{2 y_{EN}} \right) \\ b = K_{\text{NIT},N,M,2} \left(r_{\text{NIT},M} - \dfrac{k_M}{2 y_{EN}} \right) \\ c = -\dfrac{k_M}{2 y_{EN}} K_{\text{NIT},N,M,1} K_{\text{NIT},N,M,2} < 0 \end{cases}$$

If $r_{\text{NIT},M} > \dfrac{k_M}{2 y_{EN}}$ thus $ac < 0 \Leftrightarrow \Delta = b^2 - 4ac > 0 \Leftrightarrow \Delta > b^2 \Leftrightarrow \sqrt{\Delta} > |b|$.

In this case, the system has only one positive solution:

$$NH_4^* = \frac{K_{\text{NIT},N,M,2}}{2} \left(\sqrt{1 + 4 \frac{k_M}{\left(2 y_{EN} r_{\text{NIT},M} - k_M\right)} \frac{K_{\text{NIT},N,M,1}}{K_{\text{NIT},N,M,2}}} - 1 \right)$$

If $r_{\mathrm{NIT},M} < \dfrac{k_M}{2y_{EN}}$ thus $ac > 0$, supposed that $\Delta > 0$ to obtain a real solution, we have $\Delta = b^2 - 4ac > 0 \Leftrightarrow \Delta < b^2 \Leftrightarrow \sqrt{\Delta} < |b|$. But here, a and b are negative. So there is no positive solution. As we deal with concentrations, the case where $r_{\mathrm{NIT},M} < \dfrac{k_M}{2y_{EN}}$ offers no equilibrium.

The third line of the system gives:

$$y_{N_{org}}^{NO_3} j_{\mathrm{denit},M} = \frac{k_M}{2y_{EN}} \text{ with } j_{\mathrm{denit},M} = r_{\mathrm{denit},M} \frac{NO_3}{NO_3 + K_{\mathrm{DENIT},M}} N_{org}$$

$$\Leftrightarrow y_{N_{org}}^{NO_3} r_{\mathrm{denit},M} \frac{NO_3^*}{NO_3^* + K_{\mathrm{DENIT},M}} N_{org}^* = \frac{k_M}{2y_{EN}} \quad \Leftrightarrow \quad NO_3^* = \frac{k_M K_{\mathrm{DENIT},M}}{\left(2y_{EN} y_{N_{org}}^{NO_3} r_{\mathrm{denit},M} N_{org}^* - k_M\right)}$$

(5.15)

We search now for the equilibrium of organic nitrogen (fist line of the system):

$$j_{\mathrm{minox},M} + j_{\mathrm{minanox},M} + j_{\mathrm{denit},M} = \frac{k_M}{2y_{EN}}$$

$$\Leftrightarrow r_{\mathrm{MINOX},M} N_{org}^* + r_{\mathrm{MINANOX},M} \left(1 - \frac{NO_3^*}{K_{\mathrm{inhib,min},N,M} + NO_3^*}\right) N_{org}^* + \frac{k_M}{2y_{N_{org}}^{NO_3} y_{EN}} = \frac{k_M}{2y_{EN}}$$

By replacing Eq. 5.15 in the last equality we have the following second order polynomial equation:

$$a\left(N_{org}^*\right)^2 + b\left(N_{org}^*\right) + c = 0$$

with

$$\begin{cases} a = 2y_{EN} y_{N_{org}}^{NO_3} r_{\mathrm{denit},M} K_{\mathrm{inhib,min},N,M} \left(r_{\mathrm{MINOX},M} + r_{\mathrm{MINANOX},M}\right) > 0 \\ b = k_M \left[r_{\mathrm{MINOX},M} \left(K_{\mathrm{DENIT},M} - K_{\mathrm{inhib,min},N,M}\right) - K_{\mathrm{inhib,min},N,M} \left(r_{\mathrm{MINANOX},M} + \left(y_{N_{org}}^{NO_3} - 1\right) r_{\mathrm{denit},M}\right)\right] \\ c = \left(k_M{}^2 / 2y_{EN}\right) \left(\left(y_{N_{org}}^{NO_3} - 1\right) / y_{N_{org}}^{NO_3}\right) \left(K_{\mathrm{inhib,min},N,M} - K_{\mathrm{DENIT},M}\right) \end{cases}$$

In order to compare both models and because the M-model has more parameters, we made some assumptions that are presented in the Tab. 5.I. From these parameter values $c < 0$. Thus:

$$ac < 0 \Leftrightarrow \Delta = b^2 - 4ac > 0 \Leftrightarrow \Delta > b^2 \Leftrightarrow \sqrt{\Delta} > |b|$$

So this system offers only one equilibrium:

$$N_{org}^{*} = \frac{k_M \left(K_{\text{inhib,min},N,M} \left(r_{\text{MINANOX},M} + \left(y_{N_{org}}^{NO_3} - 1 \right) r_{\text{denit},M} \right) + r_{\text{MINOX},M} \left(K_{\text{inhib,min},N,M} - K_{\text{DENIT},M} \right) \right) + \sqrt{\Delta}}{4 y_{EN} y_{N_{org}}^{NO_3} r_{\text{denit},M} K_{\text{inhib,min},N,M} \left(r_{\text{MINOX},M} + r_{\text{MINANOX},M} \right)}$$

with

$$\Delta = k_M^{\,2} \left(\begin{array}{l} \left(r_{\text{MINOX},M} \left(K_{\text{DENIT},M} - K_{\text{inhib,min},N,M} \right) - K_{\text{inhib,min},N,M} \left(r_{\text{MINANOX},M} + \left(y_{N_{org}}^{NO_3} - 1 \right) r_{\text{denit},M} \right) \right)^2 \\ +4 r_{\text{denit},M} K_{\text{inhib,min},N,M} \left(y_{N_{org}}^{NO_3} - 1 \right) \left(r_{\text{MINOX},M} + r_{\text{MINANOX},M} \right) \left(K_{\text{DENIT},M} - K_{\text{inhib,min},N,M} \right) \end{array} \right)$$

As b and Δ are proportional to k_M, let $N_{\text{org}}^{*} = \sigma k_M$ with σ independent of k_M. We can replace the N_{org}^{*} in NO_3^{*} (Eq. 5.15) such that:

$$NO_3^{*} = \frac{K_{\text{DENIT},M}}{2 y_{EN} y_{N_{org}}^{NO_3} r_{\text{denit},M} \sigma - 1}$$

As σ doesn't depend on k_M, NO_3^{*} doesn't depend on k_M. Thus the unique equilibrium is:

$$\left\{ \begin{array}{l} NH_4^{*} = \frac{K_{\text{NIT},N,M,2}}{2} \left(\sqrt{1 + 4 \frac{k_M}{\left(2 y_{EN} r_{\text{NIT},M} - k_M \right)} \frac{K_{\text{NIT},N,M,1}}{K_{\text{NIT},N,M,2}}} - 1 \right), NO_3^{*} = \frac{K_{\text{DENIT},M}}{2 y_{EN} y_{N_{org}}^{NO_3} r_{\text{denit},M} \sigma - 1}, N_{org}^{*} = \sigma k_M, \\ V^{*} = 2 y_{EN} I_N / k_M, \\ e^{*} = k_M / k_E, \end{array} \right\}$$

With the following existence conditions:

$2 y_{EN} r_{\text{NIT},M} > k_M$ (called M1) and $2 y_{EN} y_{N_{org}}^{NO_3} r_{\text{denit},M} \sigma > 1$ (called M2).

NH_4^{*}, NO_3^{*} and N_{org}^{*} do not depend more on the supply of organic nitrogen compared to Ph-model. The reserve density is constant at equilibrium and also independent of the substrate supply, but depends on the ratio between the maintenance cost and the reserve turnover rate. The equilibrium of structural biomass V^{*} is proportional to the substrate supply and the maintenance rate, and constant as these parameters are considered constant.

The stability analysis

We analyse the stability of this equilibrium. To this end, we first try the analytical method, for both models (see Appendix 5.C), through the construction of the Jacobian matrix and the testing of the Routh-Hurwitz criterion. The Jacobian matrix allows to find the solution of the characteristic equation and the criterion method helps to determine how many roots of the characteristic equation have positive real parts (located in the right hand side of the complex plane), and are therefore unstable. However, it turned out that the model is too complex for this approach.

So we calculate the maximum eigenvalue of the Jacobian numerically in different environmental conditions, using the Matlab software. This numerical method can be used to analyse the local stability: the more negative is the maximal eigenvalue, the more stable is the system. But, a maximal eigenvalue of zero means that the system can be reduced, but it doesn't say anything about the stability of the equilibrium. In this case, we have verified the stability of the model through simulations under asymptotic conditions, with different parameter values. In the following models, a maximal eigenvalue of zero means a local stability.

The Ph-model

So we calculate the maximal eigenvalue numerically as function of the input of organic nitrogen and the dioxygen concentration. As the organic nitrogen is supposed to be non-saturating, we choose a maximal I_N value that is not too large.

This equilibrium is always stable (Fig. 5.12.A). The more the input of organic nitrogen increases, the less stable is the system. In order to have a good visibility of what happens, we put an absolute value (=10) for the maximal eigenvalue in the area where non equilibrium exists which means that the conditions Ph1 and Ph2 are not fulfilled. Fig. 5.11.B-C shows that equilibria exist in a very small area only.

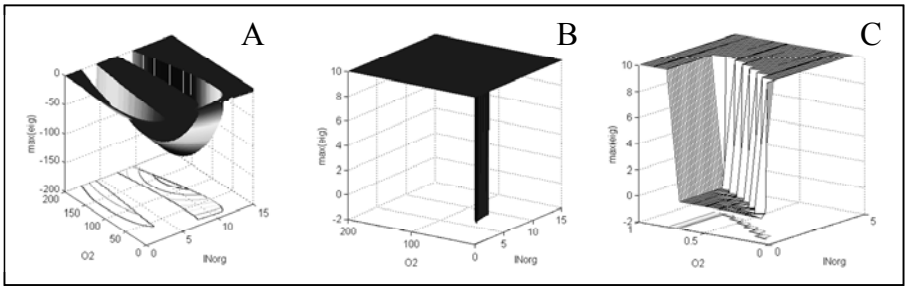

Fig. 5.12. The maximum eigenvalue of Ph-model, as functions of the input organic nitrogen and the dioxygen concentration. The projection of the 3D-graph on the plane below represents the area where the maximal eigenvalue is negative. The value at 10 represents the area where no equilibria exist. (A) without the existence conditions of the equilibriums, (B) with the existence conditions of the equilibriums, (C) like (B) but with more detail around the origin. The other parameter values come from Tab. 5.I.

We also realized an analytical study of batch cultures where the organic nitrogen input is negligible (Appendix 5.D). The result is found to be in accordance with that of chemostats and it allows knowing what happens near the origin of the axes of the graph of Fig. 5.11. Indeed, we obtain a stable equilibrium point which value depends on parameter values and a straight line constituting a set of equilibria: if the system starts on this line, there is no change, if the system starts near this line but not on it, the system evolves to the point. And if the system is stable for an input of organic nitrogen equal to zero, we can safely assume that it will be stable for small value for input.

The M-model

The Figs. 5.13 and 5.14 show the numerical calculation of the maximal eigenvalue in different conditions. The parameter values, used for the bacterial dynamics, come from Chapter 4: y_{EV} = 0.829, m = 7.8x10^{-2} d^{-1}, y_{EN} = 17.1637, k_E = 4.3704 d^{-1}, y_{PE} = 1.1797 with $k_M = y_{EP}\, m$ = 6.6x10^{-2} d^{-1}. For the chosen parameters, condition M2 for the existence of equilibria is always fulfilled.

We first study the evolution of the maximal eigenvalue with the dioxygen concentration and the organic nitrogen supply as in the previous model (Fig. 5.13). In this case, as k_M is very small, condition M1 for the existence of equilibria is mostly fulfilled except for the strictly anoxic environment, as $r_{NIT,M} = r_{nit,M}\, O_2 / (K_{nit,O,M} + O_2)$. The area, for which no equilibria exist, is then at the origin; this is not represented here for better visibility.

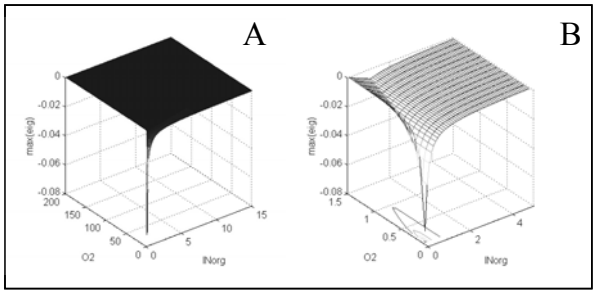

Fig. 5.13. The maximum eigenvalue of the M-model, as functions of the input organic nitrogen and the dioxygen concentration. (A) with the existence conditions of the equilibriums, (B) like (A) but with more detail around the origin. The projection of the 3D-graph on the plane below represents the area where the maximal eigenvalue is negative. The other parameter values come from Tab. 5.I.

Fig. 5.13.A-B shows that the equilibrium is clearly stable for a negligible supply of substrate and low dioxygen concentration (but fulfilling the condition M1). Furthermore, we can see a large plane for the maximal eigenvalue of zero. Some numerical simulations have demonstrated its stability. If the dioxygen concentration increases for the chosen parameter values, there is a very soon inhibition (at very small dioxygen concentrations) of some biogeochemical processes. But, the more the dioxygen concentration increases, the more the denitrification process is inhibited. This phenomenon leads to an accumulation of nitrate. As in our model, the inhibition of denitrification results from a decrease in meeting frequency when the nitrate concentration increases. Thus, when the dioxygen concentration increases, the time needed to achieve the stable equilibrium increases.

As the maintenance cost (k_M) is a very important parameter in this system, we have represented here (Fig. 5.14) the maximal eigenvalue, dependent on the organic nitrogen input and the maintenance cost and for different steady state dioxygen concentrations (0.001, 0.005, 0.01 and 200 $\mu mol\ O_2.l^{-1}$). For strictly anoxic conditions, condition M1 for the existence of equilibria is never fulfilled, as explained before. With the increase in the dioxygen concentration, k_M must quickly become very important for not-fulfilling the existence conditions M1 (for dioxygen concentration around 0.005 $\mu mol\ O_2.l^{-1}$, k_M has to be 1 d^{-1}).

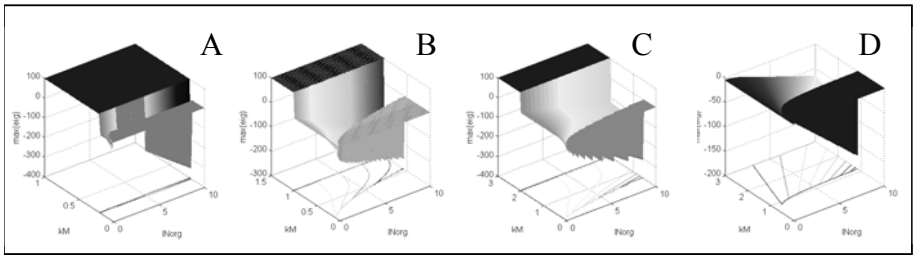

Fig. 5.14. The maximum eigenvalue of the M-model as functions of the input organic nitrogen and the maintenance cost, with existence conditions - the values at 100 represent the area where equilibria do not exist - at: (A) O2=0.001, (B) O2=0.005, (C) O2=0.01, (D) O2=200 the enlarged stability with the existence conditions of the equilibriums where. The projection of the 3D-graph on the plane below represents the area where the maximal eigenvalue is negative. The other parameter values come from Tab. 5.I.

In the same way, the maintenance cost has a small influence on the equilibrium stability and has a big impact on the equilibrium existence condition M1. The more the maintenance cost increases, the more the stability decreases. However, the more the organic nitrogen supply increases, the more the system is stable for large value of the maintenance cost. But for a small value of k_M, the equilibrium stability decreases when the organic nitrogen increases. Furthermore, the more the dioxygen concentration increases and the more the stability area increases. Thus the dioxygen concentration has a stabilizing effect on the system.

We found numerical problems for small values of the organic nitrogen supply. Indeed, for the batch case, this system gives the solution for $V^* = 0$. And for $V^* = 0$, e^* is not defined. This result is not biologically acceptable and for this model, the batch case is not studied.

5.4 Discussion

The fitting step allows: (1) to obtain parameter values of the biogeochemical processes, (2) to simulate changes in the concentrations of unknown compounds (such as the organic nitrogen). With this method, we could also simulate the unknown reaction rates (as the oxic and the anoxic mineralization rates, results not shown). Furthermore, it could help us to predict the amount of dioxygen that is used. This study shows that the reaction rates of Ph-model are well determined by the data, contrary to the concentrations of compounds. Indeed, the Ph-model simulates a higher amount of nitrate than the shown in the data. We can explain this over-estimation of the simulated nitrate by the absence of an important process in this local model: the diffusion process that occurs from the pore water to the overlying water environments. But this problem can also suggest that the formulation should include biological dynamics, which is coherent with the perturbed environment.

Given the obtained parameter values, we have simulated oscillating environments with the Ph-model and compared it with the corresponding data. The model is far from the data and it suggests that the parameter values and the empirical construction are not suitable for perturbed environments. The parameter values do not apply to different conditions.

This study of equilibria helped to reveal the behavioural differences between both models and to see if the mechanistic model allows several equilibriums (a not trivial system). It showed that, in the case of environmental perturbations, the phenomenological and the mechanistic approaches lead to different results. Indeed, if there is some organic matter supply to the sediment, for instance from a phytoplankton bloom, the Ph-model will allow the concentration of NH_4^* and N_{org}^* to increase, while the M-model will not. According to the M-model, all the supplied matter will be absorbed by the structural biomass.

This result has already been observed experimentally. Indeed, the seasonal pulses are thought to have a major influence on levels of activity of the resident microbial community in the sediment (Turley and Lochte, 1990) and at the sediment-water interface (Patching and Eardly, 1997). In order to assess the response of a deep-sea microbial population from the N.E. Atlantic to simulated fall of detrital aggregates, Turley and Lochte (1990) added sterile detritus to deep-sea microbial communities and incubated them under high pressure and low temperature. Rapid colonization, growth, and decomposition rates indicate that the deep-sea benthic microbial community can react quickly to such inputs of organic carbon to the sea bed. In the same

way, Fabiano *et al*. (2001) show that there is a clear response to the flux of labile organic matter by the smallest sized biota. Furthermore, microbial decomposition and transformation of sedimented detrital aggregates may be important in the material flow to the deep-sea and may influence the chemistry of local seawater.

Our conditions for the existence of equilibria showed the M-model are much more stable than the Ph-model.

Moreover, these results show that the dioxygen oscillations can play an important role and some parameter values are dependent on the dioxygen concentration, considered here as a function of time. The existence of NH_4^* in the Ph-model needs $I_N < R_{\mathrm{NIT},Ph}$ with $R_{\mathrm{NIT},Ph} = R_{\mathrm{nit},Ph}\ O_2\ /\ (K_{\mathrm{nit},O,Ph} + O_2)$. Under oscillating dioxygen conditions, we could obtain an accumulation of ammonium if time where $R_{\mathrm{NIT},Ph} < I_N$ (ex: anoxic conditions) is greater than the inverse; so, we can change the asymptotic behaviour, if the dioxygen concentration is oscillating, related to the oscillations amplitude and frequency, above and below the limit of the existence of the equilibrium. In the same way, the equilibrium value for nitrate could also become negative. For the M-model, for a maintenance cost equals to 1 d^{-1} (Fig. 5.14), the system is unstable when $O_2 \rightarrow 0$ and becomes stable when the dioxygen concentration increases. But, as the Ph-model and the M-model don't have the same stability behaviour in terms of area and strength, both models can give different results for the same environmental conditions.

These results show that the quality of the dioxygen supply can have its importance on the stability, and thus on the trajectories of the concentrations of compounds - a weak and constant dioxygen concentration will not give the same result than oscillating dioxygen concentration, with the same integrated amount of dioxygen. Our first idea was to determine the environmental conditions that allow higher mineralization of nitrogen in oscillating conditions than in oxic conditions. So this study demonstrates that this result is possible.

The next step would be to analyse the bifurcation diagram, to study the potential behaviour of the model. It will allow to find the full set of environmental conditions under which the mineralization of nitrogen is higher in oscillating conditions than in oxic conditions. Further, this complete model could be integrated in an early diagenetic model that accounts for transport (diffusion and advection) processes. Moreover, the macrobenthic activity implies other impacts on the bacterial populations and organic matter fate: ingestion, worm's respiration, etc.

Appendix 5.A. Model description and simplification

For nitrification of the M-model, we have:

$$j_{\text{nit},M} = r_{\text{nit},M} \frac{O_2 NH_4}{K_{\text{nit},M}\left(O_2, NH_4\right) + K_{\text{nit},N,M} O_2 + K_{\text{nit},O,M} NH_4 + O_2 NH_4}$$

$$\text{with } r_{\text{nit},M} = n^{'},\ K_{\text{nit},O,M} = \frac{n^{'}}{n_{O_2}},\ K_{\text{nit},N,M} = \frac{n^{'}}{n_{NH_4}} \text{ and}$$

$$K_{\text{nit},M}\left(O_2, NH_4\right) = -\frac{n' O_2 NH_4}{\left(\frac{n'}{n_{NH_4}} NH_4 + \frac{n'}{n_{O_2}} O_2\right)}$$

Thus:

$$\Leftrightarrow j_{\text{nit},M} = r_{\text{nit},M} O_2 \frac{NH_4}{-\frac{r_{\text{nit},M} O_2 NH_4}{\left(\frac{r_{\text{nit},M}}{K_{\text{nit},N,M}} NH_4 + \frac{r_{\text{nit},M}}{K_{\text{nit},O,M}} O_2\right)} + K_{\text{nit},N,M} O_2 + \left(K_{\text{nit},O,M} + O_2\right) NH_4}$$

$$\Leftrightarrow j_{\text{nit},M} = \frac{r_{\text{nit},M} O_2}{\left(K_{\text{nit},O,M} + O_2\right)} \frac{NH_4}{-\frac{K_{\text{nit},N,M} O_2}{\left(K_{\text{nit},O,M} + O_2\right)} \frac{NH_4}{\left(NH_4 + \frac{K_{\text{nit},N,M}}{K_{\text{nit},O,M}} O_2\right)} + \frac{K_{\text{nit},N,M} O_2}{\left(K_{\text{nit},O,M} + O_2\right)} + NH_4}$$

We obtain the following simplified nitrification formulation:

$$j_{\text{nit},M} = \frac{r_{\text{NIT},M} NH_4}{K_{\text{NIT},N,M,1}\left(1 - NH_4 \middle/ \left(NH_4 + K_{\text{NIT},N,M,2}\right)\right) + NH_4}$$

$$\Leftrightarrow \boxed{j_{\text{nit},M} = \frac{r_{\text{NIT},M} NH_4}{\left(K_{\text{NIT},N,M,1} K_{\text{NIT},N,M,2} \middle/ \left(NH_4 + K_{\text{NIT},N,M,2}\right)\right) + NH_4}}$$

with:

$$r_{\text{NIT},M} = \frac{r_{\text{nit},M} O_2}{\left(K_{\text{nit},O,M} + O_2\right)}, K_{\text{NIT},N,M,1} = \frac{K_{\text{nit},N,M} O_2}{\left(K_{\text{nit},O,M} + O_2\right)}, K_{\text{NIT},N,M,2} = \frac{K_{\text{nit},N,M}}{K_{\text{nit},O,M}} O_2$$

For denitrification, we have:

$$j_{\text{denit},M} = r_{\text{denit},M} \frac{NO_3}{K_{\text{denit},M} + NO_3} \left(1 - \frac{O_2}{K_{\text{inhib,denit,M}}\left(NO_3\right) + O_2} \right) N_{org}$$

with $K_{\text{inhib,denit},M}\left(NO_3\right) = \frac{d_{NO_3}}{d_{O_2}} NO_3 + \frac{d'}{d_{O_2}}$, $r_{\text{denit},M} = d'$ and $K_{\text{denit},M} = \frac{d'}{d_{NO_3}}$

Thus:

$$\Leftrightarrow j_{\text{denit},M} = r_{\text{denit},M} \frac{NO_3}{K_{\text{denit},M} + NO_3} \left(1 - \frac{O_2}{\frac{r_{\text{denit},M}}{d_{O_2} K_{\text{denit},M}} NO_3 + \frac{r_{\text{denit},M}}{d_{O_2}} + O_2} \right) N_{org}$$

$$\Leftrightarrow j_{\text{denit},M} = r_{\text{denit},M} \frac{NO_3}{K_{\text{denit},M} + NO_3} \left(\frac{NO_3 + K_{\text{denit},M}}{NO_3 + K_{\text{denit},M} + O_2 \frac{d_{O_2} K_{\text{denit},M}}{r_{\text{denit},M}}} \right) N_{org}$$

We obtain the following simplified denitrification formulation:

$$\boxed{j_{\text{denit},M} = r_{\text{denit},M} \frac{NO_3}{NO_3 + K_{\text{DENIT},M}} N_{org}} \text{ with}$$

$$K_{\text{DENIT},M} = K_{\text{denit},M} + O_2 \frac{d_{O_2} K_{\text{denit},M}}{r_{\text{denit},M}} .$$

	The Ph-model	*The M-model*
Biogeochemical Equations	$\begin{cases} \frac{dN_{org}}{dt} = I_{N_{org}} - J_{\text{minox},Ph} - J_{\text{mininanox},Ph} - J_{\text{denit},Ph} \\ \frac{dNH_4}{dt} = J_{\text{minox},Ph} + J_{\text{mininanox},Ph} - J_{\text{nit},Ph} + J_{\text{denit},Ph} \\ \frac{dNO_3}{dt} = J_{\text{nit},Ph} - y_{N_{org}}^{NO_3} J_{\text{denit},Ph} \end{cases}$	$\begin{cases} \frac{dN_{org}}{dt} = I_{N_{org}} - \left(j_{\text{minox},M} + j_{\text{mininanox},M} + j_{\text{denit},M}\right)V \\ \frac{dNH_4}{dt} = \left(j_{\text{minox},M} + j_{\text{mininanox},M} - j_{\text{nit},M} + j_{\text{denit},M}\right)V \\ \frac{dNO_3}{dt} = \left(j_{\text{nit},M} - y_{N_{org}}^{NO_3} j_{\text{denit},M}\right)V \end{cases}$
Bacterial dynamics	No	$\begin{cases} \frac{de}{dt} = y_{EN}\left(j_{\text{minox},M} + j_{\text{mininanox},M} + j_{\text{nit},M} + j_{\text{denit},M}\right) - k_E e \\ \frac{dV}{dt} = \frac{k_E e - k_M}{e + y_{EV}} V \end{cases}$
O_2	Oscillations: $O_2(t) = \left[M + \text{Atan}\left(C * \cos\left(Ft + P\right)\right)/D\right]A$, Anoxic: $A = 0$, Constant: $C = 0$	
Oxic mineralization	$J_{\text{min ox},Ph} = R_{\text{MINOX},Ph} N_{\text{org}}$ $R_{\text{MINOX},Ph} = R_{\text{min ox},Ph} \frac{O_2}{K_{\text{min ox},Ph} + O_2}$	$j_{\text{min ox},M} = r_{\text{MINOX},M} N_{\text{org}}$ $r_{\text{MINOX},M} = r_{\text{min ox},M} \frac{O_2}{K_{\text{min ox},M} + O_2}$, $r_{\text{min ox},M} = m'$ and $K_{\text{min ox},M} = m'/m_O$
Nitrification	$J_{\text{nit},Ph} = R_{\text{NIT},Ph} \frac{NH_4}{K_{\text{nit},N,Ph} + NH_4}$ $R_{\text{NIT},Ph} = R_{\text{nit},Ph} \frac{O_2}{K_{\text{nit},O,Ph} + O_2}$	$j_{\text{nit},M} = r_{\text{NIT},M} \frac{NH_4}{\left(K_{\text{NIT},N,M,1} K_{\text{NIT},N,M,2} / \left(NH_4 + K_{\text{NIT},N,M,2}\right)\right) + NH_4}$ $r_{\text{NIT},M} = \frac{r_{\text{nit},M} O_2}{\left(K_{\text{nit},O,M} + O_2\right)}, K_{\text{NIT},N,M,1} = \frac{K_{\text{nit},N,M} O_2}{\left(K_{\text{nit},O,M} + O_2\right)}, K_{\text{NIT},N,M,2} = \frac{K_{\text{nit},N,M}}{K_{\text{nit},O,M}} O_2$ $r_{\text{nit},M} = n'$, $K_{\text{nit},O,M} = n'/n_O$, $K_{\text{nit},N,M} = n'/n_{NH}$
Denitrification	$J_{\text{denit},Ph} = R_{\text{DENIT},Ph} \frac{NO_3}{K_{\text{denit},Ph} + NO_3} N_{org}$ $R_{\text{DENIT},Ph} = R_{\text{denit},Ph}\left(1 - \frac{O_2}{K_{\text{inhib,denit},Ph} + O_2}\right)$	$j_{\text{denit},M} = r_{\text{denit},M} \frac{NO_3}{NO_3 + K_{\text{DENIT},M}} N_{org}$ $K_{\text{DENIT},M} = K_{\text{denit},M} + O_2 \frac{d_{O_2} K_{\text{denit},M}}{r_{\text{denit},M}}$, $r_{\text{denit},M} = d'$ and $K_{\text{denit},M} = d'/d_{NO}$
Anoxic mineralization	$J_{\text{mininanox},Ph} = R_{\text{MINANOX},Ph}\left(\frac{K_{\text{inhib,min},N,Ph}}{K_{\text{inhib,min},N,Ph} + NO_3}\right) N_{org}$ $R_{\text{MINANOX},Ph} = R_{\text{mininanox},Ph}\left(\frac{K_{\text{inhib,min},O,Ph}}{K_{\text{inhib,min},O,Ph} + O_2}\right)$	$j_{\text{mininanox},M} = r_{\text{MINANOX},M}\left(\frac{K_{\text{inhib,min},N,M}}{K_{\text{inhib,min},N,M} + NO_3}\right) N_{org}$ $r_{\text{MINANOX},M} = r_{\text{mininanox},M}\left(K_{\text{inhib,min},O,M} / \left(K_{\text{inhib,min},O,M} + O_2\right)\right)$ $r_{\text{mininanox},M} = aa'/\left(a + a'\right)$, $K_{\text{inhib,min},O,M} = \left(a + a'\right)/a_O$ and $K_{\text{inhib,min},N,M}(O_2) = \left(a + a' + a_{O_2} O_2\right)/a_{NO_3}$

Appendix 5.B: The meaning of biogeochemical models

A negative value of the equilibrium or of the variables has no biological meaning. We have to verify that this does not happen for all models:

$$\text{if } X = 0 \Rightarrow \frac{dX}{dt} \geq 0$$

We show that both models respect this condition. This condition proves firstly that a negative equilibrium is unstable and secondly that you cannot obtain a negative equilibrium when the initial value is positive.

$= 0$	*The Ph-model*	*The M-model*
N_{org}	$\frac{dN_{org}}{dt} = I_{N_{org}} \geq 0$	$\frac{dN_{org}}{dt} = I_{N_{org}} \geq 0$
NO_3	$\frac{dNO_3}{dt} = J_{\text{nit},Ph} \geq 0$	$\frac{dNO_3}{dt} = \left(j_{\text{nit},M}\right)V \geq 0$
NH_4	$\frac{dNH_4}{dt} = J_{\text{minox},Ph} + J_{\text{minanox},Ph} + J_{\text{denit},Ph} \geq 0$	$\frac{dNH_4}{dt} = \left(j_{\text{minox},M} + j_{\text{minanox},M} + j_{\text{denit},M}\right)V \geq 0$
e	No	$\frac{de}{dt} = y_{EN}\left(j_{\text{minox},M} + j_{\text{minanox},M} + j_{\text{nit},M} + j_{\text{denit},M}\right) \geq 0$
V	No	$\frac{dV}{dt} = 0$

Appendix 5.C: Stability analysis – analytical way

We present in this appendix the analytical approach. We study the stability of the equilibrium. Let us consider a system of three equations. We construct the corresponding Jacobian matrix *J*:

$$\begin{cases} \dfrac{dx}{dt} = f(x,y,z) \\ \dfrac{dy}{dt} = g(x,y,z) \\ \dfrac{dz}{dt} = h(x,y,z) \end{cases} \quad \Leftrightarrow \quad J = \begin{pmatrix} \dfrac{\partial f}{\partial x} & \dfrac{\partial f}{\partial y} & \dfrac{\partial f}{\partial z} \\ \dfrac{\partial g}{\partial x} & \dfrac{\partial g}{\partial y} & \dfrac{\partial g}{\partial z} \\ \dfrac{\partial h}{\partial x} & \dfrac{\partial h}{\partial y} & \dfrac{\partial h}{\partial z} \end{pmatrix} = \begin{pmatrix} A1 & A2 & A3 \\ B1 & B2 & B3 \\ C1 & C2 & C3 \end{pmatrix}$$

We can determine the eigenvalues of the Jacobian matrix, with the following calculus of the determinant:

$$P(\lambda) = |J - \lambda I_3| = \begin{vmatrix} A1-\lambda & A2 & A3 \\ B1 & B2-\lambda & B3 \\ C1 & C2 & C3-\lambda \end{vmatrix}$$

$$\Leftrightarrow \quad P(\lambda) = \lambda^3 + a_1\lambda^2 + a_2\lambda + a_3 = 0 \qquad (5.C.1)$$

This root of the polynomial of the third degree is called the characteristic equation. If at least one of the eigenvalues is equal to zero, the solution of the equation is easy. And with the sign of these eigenvalues, we can determine the stability of the equilibrium. If the number of eigenvalues exceeds two, we use a Routh-Hurwitz (RH) criterion. This method aims to determine how many roots of the characteristic equation (Eq. 5.C.1) have positive parts (located on the right hand side in the complex plane), and are therefore unstable. For the considered system, we have:

Routh array

$$\begin{matrix} \lambda^3 & 1 & a_2 \\ \lambda^2 & a_1 & a_3 \\ \lambda & b_1 & 0 \\ 1 & a_3 & \end{matrix} \qquad \text{with} \quad b_1 = (a_1a_2 - a_3)/a_1$$

The number of poles in the right half plane (unstable roots) equals the number of sign changes in the first column of the Routh array. We search for the sign of the coefficient in the first row. As an example, for the Ph-model we found:

$$a_1 = R_{\mathrm{MINOX},Ph} + \frac{K_{\mathrm{inhib,min},N,Ph} R_{\mathrm{MINANOX},Ph}}{K_{\mathrm{inhib,min},N,Ph} + NO_3^*} + R_{\mathrm{NIT},Ph} \frac{K_{\mathrm{nit},N,Ph}}{\left(K_{\mathrm{nit},N,Ph} + NH_4^*\right)^2} + R_{\mathrm{DENIT},Ph} \frac{NO_3^* \left(K_{\mathrm{denit},Ph} + NO_3^*\right) + y_{N_{org}}^{NO_3} K_{\mathrm{denit},Ph} N_{org}^*}{\left(K_{\mathrm{denit},Ph} + NO_3^*\right)^2}$$

$$a_2 = R_{\mathrm{NIT},Ph} \frac{K_{\mathrm{nit},N,Ph}}{\left(K_{\mathrm{nit},N,Ph} + NH_4^*\right)^2} \left(R_{\mathrm{DENIT},Ph} \frac{NO_3^*}{K_{\mathrm{denit},Ph} + NO_3^*} + \frac{K_{\mathrm{inhib,min},N,Ph} R_{\mathrm{MINANOX},Ph}}{\left(K_{\mathrm{inhib,min},N,Ph} + NO_3^*\right)^2} \left(K_{\mathrm{inhib,min},N,Ph} + NO_3^* + N_{org}^*\right) + R_{\mathrm{MINOX},Ph} + R_{\mathrm{DENIT},Ph} \frac{K_{\mathrm{denit},Ph} N_{org}^* \left(y_{N_{org}}^{NO_3} - 1\right)}{\left(K_{\mathrm{denit},Ph} + NO_3^*\right)^2} \right)$$

$$+ \frac{R_{\mathrm{DENIT},Ph}}{\left(K_{\mathrm{denit},Ph} + NO_3^*\right)^2} N_{org}^* y_{N_{org}}^{NO_3} \left(\frac{K_{\mathrm{inhib,min},N,Ph} R_{\mathrm{MINANOX},Ph} \left(NO_3^{*2} + K_{\mathrm{denit},Ph} \left(K_{\mathrm{inhib,min},N,Ph} + 2NO_3^*\right)\right)}{\left(K_{\mathrm{inhib,min},N,Ph} + NO_3^*\right)^2} + K_{\mathrm{denit},Ph} R_{\mathrm{MINOX},Ph} \right)$$

$$a_3 = \frac{R_{\mathrm{NIT},Ph} K_{\mathrm{nit},N,Ph}}{\left(K_{\mathrm{nit},N,Ph} + NH_4^*\right)^2} \frac{R_{\mathrm{DENIT},Ph}}{\left(K_{\mathrm{denit},Ph} + NO_3^*\right)^2} N_{org}^* y_{N_{org}}^{NO_3} \left(\frac{R_{\mathrm{MINANOX},Ph} K_{\mathrm{inhib,min},N,Ph} \left(NO_3^{*2} + K_{\mathrm{denit},Ph} \left(K_{\mathrm{inhib,min},N,Ph} + 2NO_3^*\right)\right)}{\left(K_{\mathrm{inhib,min},N,Ph} + NO_3^*\right)^2} + K_{\mathrm{denit},Ph} R_{\mathrm{MINOX},Ph} \right)$$

Thus $a_3 > 0$ whatever the parameter values are and $a_2 > 0$ for the chosen parameter values (Tab. 5.I). But b_1 is not evidently positive or negative. Thus, for complex model, we cannot easily define the sign of these expressions. So this method doesn't help to determine the stability of the Ph- and the M-models.

Appendix 5.D: Batch cultures

The particular case of $I_N = 0$ corresponds to the batch case where there is some initial substrate at the beginning of the experiment but no continuous input.

For the Ph-model, we find two equilibria, a point and a straight line:

$$\left\{ NH_4^* = 0, N_{org}^* = 0, NO_3^* = \frac{K_{\mathrm{denit},Ph}}{y_{N_{org}}^{NO_3} R_{\mathrm{DENIT},Ph} \sigma - 1} \right\} \text{.and } \left\{ N_{org}^* = 0, NH_4^* = 0 \right\}$$

In the same way we construct the Jacobian matrix; and we calculate the determinant and the trace of this matrix for each equilibrium.

For the point, we have:

$$Det\left(J_{I_{N_{org}}=0}\right) = 0 \text{ and } Tr\left(J_{I_{N_{org}}=0}\right) = -\frac{R_{\mathrm{NIT},Ph}}{K_{\mathrm{nit},N,Ph}} < 0$$

The determinant equal to zero indicates that at least one of the eigenvalues is equal to zero. By calculating them, we find:

$$\left\{ \lambda_1 = 0, \lambda_2 = 0, \lambda_3 = -\frac{R_{\mathrm{NIT},Ph}}{K_{\mathrm{nit},N,Ph}} \right\}$$

So this system is stable and can be reduced to one dimension.

For the straight line, we have: $Det\left(J_{I_{N_{org}}=0}\right)=0$ and

$$Tr\left(J_{I_N=0}\right)=-R_{\mathrm{MINOX},Ph}-\frac{R_{\mathrm{NIT},Ph}}{K_{\mathrm{nit},N,Ph}}-R_{\mathrm{MINANOX},Ph}\left(\frac{K_{\mathrm{inhib,min},N,Ph}}{K_{\mathrm{inhib,min},N,Ph}+NO_3^*}\right)-R_{\mathrm{DENIT},Ph}\frac{NO_3^*}{K_{\mathrm{denit},Ph}+NO_3^*}<0$$

By calculating the eigenvalues, we find:

$$\left\{\lambda_1=0,\lambda_2=-R_{\mathrm{MINOX},Ph}-R_{\mathrm{MINANOX},Ph}\left(\frac{K_{\mathrm{inhib,min},N,Ph}}{K_{\mathrm{inhib,min},N,Ph}+NO_3^*}\right)-R_{\mathrm{DENIT},Ph}\frac{NO_3^*}{K_{\mathrm{denit},Ph}+NO_3^*},\lambda_3=-\frac{R_{\mathrm{NIT},Ph}}{K_{\mathrm{nit},N,Ph}}\right\}$$

So this system is also stable and can be reduced in this case to two dimensions.

References

Aller, R.C., and De Master, D.J. (1984) Estimates of particle flux and reworking at the deep-sea floor using 234 Th/238 U disequilibrium. *Earth and Planetary Science Letters* **67**: 308-318.

Anderson, T.R., and Williams, P.J.l.B. (1998) Modelling the seasonal cycle of dissolved organic carbon at station E1 in the English Channel. *Est Coastal Shelf Science* **46**: 93-109.

Anderson, T.R., and Williams, P.J.l.B. (1999) A one dimensional model of dissolved organic carbon cycling in the water column incorporating combined biological-photochemical decomposition. *Global Biogeochemistry Cycles* **13**: 337-349.

Anderson, T.R., and Ducklow, H.W. (2001) Microbial loop carbon cycling in ocean environments studied using a simple steady-state model. *Aquatic Microbiology Ecology* **26**: 37-49.

Archuleta, R.J., Hoppes, P.Y., and Primm, T.P. (2005) Mycobacterium avium enters a state of metabolic dormancy in response to starvation. *Tuberculosis* **in press**.

Auger, P., and Poggiale, J.C. (1998) Aggregation and Emergence in Systems of Ordinary Differential Equations. *Mathematical and Computer Modelling* **27**: 1-22.

Barcina, I., Lebaron, P., and Vives-Rego, J. (1997) Survival of allochthonous bacteria in aquatic systems: a biological approach. *FEMS Microbiology Ecology* **23**: 1-9.

Baretta-Bekker, J.G., Baretta, J.W., and Rasmussen, E.K. (1995) The microbial food web in the European Regional Seas Ecosystem Model. *Netherlands Journal of Sea Research* **33**: 363-379.

Benninger, L.K., Aller, R.C., Cochran, J.K., and Turekian, K.K. (1979) Effects of biological sediment mixing on the 210 Pb chronology and trace metal distribution in a Long Island Sound sediment core. *Earth and Planetary Science Letters* **43**: 241-259.

Berner, R.A. (1980) *Early Diagenesis: A Theoretical Approach.* Princeton, NJ, U.S.A.: Princeton University Press.

Blackburn, N., Zweifel, U.L., and Hagström, Å. (1996) Cycling of marine dissolved organic matter. II. A model analysis. *Aquatic Microbiology Ecology* **11**: 79-90.

Bonin, P., Gilewicz, M., and Bertrand, J.C. (1992) Effects of oxygen on Pseudomonas nautica on nalkane with or without nitrate. *Archives of Microbiology* **157**.

Boudreau, B.P. (1986) Mathematics of tracer mixing in sediments. I-spatially dependent diffusive mixing. II-non local mixing and biological conveyor-belt phenomena. *American Journal Sciences* **286**: 161-238.

Boudreau, B.P. (1996) A method-of-lines code for carbon and nutrient diagenesis in aquatic sediments. *Computational Geosciences* **22**: 479-496.

Boudreau, B.P. (1997) *Diagenetic models and their implementation: modelling transport and reactions in aquatic sediments.* New York: Springer-Verlag Berlin Heidelberg.

Boudreau, B.P. (1999) A theoretical investigation of the organic carbon-microbial biomass relation in sediments. *Aquatic Microbiology Ecology* **17**: 181-189.

Brandt, B.W. (2002) Realistic characterizations of biodegradation. Ph.D. thesis. Amsterdam: Vrije Universiteit, pp. 108.

Brandt, B.W., van Leeuwen, I.M.M., and Kooijman, S.A.L.M. (2003) A general model for multiple substrate biodegradation. Application to co-metabolism of structurally non-analogous compounds. *Water Research* **37**: 4843-4854.

Brandt, B.W., Kelpin, F.D.L., Van Leeuwen, I.M.M., and Kooijman, S.A.L.M. (2004) Modelling microbial adaptation to changing availability of substrates. *Water Research* **38**: 1003-1013.

Choi, J., François-Carcaillet, F., and Boudreau, B.P. (2002) Lattice-automaton bioturbation simulator (LABS) : Implementation for small deposit feeders. *Computational Geosciences* **28**: 213-222.

Crank, J. (1976) *The mathematics of diffusion* England: Oxford University Press.

Dawes, E.A. (1976) *Endogenous metabolism and the survival of starved prokaryotes*. Cambridge: Cambridge University Press.

Dawes, E.A. (1985) *Starvation, survival and energy reserves.* London: Academic Press.

Dearman, J.R., Taylor, A.H., and Davidson, K. (2003) Influence of autotroph model complexity on simulations of microbial communities in marine mesocosms. *Marine Ecology Progress Series* **250**: 13-28.

Dilão, R., and Domingos, T. (2000) A general approach to the modelling of trophic chains. *Ecological Modelling* **132**: 191-202.

Douglas, J., and Rachford, H. (1956) On the numerical solution of the heat conduction problem in two and three space variables. *Transactions of American Mathematical Society* **82**: 421-439.

Downing, W.L., and Downing, J.A. (1993) Molluscan shell growth and loss. *Nature (Lond.)*: 362-506.

Droop, M.R. (1968) Vitamin B12 and marine ecology. IV. The kinetics of uptake, growth and inhibition in Monochrysis lutheri. *Journal of Marine Biology Assessment U.K.* **48**: 689-733.

Evers, A.G. (1991a) A model for light-limited continuous cultures: growth, shading and maintenance. *Biotechnology and Bioengineering* **38**: 254-259.

Evers, A.G. (1991b) Growth, starvation and storage in micro-organisms. Ph.D. Thesis. Amsterdam: Vrije Universiteit, pp. 116.

Fabiano, M., Pusceddu, A., Dell'Anno, A., Armeni, M., Vanucci, S., Lampitt, R.S., Wolff, G.A., and Danovaro, R. (2001) Fluxes of phytopigments and labile organic matter to the deep ocean in the NE Atlantic Ocean. *Progress In Oceanography* **50**: 89-104.

Fenchel, T. (1996) Worm burrows and oxic microniches in marine sediments. 1. Spatial and temporal scales. *Marine Biology* **127**: 289-296.

Ferzinger, J.H., and Peric, M. (1999) *Computational methods for fluid dynamics*.

Fisher, J.B., Lick, W.J., McCall, P.L., and Robbins, J.A. (1980) Vertical mixing of lake sediments by Tubificid Oligochaetes. *Journal of Geophysical Research* **85**: 3997-4006.

François-Carcaillet, F., Poggiale, J.C., Durbec, J.P., and Stora, G. (1997) A new approach for the modelling of sediment reworking induced by a macrobenthic community. *Acta Biotheoretica* **45**: 295-319.

François-Carcaillet, F. (1999) Mise au point d'un nouveau modèle de bioturbation pour une approche fonctionnelle du remaniement sédimentaire lié à l'activité des communautés macrobenthiques. Thèse de Docteur en Science. France: Université Aix-Marseille II, pp. 110.

Garby, L., and Larsen, P.S. (1995) *Bioenergetics: Its Thermodynamic Foundations*. New York: Cambridge University Press.

Gayon, U., and Dupetit, G. (1882) Sur la fermentation des nitrates. *Compte Rendu de l'Academie des Sciences* **95**: 644-646.

Genoud, M. (1988) Energetic strategies of shrews : ecological constraints and evolutionary implications. *Mammal Review* **4**: 173-193.

Gilbert, F., Hulth, S., Grossi, V., and Aller, R.C. (in preparation) Redox oscillation and benthic nitrogen mineralization: an experimental simulation approach.

Goldberg, E.D., and Koide, M. (1962) Geochronological studies of deep-sea sediments by the ionium/thorium method. *Geochimica et Cosmochimica Acta* **26**: 417-450.

Goldman, J.C., and Dennett, M.R. (2000) Growth of marine bacteria in batch and continuous culture under carbon and nitrogen limitation. *Limnology Oceanography* **45**: 789-800.

Guinasso, N.L., and Schink, D.R. (1975) Quantitative estimates of biological mixing rates in abyssal sediments. *Journal of Geophysical Research* **80**: 3032-3043.

Gurney, W.S.C., Jones, W., Veitch, A.R., and Nisbet, R.M. (2003) Resource allocation, hyperphagia and compensatory growth in juveniles. *Ecology* **84**: 2777-2787.

Gurney, W.S.C., and Nisbet, R.M. (2004) Resource allocation, hyperphagia and compensatory growth. *Bulletin of Mathematical Biology* **66**: 1731-1753.

Hanegraaf, P.P.F., and Muller, E.B. (2001) The dynamics of the macromolecular composition of biomass. *Journal of Theoretical Biology* **212**: 237-251.

Harvey, R.J., Marr, A.G., and Painter, P.R. (1967) Kinetics of growth of individual cells of Escherishia coli and Azotobacter agilis. *Journal of Bacteriology* **93**: 605-617.

Kooi, B.W., and Kooijman, S.A.L.M. (1994b) The transient behaviour of food chains in chemostats. *Journal of Theoretical Biology* **170**: 87-94.

Kooijman, S.A.L.M., Muller, E.B., and Stouthamer, A.H. (1991) Microbial dynamics on the basis of individual budgets. *Antonie van Leeuwenhoek* **60**: 159-174.

Kooijman, S.A.L.M. (1993) *Dynamic energy budgets in biological systems. Theory and applications in ecotoxicology*.

Kooijman, S.A.L.M. (1998) The synthesizing unit as model for the stoichiometric fusion and branching of metabolic fluxes. *Biophysical Chemistry* **73**: 179-188.

Kooijman, S.A.L.M. (2000) *Dynamic Energy and Mass Budgets in Biological Systems*. Cambridge.

Kooijman, S.A.L.M., Auger, P., Poggiale, J.C., and Kooi, B.W. (2003) Quantitative steps in symbiogenesis and the evolution of homeostasis. *Biol. Reviews* **78**: 435-463.

Kuijper, L.D.J. (2004) The role of trophic flows in food web dynamics. Amsterdam: Vrije Unervisiteit, pp. 126.

Kuijper, L.D.J., Anderson, T.R., and Kooijman, S.A.L.M. (2004) C and N gross efficiencies of copepod egg production studies using a

Dynamic Energy Budget model. *Journal of Plankton Research* **26**: 213-226.

Lancelot, C., Staneva, J., Van Eeckhour, D., Beckers, J.M., and Stanev, E. (2002) Modelling the Danube-influenced north-western continental shelf of the Black Sea. II: Ecosystem response to changes in nutrient delivery by the Danube River after its damming in 1972. *Est Coast Shelf Sciences* **54**: 473-479.

Lawton, J.H. (1994) What do species do in ecosystems? *Oikos* **71**: 367-374.

Lumey, L.H., Stein, A.D., and Ravelli, A.C.J. (1995) Timing of prenatal starvation in women and birth weight in their first and second born offspring: the Dutch famine birth cohort study. *European Journal of Obstetrics Gynecology Reproduction Biology* **61**: 23-30.

Madigan, M.T., Martino, J.M., and Parker, J. (2003) *Brock biology of microorganisms.* United States of America: Pearson Education International.

Marr, A.G., and Ingraham, J.L. (1962) Effect of temperature on the composition of fatty acids in Escherishia coli. *Journal of Bacteriology* **84**: 1260-1267.

Marr, A.G., Nilson, E.H., and Clark, D.J. (1963) The maintenance requirement of Escherishia coli. *Annals of the New York Academy of Sciences* **102**: 536-548.

Matisoff, G. (1982) *Mathematical models of bioturbation.* NY: Plenum Press London.

Meese, E.A. (1998) *SMLIB v. 1.1 a Fortran 90 library for sparse matrix calculations.* Trondheim.

Meysman, F.J.R., Boudreau, B.P., and Middelburg, J.J. (2003) Relations between local, nonlocal, discrete and continuous models of bioturbation. *Journal of Marine Research* **61**: 391-410.

Monod, J. (1942) *Recherches sur la croissance des cultures bactériennes.* Paris.

Morita, R.Y. (1985) *Starvation and miniaturisation of heterotrophs, with special emphasis on maintenance of the starved viable state. In: Bacteria in their natural environments (M. Fletcher and G.D. Floodgate, eds.)*. London.

Muller, E.B., and Nisbet, R.M. (2000) Survival and production in variable resource environments. *Bulletin of Mathematical Biology* **62**: 1163-1189.

Patching, J.W., and Eardly, D. (1997) Bacterial biomass and activity in the deep waters of the eastern Atlantic-evidence of a barophilic community. *Deep Sea Research Part I: Oceanographic Research Papers* **44**: 1655-1670.

Peaceman, D.W., and Rachford, H.H. (1955) The numerical solution of parabolic and elliptic differential equations. *SIAM* **3**: 28-42.

Péry, A.R.R., Mons, R., Flammarion, P., Lagadic, L., and Garric, J. (2002) A modelling approach to link food availability, growth, emergence, and reproduction for the midge Chironomus riparius. *Environmental Toxicology and Chemistry* **21**: 2507–2513.

Pirt, S.J. (1965) The maintenance energy of bacteria in growing cultures. *Process Royal Society London B* **163**: 224-231.

Postgate, J.R. (1990) The microbes that would not die. *New Scientist* **127**: 46-49.

Rabouille, C., and Gaillard, J.F. (1991) Towards the EDGE : early diagenetic global explanations. A model depicting the early diagenesis of organic matter, O2, NO3, Mn, and PO4. *Geochimica et Cosmochimica Acta* **55**: 2511-2525.

Rabouille, C., Witbaard, R., and Duineveld, G.C.A. (2001) Annual and interannual variability of sedimentary recycling studied with a non-steady-state application to the North Atlantic Ocean (BENGAL site). *Progress in Oceanography* **50**: 147-170.

Ratledge, C., Boulton, C.A., and Evans, C.T. (1984) *Continuous culture studies of lipid production by oleaginous microorganisms.* Chichester.

Rice, D.L., Bianchi, T.S., and Roper, E.H. (1986) Experimental studies of sediment reworking and growth of Scoloplos spp. (Orbiniidae : polychaeta). *Marine Ecology Progress Series* **30**: 9-19.

Robbins, J.A. (1986) A model of particle selective transport of tracers in sediments with conveyor-belt deposit feeders. *Journal of Geophysical Research* **91**: 8542-8558.

Scholten, J.C.M., van Bodegom, P.M., Vogelaar, J., van Ittersum, A., Hordijk, K., Roelofsen, W., and Stams, A.J.M. (2002) Effect of sulfate and nitrate on acetate conversion by anaerobic microorganisms in a freshwater sediment. *FEMS Microbiology Ecology* **42**: 375-385.

Soetaert, K., Herman, P.M.J., and Middelburg, J.J. (1996) A model of early diagenetic processes from the shelf to abyssal depths. *Geochimica et Cosmochimica Acta* **60**: 1019-1040.

Spitz, Y.H., Moisan, J.R., and Abbott, M.R. (2001) Configuring an ecosystem model using data from the Bermuda Atlantic Times Series (BATS). *Deep-Sea Research Part II* **48**: 1733-1768.

Talin, F., Tolla, C., Rabouille, C., and Poggiale, J.C. (2003) Relations between bacterial biomass and carbon cycle in marine sediments: An early diagenetic model. *Acta Biotheoretica* **51**: 295-315.

Tolla, C., Kooijman, S.A.L.M., and Poggiale, J.C. (Submitted) A kinetic inhibition mechanism for maintenance. *Journal of Theoretical Biology*.

Turley, C.M., and Lochte, K. (1990) Microbial response to the input of fresh detritus to the deep-sea bed. *Global and Planetary Change* **3**: 3-23.

van der Veer, H.W., Kooijman, S.A.L.M., and van der Meer, J. (2001) Intra- and interspecific comparison of energy flow in north atlantic flatfish species by means of dynamic energy budgets. *Journal of Sea Research* **45**: 303-320.

van der Vorst, H.A. (1992) BI-CGSTAB : a fast and smoothly converging variant of BI-CG for the solution of nonsymmetric linear systems. *SIAM Journal of Science Computing* **13**: 631-644.

van Haren, R.J.F., and Kooijman, S.A.L.M. (1993) Application of the dynamic energy budget model to Mytilus edulis (L). *Netherlands Journal of Sea Research* **31**: 119-133.

Wardle, D.A., Zackrisson, O., Hornberg, G., and Gallet, C. (1997) The influence of island area on ecosystem properties. *Science* **277**: 1296-1299.

Appendix

Appendix A. Table of nomenclature

State variables and parameters – Table of notation, units, description and initial value of state variables and parameters used in the manuscript. The following symbols are used for the dimensions: -, without unit; #*i*, unit of *i* (number, mass or concentration) ; *t*, time which vary according to the study (Kooijman, 2000).

Chapter 2: *t*: *d*, #: $\mu mol.l^{-1}$; Chapter 3: *t*: *h*, #: $mmol.l^{-1}$; Chapter 4: *t*: *h*, #: $g.l^{-1}$, *E* represents the nitrogen reserve ($gN.l^{-1}$) and *V* is in gram of structural biomass ($gV.l^{-1}$); Chapter 5: *t*: *d*, #: $\mu mol.l^{-1}$, E and V are expressed in $\mu mol\ N.l^{-1}$.

Notation	Units	Description
		State Variables
C	$\#C$	Particular Organic Carbon (POC)
O_2	$\#O_2$	Dioxygen
NO_3, N_{org}, NH_4	$\#N$	Nitrate, organic nitrogen and ammonium
X or S	$\#X$ or $\#S$	Substrate
E	$\#E$	Reserve of the microbial population
V	$\#V$	Structural biomass of the microbial population
e	$\#E.\#V^{-1}$	Reserve density (reserve by unit of structure) $e = E/V$
B	$\#B$	Bacterial biomass $B = V + \varepsilon E$
P	$\#P$	Products of the reactions
		Functions
I_X	$\#X.t^{-1}$	Substrate supply rate
$f(X)$	-	Michaelis-Menten kinetics $f(X) = X/(X+K_X)$
j_i^{Π}	$\#i.\#V^{-1}.t^{-1}$	Specific flux of compound *i* (*X*, *E*, *V* and *P*) associated to the process Π (A: assimilation, G: growth, M: maintenance)

J_i^{Π}	$\#i.t^{-1}$	Absolute flux of compound i associated to the process Π $J_i^{\Pi} = j_i^{\Pi} V$
θ_{ij}	-	SU fraction associated to a biogeochemical process, at binding state i and j (free, occupied by one or several substrate bound)
θ_{ij}*	-	SU fraction at steady state associated to a biogeochemical process, where i and j can be free or occupied
e_S	$\#E.\#V^{-1}$	Threshold value of the reserve density setting off the switch between the reserve and the structure use in the maintenance

Parameters

Physical and numerical geometry		
z_{max}	cm	Maximum depth of the sedimentary column
N	-	Grid number
Δz	cm	Space step (for the first 8 cm)
Δt	cm	Time step
Physical fields and constants		
W	$cm.t^{-1}$	Sedimentation velocity
D_O	$cm^2.t^{-1}$	Overall diffusion coefficient for dioxygen (0 – 6 cm)
D_{NO}	$cm^2.t^{-1}$	Overall diffusion coefficient for nitrate (0 – 6 cm)
$D_{M\,O}$	$cm^2.t^{-1}$	Molecular diffusion coefficient for dioxygen
$D_{M\,NO}$	$cm^2.t^{-1}$	Molecular diffusion coefficient for nitrate
ϕ	- (%)	Porosity
Biological		
D_B and D_C	$cm^2.t^{-1}$	Overall biodiffusion coefficient for bacteria and POC (0 – 6 cm)
α_{Bac}	$(\#C)^{-1}$	Transformation rate of POC in bacterial biomass
γ_B	$\%.(\#C)^{-1}$	Proportionality coefficient to POC for environment capacity of bacterial
r	t^{-1}	Specific growth rate of bacterial biomass
h_E *or* k_E	t^{-1}	Reserve turnover rate
k_M	$\#E.(\#V)^{-1}.t^{-1}$	Maintenance cost
g	$\#E.(\#V)^{-1}$	Growth cost
m	t^{-1}	Ratio between maintenance and growth costs
y_{ij}	$\#i.(\#j)^{-1}$	Yield coefficient coupling the mass flux i to the mass flux j
e_0	$\#E.\#V^{-1}$	Initial reserve density
Biogeochemical		
k_i	$(\#V)^{-1}.t^{-1}$	Binding rate of compounds i on the SU fraction association to a biogeochemical process k_i = m_i for oxic mineralization, a_i for anoxic mineralization, d_i for denitrification and n_i for nitrification

k'	t^{-1}	Releasing rate of the SU fraction associated to a biogeochemical process $k' = m'$ for oxic mineralization, a' for anoxic mineralization, d' for denitrification and n' for nitrification
ρ_i	-	Binding probability of compound i on the free SUs fraction
ρ_{ij}	-	Binding probability of compound i on the SU fraction with the compound j already bound
$j_{i\Pi m}$	t^{-1}	Maximal using rate of compounds i in the process Π
y_j^i	$\#i.(\#j)^{-1}$	Stoichiometric coefficient of the compound i used by compound j degraded associated to a biogeochemical process
R_{minox}, R_{minanox}, R_{denit}	t^{-1}	Maximal absolute rate of the oxic and anoxic mineralization and the denitrification
R_{nit}	$\#N.t^{-1}$	Maximal absolute rate of the nitrification
r_{minox}, r_{minanox}, r_{denit}	$(\#V)^{-1}.t^{-1}$	Maximal specific rate (by unit of structure) of the oxic and anoxic mineralization and the denitrification
r_{nit}	$\#N.(\#V)^{-1}.t^{-1}$	Maximal specific rate of the nitrification
K_X	$\#X$	Half Saturation Constant (HSC) in a process
$K_{\text{minox},*}$	$\#O_2$	HSC of the dioxygen for the oxic mineralization in the model *
$K_{\text{nit},O,*}$	$\#O_2$	HSC of the dioxygen for the nitrification in the model *
$K_{\text{denit},*}$	$\#N$	HSC of the nitrate for the denitrification in the model *
$K_{\text{nit},N,*}$	$\#N$	HSC of the organic nitrogen for the nitrification in the model *
$K_{\text{inhib,denit},*}$	$\#O_2$	Inhibition constant by dioxygen for the denitrification in the model *
$K_{\text{inhib,min},O,*}$	$\#O_2$	Inhibition constant by dioxygen for the anoxic mineralization in the model *
$K_{\text{inhib,min},N,*}$	$\#N$	Inhibition constant by the nitrate in the anoxic mineralization in the model *
α	-	Proportionality coefficient in maintenance

Appendix B. Relations between bacterial biomass and carbon cycle in marine sediments: An early diagenetic model.

Francis Talin, Caroline Tolla, Christophe Rabouille and Jean-Christophe Poggiale

Published in *Acta Biotheoretica*

Abstract

A new model for early diagenetic processes has been developed through a new formulation explicitly accounting for a microbial population dynamics. Following a mechanistic approach based on enzymatic reactions, a new model has been proposed for oxic mineralization and denitrification. It incorporates dynamics of bacterial metabolism. We find a general formulation for inhibition processes for which some of other mathematical relations are particular cases.

Moreover a fast numerical algorithm has been developed. It allows us to perform simulations of different diagenetic models in non steady states. We use this algorithm to compare our model to a classical one (Soetaert et al, 1996). Dynamical evolutions since a perturbation of particulate organic carbon (POC) input are studied for both models.

The results are very similar for stationary cases. But with variable inputs, the bacterial biomass dynamics brings about noticeable differences, which are discussed.

Keywords: maintenance - inhibition formulation - DEB theory - Synthesizing Units.

Appendix C. A kinetic inhibition mechanism for maintenance.

Caroline Tolla, Sebastiaan A. L. M. Kooijman, Jean-Christophe Poggiale

Submitted to *Journal of Theoretical Biology*.

Abstract

To fulfil their maintenance costs, most species use mobile pools of metabolites (reserve) in favourable conditions, but can also use less mobile pools (structure) under food-limiting conditions. While the Marr-Pirt model always pays maintenance costs from structure, the presence of reserve inhibits the use of structure for maintenance purposes. The standard Dynamic Energy Budgets (DEB) model captures this by simply supplementing all costs that could not be paid from reserve with structure. This is less realistic at the biochemical level, and involves a sudden use of structure that can complicate the analysis of the model properties. We here propose a new inhibition formulation for the preferential use of reserve above structure in maintenance that avoids sudden changes in the metabolites use. It is based on the application of the DEB theory for synthesizing units, which can easily become rather complex for demand processes, such as the maintenance process. We found, however, a simple explicit expression for the use of reserve and structure for maintenance purposes and compared the numerical behaviour with that of the Marr-Pirt model in oscillating conditions, by using parameter values from a fit of the models to data on yeasts in a batch culture. We conclude that our model can better handle variable environments. This new inhibition formulation has a wide applicability in modelling metabolic processes.

Keywords: maintenance - inhibition formulation - DEB theory - Synthesizing Units.

Appendix D. Modelling the impact of Tubificid worms (Oligochaeta) on oxygen concentrations in hyporheic sediments: importance of vertical distributions.

Florian Mermillod-Blondin, Jean-Christophe Poggiale, Caroline Tolla, Wilfried Thuiller, Pierre Auger and Michel Creuzé des Châtelliers

Submitted to *Canadian Journal of Fisheries Aquatic Sciences*.

Abstract

The aim of the study was to present a model to simulate the influence of tubificids (*Tubifex* and *Limnodrilus*) on O_2 concentrations in hyporheic sediments. A mathematical model was developed to reproduce vertical distribution of O_2 in experimental columns of sediments. Vertical column was simulated as a grid with cells of 1-cm depth each. The model took into account the hydrodynamic properties, the microbial respiration, and the stimulation effect of tubificids on microbial activity in the system. A coupling was made between the microbial stimulation by worms and their distribution in columns. The results of the model were compared to experimental data sets with the aim to test the importance of worm identity on aerobic processes. We hypothesized that two groups of worms (*Tubifex* and *Limnodrilus*) would present different vertical distributions in sediments and then would affect differently oxygen gradients in sediments. The spatial model gave a good assessment of the impact of tubificids on O_2 concentrations in the sediment. According to our hypothesis, the worm impact depended on the fluctuations of tubificid distributions that were linked to worm identity. Finally, the model suggests that factors affecting worm distribution in sediments have a significant impact on the biogeochemical functioning of the system.

Keywords: simulation - worms identity - microcosme - O_2 concentration.

Summary

Modelling Microbial Populations in Variable Environments

This thesis expands on a realistic characterisation of the links between microbial populations and their environment. Natural environments are mostly complex, with a lot of factors that can interplay. For example, the influence of food quality in ecosystems is the notion that all organisms need multiple elements in their nutrition. Furthermore, these environments are forced by perturbations in time and space. As an example, the variability in the amount of their resources can influence the fate of the considered populations.

Classical models analysing the microbial dynamics are empirical and based on experiments realised in equilibrium situations. They mostly use Michaelis-Menten kinetics as a base for the absorption process, and a Liebig's law for multi-substrate transformations. The Liebig's law allows a switch between different metabolic modes, depending on which element limits biomass growth. This switch makes the mathematical and the numerical analysis of such models awkward. Furthermore, these empirical formulations do not achieve the thermodynamics involved in biochemical transformations. Consequently, they are only appropriate for really simple environments but not for more complex ones such as multi-substrate natural systems.

This thesis provides a mechanistic modelling approach to treat these aspects of microbial dynamics in variable environments. This approach is based on the Dynamics Energy Budget (DEB) theory which considers some evidences such as:

- the mass conservation law must be fulfilled. This characteristic is achieved thanks to the individual scale consideration in the model formulation as mass and energy balances are most clear at this level.

- the element composition of an organism may differ substantially from the element composition of its food. In the mechanistic model, the differentiation in mobile (reserve) and non-mobile (structural biomass) matter derivates from this observation.
- the processes occurring at the individual level can be described from enzymatic kinetics. The synthesizing units (SUs) can be considered as a simple generalisation of the classical concepts of enzyme. This reasoning allows to obtain parameters value that can be reused.

Chapter 1 introduces the context, the problematic and presents our development. Then, from one chapter to another one, we improve the mechanistic model with different levels of details concerning the microbial population and its interaction with its environment.

Chapter 2 incorporates the dynamics of bacterial metabolism in classical models analysing the organic matter degradation and proposes a new model based on enzymatic reactions for oxic mineralization and denitrification. We find a general formulation for inhibition processes for which some of other mathematical relations are particular cases. We compare our model to a classical one through simulations. Both models show very similar results for stationary cases, but with variable inputs, the model that accounts for bacterial biomass dynamics shows noticeable differences, which are discussed.

Chapter 3 compares classical empirical models that analyse the microbial dynamics (the models by Monod and Droop) with a DEB based model through an application to a set of data. The Monod model shows intrinsic failing. The two other models offer a good fit to the data but show strong differences in parameter values. This chapter highlights the problematic of the complementarity between experimentation and modelling. Indeed, the strong variability in parameter values from one condition to another one in simplified model can come from some essential processes not taken into account; but the model complexity in terms of numbers of parameters and variables must match the availability of data. Although too complex for this particular data set, the DEB model obtains parameter values that are useful for perturbation studies.

Chapter 4 proposes an improvement of the standard DEB model for bacterial communities dynamics by giving a new description of adaptation in case of nutrients depletion: the shrinking process. To fulfil their maintenance costs, most species use mobile pools of metabolites (reserve) in favourable conditions, but can also use less mobile pools (structure) under food-limiting conditions. As the presence of reserve inhibits the use of structure, this leads to a new inhibition formulation, based on SUs, for maintenance which is

controlled by product formation (demand system). The standard DEB model, based on an empirical switch, is less realistic at the biochemical level, and involves a sudden use of structure that can complicate the analysis of the model properties. We compared the numerical behaviour with that of the Marr-Pirt model in oscillating conditions, by using parameter values from a fit of the models to data on yeasts in a batch culture. We conclude that our model can better handle variable environments.

From previous work, Chapter 5 proposes an improvement of the description of substrate interactions in biogeochemical models, focusing on the nitrogen cycle, and studies the impact of benthic population on the expression of bacterial metabolism. The principal effect of macrobenthic activities on microbial communities considered here is changing the environmental oxygenation (RedOx oscillations). We applied here the formulations developed in Chapters 2 and 4 on a supply system corresponding to biogeochemical processes: inhibition of a biogeochemical process of the nitrogen cycle by the presence of an inhibitory compound (as dioxygen for anaerobic processes). We compare, through a theoretical and a numerical analysis, the usual (phenomenological) model based on Michaelis-Menten formulations with a DEB based model. Simulating oscillations, the usual model suggests that the empirical formulation is not suitable for perturbed environments. The theoretical analysis shows that the phenomenological and the mechanistic approaches lead to different results in the case of environmental perturbations. The mechanistic model, more stable than the phenomenological one, points out the absorption of the supplied matter by the structural biomass. This result has already been observed experimentally. The mechanistic model support some unexpected experimental results found in the literature.

The work presented in this dissertation yields a number of general ideas (*i*) on the interactions between microbial populations and their environments by considering their functionality; (*ii*) on the modelling problematic: the compromise between complexity and obtained informations, the link between data and modelling, the importance of the modelling approach.

The models developped here can now suggest new experiments: which parameters must be measured, what is the measure frequency that allows to obtain new knowledge, what is the good time scale in order to obtain data at several dynamics levels (ex: biochemical and biological) with a minimum cost. Furthermore, the mechanistic formulations can help to understand the physiological state of the individual and can have a wide applicability in modelling metabolic processes.

Samenvatting

Modelling Microbial Populations in Variable Environments

This thesis expands on a realistic characterisation of the links between microbial populations and their environment. Natural environments are mostly complex, with a lot of factors that can interplay. For example, the influence of food quality in ecosystems is the notion that all organisms need multiple elements in their nutrition. Furthermore, these environments are forced by perturbations in time and space. As an example, the variability in the amount of their resources can influence the fate of the considered populations.

Classical models analysing the microbial dynamics are empirical and based on experiments realised in equilibrium situations. They mostly use Michaelis-Menten kinetics as a base for the absorption process, and a Liebig's law for multi-substrate transformations. The Liebig's law allows a switch between different metabolic modes, depending on which element limits biomass growth. This switch makes the mathematical and the numerical analysis of such models awkward. Furthermore, these empirical formulations do not achieve the thermodynamics involved in biochemical transformations. Consequently, they are only appropriate for really simple environments but not for more complex ones such as multi-substrate natural systems.

This thesis provides a mechanistic modelling approach to treat these aspects of microbial dynamics in variable environments. This approach is based on the Dynamics Energy Budget (DEB) theory which considers some evidences such as:

- the mass conservation law must be fulfilled. This characteristic is achieved thanks to the individual scale consideration in the model formulation as mass and energy balances are most clear at this level.

- the element composition of an organism may differ substantially from the element composition of its food. In the mechanistic model, the differentiation in mobile (reserve) and non-mobile (structural biomass) matter derivates from this observation.
- the processes occurring at the individual level can be described from enzymatic kinetics. The synthesizing units (SUs) can be considered as a simple generalisation of the classical concepts of enzyme. This reasoning allows to obtain parameters value that can be reused.

Chapter 1 introduces the context, the problematic and presents our development. Then, from one chapter to another one, we improve the mechanistic model with different levels of details concerning the microbial population and its interaction with its environment.

Chapter 2 incorporates the dynamics of bacterial metabolism in classical models analysing the organic matter degradation and proposes a new model based on enzymatic reactions for oxic mineralization and denitrification. We find a general formulation for inhibition processes for which some of other mathematical relations are particular cases. We compare our model to a classical one through simulations. Both models show very similar results for stationary cases, but with variable inputs, the model that accounts for bacterial biomass dynamics shows noticeable differences, which are discussed.

Chapter 3 compares classical empirical models that analyse the microbial dynamics (the models by Monod and Droop) with a DEB based model through an application to a set of data. The Monod model shows intrinsic failing. The two other models offer a good fit to the data but show strong differences in parameter values. This chapter highlights the problematic of the complementarity between experimentation and modelling. Indeed, the strong variability in parameter values from one condition to another one in simplified model can come from some essential processes not taken into account; but the model complexity in terms of numbers of parameters and variables must match the availability of data. Although too complex for this particular data set, the DEB model obtains parameter values that are useful for perturbation studies.

Chapter 4 proposes an improvement of the standard DEB model for bacterial communities dynamics by giving a new description of adaptation in case of nutrients depletion: the shrinking process. To fulfil their maintenance costs, most species use mobile pools of metabolites (reserve) in favourable conditions, but can also use less mobile pools (structure) under food-limiting conditions. As the presence of reserve inhibits the use of structure, this leads to a new inhibition formulation, based on SUs, for maintenance which is

controlled by product formation (demand system). The standard DEB model, based on an empirical switch, is less realistic at the biochemical level, and involves a sudden use of structure that can complicate the analysis of the model properties. We compared the numerical behaviour with that of the Marr-Pirt model in oscillating conditions, by using parameter values from a fit of the models to data on yeasts in a batch culture. We conclude that our model can better handle variable environments.

From previous work, Chapter 5 proposes an improvement of the description of substrate interactions in biogeochemical models, focusing on the nitrogen cycle, and studies the impact of benthic population on the expression of bacterial metabolism. The principal effect of macrobenthic activities on microbial communities considered here is changing the environmental oxygenation (RedOx oscillations). We applied here the formulations developed in Chapters 2 and 4 on a supply system corresponding to biogeochemical processes: inhibition of a biogeochemical process of the nitrogen cycle by the presence of an inhibitory compound (as dioxygen for anaerobic processes). We compare, through a theoretical and a numerical analysis, the usual (phenomenological) model based on Michaelis-Menten formulations with a DEB based model. Simulating oscillations, the usual model suggests that the empirical formulation is not suitable for perturbed environments. The theoretical analysis shows that the phenomenological and the mechanistic approaches lead to different results in the case of environmental perturbations. The mechanistic model, more stable than the phenomenological one, points out the absorption of the supplied matter by the structural biomass. This result has already been observed experimentally. The mechanistic model support some unexpected experimental results found in the literature.

The work presented in this dissertation yields a number of general ideas (*i*) on the interactions between microbial populations and their environments by considering their functionality; (*ii*) on the modelling problematic: the compromise between complexity and obtained informations, the link between data and modelling, the importance of the modelling approach.

The models developped here can now suggest new experiments: which parameters must be measured, what is the measure frequency that allows to obtain new knowledge, what is the good time scale in order to obtain data at several dynamics levels (ex: biochemical and biological) with a minimum cost. Furthermore, the mechanistic formulations can help to understand the physiological state of the individual and can have a wide applicability in modelling metabolic processes.

Dankwoord

First, I would like to thank my french PhD supervisor Jean-Christophe POGGIALE who transmitted his interest for modelling to me during my whole university programme. With a lot of patience and listening, he guided me through the discovery.

Many thanks also to Sebastiaan KOOIJMAN who was always available for open discussion and advice. Furthermore, he judged my work and helped me in the DEB theory and understanding the Dutch life.

I also sincerely thank Pierre AUGER, Peter van BODEGOM, Ulf DIECKMANN, Rob HENGEVELD, Bote KOOI, Jaap van der MEER who honour me for judging my work and accepting the jury role for this PhD defence.

I thank Tineke TROOST for her enthusiastic welcome in Netherlands and her joie de vivre and David NERINI and Claude MANTE for their support and their humour.

I don't forget to thank a lot all who brought me their good or bad mood: Guy JAYME, Maurice LIBES, Franck GILBERT, etc.

In particular, I would like to thank Rodin KAUFMANN and my friends Emilie BONNIN, Agnès BOURRET, Julie GATTI and Melilotus THYSSEN.

Finally, I direct tenders thanks to my mother who brought me her relentless support and her trust.

Thank you.

Caroline